

**DEVELOPMENT OF A REGENERABLE GLUCOSE BIOSENSOR
PROBE FOR BIOPROCESS MONITORING**

MICHAEL R. PHELPS

B. Eng., The Royal Military College of Canada, 1990

A THESIS SUBMITTED IN PARTIAL FULFILLMENT OF
THE REQUIREMENTS FOR THE DEGREE OF
MASTER OF APPLIED SCIENCE
in
THE FACULTY OF GRADUATE STUDIES
DEPARTMENT OF CHEMICAL ENGINEERING

We accept this thesis as conforming to the required standard




THE UNIVERSITY OF BRITISH COLUMBIA

October 1993

© Michael R. Phelps, 1993

In presenting this thesis in partial fulfilment of the requirements for an advanced degree at the University of British Columbia, I agree that the Library shall make it freely available for reference and study. I further agree that permission for extensive copying of this thesis for scholarly purposes may be granted by the head of my department or by his or her representatives. It is understood that copying or publication of this thesis for financial gain shall not be allowed without my written permission.

(Signature)



Department of Chemical Engineering

The University of British Columbia
Vancouver, Canada

Date September 28, 1993

ABSTRACT

The implementation and commercialization of enzyme-based biosensors for on-line bioprocess monitoring and control has been slowed by problems relating to the *in situ* sterilizability of the probe and the stability of the enzyme component. A novel technology is presented here which addresses both of these difficulties. The approach is based on the reversible immobilization of enzymes conjugated with the cellulose binding domain (CBD) of cellulases from *Cellulomonas fimi*. A regenerable biosensor probe is configured with a cellulose matrix onto which the solubilized enzyme-CBD conjugate can be repeatedly loaded (via the attachment of the CBD) and subsequently eluted by perfusing the cellulose matrix with the appropriate loading or eluting solution.

The chemical conjugation of the enzyme glucose oxidase (GOx) with CBD by glutaraldehyde is described. The GOx-CBD conjugate retained the enzymatic activity of the glucose oxidase and the binding affinity of the CBD. The GOx-CBD conjugate was used in an experimental glucose biosensor based on a platinum rotating disk electrode fitted with a cellulose immobilization matrix to demonstrate the feasibility of multiple cycles of loading and elution of the conjugate and to develop suitable protocols and reagents for the loading and elution procedures. A prototype glucose biosensor and reagent flow system were designed and built for use in fermentation monitoring. A custom-designed membrane system consisting of a sterilizable, glucose-permeable outer Nafion membrane for the sensor and a cellulose acetate coating on the indicating electrode was developed for use in a microbial fermentation. The prototype glucose biosensor was used successfully to monitor medium glucose concentration for 16.5 continuous hours during a 20 L fed-batch cultivation of *E. coli* in minimal medium. Michaelis-Menten enzyme kinetics were used as an empirical model for the calibration of the experimental biosensor. The development of a computer-controlled prototype glucose biosensor and fermentation monitoring system is discussed.

These results are the first to demonstrate the concept, feasibility, and utility of a regenerable biosensor based on reversible immobilization of the enzyme using CBD technology and represent a significant step toward better instrumentation for fermentation monitoring and control.

TABLE OF CONTENTS

	Page
ABSTRACT.....	ii
TABLE OF CONTENTS	iv
LIST OF TABLES	vii
LIST OF FIGURES	viii
ACKNOWLEDGEMENTS.....	x
INTRODUCTION	1
CHAPTER 1 LITERATURE REVIEW	4
1.1 BIOSENSOR DEVELOPMENT.....	4
1.1.1 Introduction.....	4
1.1.2 Enhancing Long Term Stability.....	8
1.1.3 Cellulose Binding Domain Technology.....	10
1.2 GLUCOSE MONITORING AND CONTROL.....	12
1.2.1 Optimization of Bioprocesses.....	12
1.2.2 Strategies for Glucose Monitoring and Control	14
1.2.3 <i>In situ</i> Enzyme Electrode Probes.....	18
CHAPTER 2 BACKGROUND AND THEORY	22
2.1 INTRODUCTION.....	22
2.2 ENZYME ELECTRODE COMPONENTS	22
2.3 BIOCHEMICAL CONSIDERATIONS.....	24
2.4 ELECTROCHEMICAL CONSIDERATIONS	26
2.5 MODELLING CONSIDERATIONS.....	28
2.5.1 Assumptions and Approximations	30
2.5.2 Diffusion Equations	32
2.5.3 Enzyme Reaction-Rate Equations	33

2.5.4	The General Modelling Approach	37
2.5.5	Multi-layer Modelling	39
2.6	PRINCIPLE OF OPERATION.....	41
CHAPTER 3 SYNTHESIS AND CHARACTERIZATION OF THE GLUCOSE		
	OXIDASE - [CELLULOSE BINDING DOMAIN] CONJUGATE.....	46
3.1	INTRODUCTION.....	46
3.2	MATERIALS AND METHODS	46
3.2.1	Enzymes and Chemicals	46
3.2.2	Enzyme-CBD Conjugations	47
3.2.3	Total Protein and Enzyme Activity Assays	48
3.2.4	Gel Electrophoresis and Immunoblotting.....	49
3.3	RESULTS AND DISCUSSION	49
CHAPTER 4 DEMONSTRATION OF THE FEASIBILITY OF A REGENERABLE		
	GLUCOSE BIOSENSOR.....	54
4.1	INTRODUCTION.....	54
4.2	MATERIALS AND METHODS	54
4.2.1	Instrumentation.....	54
4.2.2	Experimental Glucose Biosensor Preparation	55
4.3	RESULTS AND DISCUSSION	56
CHAPTER 5 DESIGN AND CHARACTERIZATION OF THE EXPERIMENTAL		
	GLUCOSE BIOSENSOR PROTOTYPE.....	66
5.1	INTRODUCTION.....	66
5.2	MATERIALS AND METHODS	66
5.2.1	Prototype Design and Construction.....	66
5.2.2	Prototype Characterization Experiments	77
5.2.3	Glucose Monitoring During Fed-Batch Cultivation of <i>E. coli</i>	80

5.3	RESULTS AND DISCUSSION	81
5.3.1	Prototype Characterization.....	82
5.3.2	Glucose Monitoring During Fed-Batch Cultivation of <i>E. coli</i>	99
CHAPTER 6	CONCLUSIONS	111
6.1	CONCLUDING REMARKS	111
6.2	FUTURE WORK	114
NOMENCLATURE SUMMARY		117
REFERENCES		119
APPENDIX	SAMPLE STRIP CHART RECORD	130

LIST OF TABLES

Table 1.1	Industrially important enzymatic assays requiring oxidase enzymes.	6
Table 3.1	Specific activity of various samples of soluble GOx-CBD conjugate.	53
Table 4.1	Properties of the cellulose matrices used in the experimental glucose biosensor system.	59
Table 4.2	Apparent enzyme kinetic data derived from the calibration data of Figure 4.2.	63
Table 5.1	Characteristics of different membranes tested as potential outer membranes for the glucose biosensor prototype.	84
Table 5.2	Prototype sensor calibration constants for the first and second enzyme loadings.	105

LIST OF FIGURES

Figure 1.1	Schematic representation of the cellulase exoglucanase from <i>C. fimi</i>	10
Figure 2.1	Schematic diagram of a glucose sensitive enzyme electrode.	23
Figure 2.2	Schematic diagram of a biosensor based on CBD-immobilized enzymes. .	43
Figure 2.3	Process flow diagram demonstrating the principle of operation of a fermentation monitoring system using the renewable biosensor probe.	43
Figure 3.1	A. Gel electrophoresis (SDS-PAGE) of the GOx-CBD conjugate. B. Western blot of the gel in A.	51
Figure 4.1	Typical calibration data for the experimental glucose biosensor.	58
Figure 4.2	Calibration data for multiple cycles of loading and elution of the GOx-CBD conjugate.	60
Figure 4.3	Lineweaver-Burk plot of the calibration data in Figure 4.2.	61
Figure 5.1	Construction of the Ingold CO ₂ probe.	67
Figure 5.2	Diagram of the internal electrode assembly.	71
Figure 5.3	Stainless steel adapter for mounting the internal electrode unit.	73
Figure 5.4	Schematic diagram of the biosensor prototype showing the reagent flow system and instrumentation.	75
Figure 5.5	Stainless steel dummy electrode.	78
Figure 5.6	Comparison of the response of different cellulose acetate coated Pt electrodes to hydrogen peroxide.	87
Figure 5.7	Normalized calibration data for the prototype biosensor in PBS and Luria broth (L-B) using different membranes.	89
Figure 5.8	Sensor equilibration time after insertion in Luria broth using different membranes.	92

Figure 5.9	Normalized calibration data for the prototype sensor in PBS and Luria broth (L-B) using the Nafion membrane before and after autoclaving.....	94
Figure 5.10	Effect of temperature on the sensor signal at steady-state.....	95
Figure 5.11	Effect of medium pH on the sensor signal at steady-state.	95
Figure 5.12	Effect of medium dissolved oxygen tension on the sensor signal at steady-state.	97
Figure 5.13	Time-course of the fermenter variables during fed-batch cultivation of <i>E. coli</i> in a 20 L fermenter.	102
Figure 5.14	Medium glucose concentration measured by the prototype glucose sensor and the Beckman off-line glucose analyzer during fed-batch cultivation of <i>E. coli</i> in minimal medium (M-9) in a 20 L fermenter.....	103
Figure 5.15	Cross-correlation plots of the prototype glucose sensor output and the Beckman off-line glucose analyzer results.....	107
Figure 5.16	Ratio of the Beckman glucose analyzer results and the prototype glucose sensor output calculated at various points in time after fresh enzyme was loaded.	110

ACKNOWLEDGEMENTS

I would like to thank my supervisor, Dr. Robin Turner, for his helpful advice and guidance throughout the course of my thesis work, and for his support and encouragement when it was needed. I would also like to thank the members of my supervisory committee, Dr. Doug Kilburn, Dr. John Hobbs and Dr. Ken Pinder, for their useful discussions and examination of this thesis.

I would also like to acknowledge the expert technical assistance of the technicians, students, and staff in the Biotechnology Laboratory and the Department of Chemical Engineering at the University of British Columbia. I am especially grateful to Dr. Edgar Ong and Dr. Andrew Wierzba for their technical assistance in purifying and characterizing the GOx-CBD conjugate, to Gary Lesnicki for his help in the fermenter pilot plant, and to Diane Hasenwinkle and Eric Jervis for their assistance and advice regarding the cultivation of *E. coli* in minimal medium.

Finally, I would like to acknowledge the financial support for this work provided by the Natural Sciences and Engineering Research Council of Canada (NSERC).

INTRODUCTION

The increasing commercial importance of bioprocesses has stimulated research in fermentation monitoring in order to optimize the performance of bioreactors. The specificity and selectivity provided by the biological component of biosensors offer enormous potential, in principle, for continuous, on-line analysis in complex fermentation media. Numerous examples of amperometric enzyme electrode biosensors have been described in the literature (Brooks et al., 1991; Mascini and Palleschi, 1989). However, the development and implementation of these biosensors for bioprocess control has been slowed by problems relating to the sterilizability and stability of enzyme-based probes in bioreactors. In this thesis, a novel enzyme immobilization technology is used in the development of a biosensor for bioprocess control which potentially addresses both of these shortcomings.

The new technology is based on the reversible immobilization of enzymes via conjugation with the cellulose binding domain (CBD) of cellulases from *Cellulomonas fimi*. These cellulases have a modular structure consisting of two or more structurally separate domains (Kilburn et al., 1992). The binding domain functions independently of the catalytic domain and can be chemically or genetically conjugated to other proteins (e.g. enzymes) which then bind strongly to cellulose. Under the appropriate solution conditions, the binding can be disrupted and the conjugate protein eluted from the cellulose matrix. In this work, the CBD is chemically conjugated to glucose oxidase to develop a regenerable glucose biosensor using reversibly immobilized enzyme.

Briefly, the hardware for the regenerable biosensor system consists of a platinum indicating electrode, a porous cellulose matrix, and a protective dialysis membrane, all incorporated into a stainless steel probe for insertion into the bioreactor. The rate of H_2O_2 evolution from the enzyme-catalyzed oxidation of glucose is measured amperometrically at the platinum electrode. The cellulose matrix for immobilization of the

enzyme-CBD conjugate is incorporated into the enzyme chamber of the sensor body, sandwiched between the surface of the indicating electrode and the dialysis membrane. Inlet and outlet tubing in the probe body allow perfusion of the cellulose matrix with the enzyme-CBD conjugate solution and/or the elution buffer. The basic design is similar to that presently employed in commercial CO₂ probes (Ingold, 1990).

After the steam sterilization of the bioreactor and the probe body, the sensor is loaded by perfusing the cellulose matrix with the enzyme-CBD conjugate solution, resulting in attachment of the enzyme via the CBD. The sensor is calibrated by inoculation of the fermenter, and an internal calibration check can be performed periodically during the fermentation. If the enzyme activity deteriorates to an unacceptable degree, the sensor can be regenerated without interrupting the fermentation by perfusing the cellulose matrix with elution buffer to remove the attached enzyme. The sensor is then reloaded with enzyme-CBD conjugate as before, and recalibrated to continue monitoring the fermentation.

The advantage of this design is that the complete process of diagnosis, regeneration, and recalibration could potentially be performed *in situ* and under computer control. The applications of the system can be expanded by conjugating the CBD to other enzymes, such that the sensor hardware could be used for monitoring a variety of different analytes.

The primary purpose of this work is to develop the technology for regenerable biosensors based on enzyme-CBD conjugates. Specifically, the objectives of this thesis are:

1. To synthesize and characterize a chemical conjugate of glucose oxidase and cellulose binding domain.
2. To demonstrate the feasibility of the concept of a regenerable glucose biosensor based on the GOx-CBD conjugate protein.

3. To demonstrate the potential of the CBD technology for the development of on-line bioprocess sensors by designing, constructing, and testing an experimental biosensor prototype that can be used for glucose monitoring during a microbial fermentation.

CHAPTER 1

LITERATURE REVIEW

1.1 BIOSENSOR DEVELOPMENT

1.1.1 Introduction

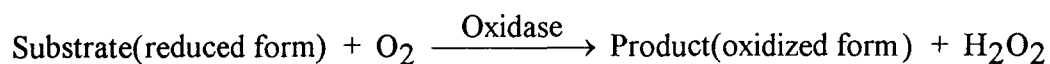
The Clark oxygen electrode (Clark, 1956) can be said to be the cornerstone of modern biosensor technology. The electrode detected dissolved oxygen polarographically and was used for monitoring blood dissolved oxygen levels in patients during surgery (Schultz, 1991). In 1962, Clark and Lyons first conceived of a glucose sensor based on the Clark oxygen electrode (Clark and Lyons, 1962). Glucose oxidase was immobilized in a gel on the surface of the oxygen electrode, and the rate of consumption of oxygen during the enzymatic oxidation of glucose could be related to the blood glucose concentration. Updike and Hicks coined the term "enzyme electrode" in 1967 and developed the idea one step further (Updike and Hicks, 1967) by incorporating an oxygen electrode without immobilized enzyme into the sensor system. A differential measurement could then be performed to correct for variation of the background oxygen concentration. In 1969, Guilbault designed an enzyme electrode for the measurement of urea in body fluids using the enzyme urease (Guilbault and Montalvo, 1969). The ammonium ion produced by the enzyme-catalyzed reaction of urea was detected potentiometrically using an ion selective electrode (ISE). In 1970, Clark patented the idea of using a platinum electrode for the amperometric detection of hydrogen peroxide produced in the oxidation of glucose by glucose oxidase (Clark, 1970). This development became the basis for the commercially available laboratory glucose analyzer marketed by the Yellow Springs Instrument Company (Yellow Springs, Ohio, U.S.A.).

Since the enzyme electrode was first conceived, a significant interest has developed in the field of biosensors because of the simplicity and selectivity of these sensors. A dramatic increase in biosensor interest began in the 1980's, evident by the publication of a new international journal Biosensors (Stoecker and Yacynych, 1990). The rapid growth of biotechnology in the last decade has now created a demand for more and better on-line sensors that can be interfaced with computers to control and optimize bioprocesses. Numerous enzyme electrode configurations have been published, and the amount of research activity today is too great to be covered in a single review (Freitag, 1993). Present-day applications of biosensors can be found in industrial bioprocess monitoring, environmental monitoring, the food and drink industry, and clinical and *in vivo* applications in medicine (Schultz, 1991; Reach and Wilson, 1992).

The work in this thesis will concentrate on biosensors for fermentation monitoring and industrial bioprocess control. The focus will be on the development of the technology for a regenerable glucose biosensor using glucose oxidase (GOx) because of the importance of glucose as the main carbon source and growth-limiting substrate in industrial fermentations (Filippini et al., 1991; Huang et al., 1991; Freitag, 1993). However, it should be understood that the technology developed here could, in principle, be used in conjunction with numerous other oxidase enzymes to monitor other industrially important analytes (see Table 1.1).

The oxidation of glucose by glucose oxidase in the presence of oxygen results in the production of gluconolactone and hydrogen peroxide. A number of different transducers, such as electrochemical detectors, optical detectors, and calorimeters, have been used to measure the rate of the enzyme-catalyzed reaction and provide a useable electrical signal for further analysis. Calorimetry is a highly versatile technique as it can be applied to virtually any enzymic reaction (Guilbault and Luong, 1989). However, the sensitivity and measuring range are relatively low, depending on the heat output of the

Table 1.1. Industrially important enzymatic assays requiring oxidase enzymes. The general oxidase enzyme-catalyzed reaction is of the form:



SUBSTRATE (Reduced Form)	ENZYME CATALYST	PRODUCT (Oxidized Form)
β-D-Glucose	Glucose Oxidase	δ-Gluconolactone
L-Lactate	L-Lactate Oxidase	Pyruvate
Ethyl Alcohol	Alcohol Oxidase	Acetaldehyhde
Lactose	Galactose Oxidase	Galactose Dialdehyde
Glycerol	Galactose Oxidase	Glyceraldehyde
Cholesterol	Cholesterol Oxidase	4-cholesten-3-one
Pyruvate	Pyruvate Oxidase	Acetyl Phosphate
Uric Acid	Uricase	Allantoin
Acetaldehyde	Aldehyde Oxidase	Acetate
Xanthine	Xanthine Oxidase	Urate
Choline	Choline Oxidase	Betaine
L-Glutamate	L-Glutamate Oxidase	α-Ketoglutarate
Acetylcholine*	Acetylcholine Esterase	Choline
L-Glutamine*	L-Glutaminase	L-Glutamate
Maltose*	Glucoamylase	β-D-Glucose
Starch*	Amyloglucosidase	β-D-Glucose
Sucrose*	Invertase + Mutarotase	β-D-Glucose

* Assays that require a multi-enzyme system.

given reaction, and difficulties have been encountered ensuring that the reference temperature is constant (± 0.01 °C) (Chaplin and Bucke, 1990). Huang et al. (1991) have coupled the luminescent reaction of luminol and H_2O_2 in the presence of horseradish peroxidase with the glucose oxidase catalyzed oxidation of glucose and used an optical detector for signal transduction. The advantages of optical sensors are high sensitivity, stable calibration, and no requirement for a reference electrode. However, optical detectors are expensive and are not suitable for use as on-line, *in situ*, sensors due to the interference from turbid, coloured media and the effect of background light. Electrochemical transducers are most commonly used for reasons of simplicity, high sensitivity, and low cost. Many examples have been cited in the literature (Kobos, 1980; Mascini and Palleschi, 1989; Hendry et al., 1990). Signal transduction can be based on either the amperometric detection of oxygen consumption or hydrogen peroxide production, or the potentiometric determination of the local pH change due to the production of gluconic acid. The greatest drawback of the potentiometric method is that the quantification of pH change necessitates a weakly buffered measurement solution if a significant change in pH is to be observed. In addition, the sensitivity of potentiometric sensors is governed by the Nernst equation, which dictates a logarithmic dependence of the signal on the hydrogen ion concentration. The biosensor developed in this thesis employs the principle of amperometric detection of hydrogen peroxide production at a platinum indicating electrode. The electrical current output from amperometric sensors is related to the rate of reaction by Faraday's law and the sensor response will, in theory, be linear. In addition, amperometric sensors are not as sensitive to changes in medium pH as potentiometric sensors and can be used in buffered media.

1.1.2 Enhancing Long Term Stability

Despite the number of biosensor research papers published each year in the scientific literature, relatively few biosensors are commercially available. Unfortunately, many practical problems remain which have prevented the widespread application of biosensors under real conditions and these have not been successfully addressed in the literature to date. The development and commercialization of biosensors has been slowed by problems of instability and drift of the sensor signal, narrow measuring range for the analyte, and long response times.

The problems of long term stability can be attributed to changes in the enzyme component, such as inhibition or deactivation by components of the analyte medium. Drift of the sensor signal over time may be due to time-dependent changes in the sensor calibration constants, which are caused by membrane fouling or electrode poisoning. Many of these issues can be alleviated to some extent by careful selection of the sensor membrane(s). Permselective membranes for amperometric biosensing have been reviewed in the literature (Wang, 1992). In addition, the sensor can be recalibrated periodically to correct for changes in the calibration constants. The denaturation of the enzyme over time is irreversible, however, and although the lifetime of the enzyme may be prolonged in some cases, replacement of the enzyme when the activity has degraded to an unsatisfactory degree will eventually be necessary. The capability to replace the enzyme component of the sensor would not only extend the sensor operating lifetime but would allow for the substitution of other enzymes in order to change the analyte specificity of the sensor.

A few sensor systems have been described in the literature with the capacity for enzyme replacement. Brooks et al. (1987/88) and Bradley and Schmid (1991) have described the immobilization of the enzyme on graphite discs which could be replaced manually. In the ideal case, the enzyme would be reversibly immobilized, such that the

enzyme could be exchanged *in situ*, without dismantling the sensor or interrupting the fermentation.

Reversible enzyme immobilization techniques have been reported in the literature. Pieters and Bardeletti (1992) described the immobilization of enzymes to magnetic beads, which could then be manipulated using magnetic fields. The technique has been used in waste-water treatment, affinity separation processes, cell sorting, immunoassays, and drug delivery (Pieters and Bardeletti, 1992). Miyabayashi et al., (1989) reported a potentiometric enzyme electrode using chymotrypsin deposited on magnetic particles, which were then trapped in a magnetic field at the indicating electrode. The time to reach steady state response was 30 minutes. The immobilization of glucose oxidase to magnetic particles was described by Pieters and Bardeletti (1992), and it may be possible to apply this technique to an amperometric glucose biosensor.

Glucose oxidase has been reversibly immobilized in an enzyme reactor coupled to a flow injection analysis system using a chain of biospecific reactions based on the binding of biotin-labelled (i.e., biotinylated) antibodies to an avidin coated matrix (de Alwis and Wilson, 1989). Biotinylated antibodies and streptavidin-labelled reporter enzymes (such as alkaline phosphatase or horseradish peroxidase) are commercially available, and the biotin/streptavidin system has been exploited for immunoassays (Brillhart and Ngo, 1991). de Alwis and Wilson covalently attached avidin to a packed column, followed by attachment of biotinylated anti-glucose oxidase antibodies, which would then bind glucose oxidase to the reactor column. The high affinity and strength of the avidin-biotin linkage ($K_d = 10^{-15} \text{ M}^{-1}$) was considered to be irreversible in this case, although the binding could be disrupted by 6 M guanidine, pH 1.5. The enzyme was eluted from the column without affecting the avidin-biotin linkage by disrupting the antibody-enzyme bond using 0.1 M phosphate buffer, pH 2.0, and fresh enzyme could then be attached by washing the column with a solution of glucose oxidase. The enzyme could be loaded and eluted repeatedly.

1.1.3 Cellulose Binding Domain Technology

The glucose biosensor developed in this thesis uses a novel technique for the reversible immobilization of enzymes based on the cellulose binding domain (CBD) of the cellulases from *C. fimi*. These cellulases have been shown to consist of two or more structurally distinct and independently functioning catalytic and binding domains (Gilkes et al., 1991). The cellulose binding domain of the cellulase exoglucanase, shown in Figure 2.2, has been expressed in *E. coli* to obtain the isolated CBD polypeptide (CBD_{Cex}) (Ong et al., 1993). Proteins conjugated to CBD (by genetic or chemical methods) have acquired the ability to bind reversibly to cellulose. The exact nature of the binding mechanism has not been determined, however the binding to cellulose has been reported to be virtually instantaneous. Previously published CBD binding studies indicated that adsorption of the CBD to cellulose was complete within the shortest incubation time feasible under the conditions of the experiment (i.e., 0.2 minutes) (Gilkes et al., 1992), but the actual adsorption kinetics are likely much faster.

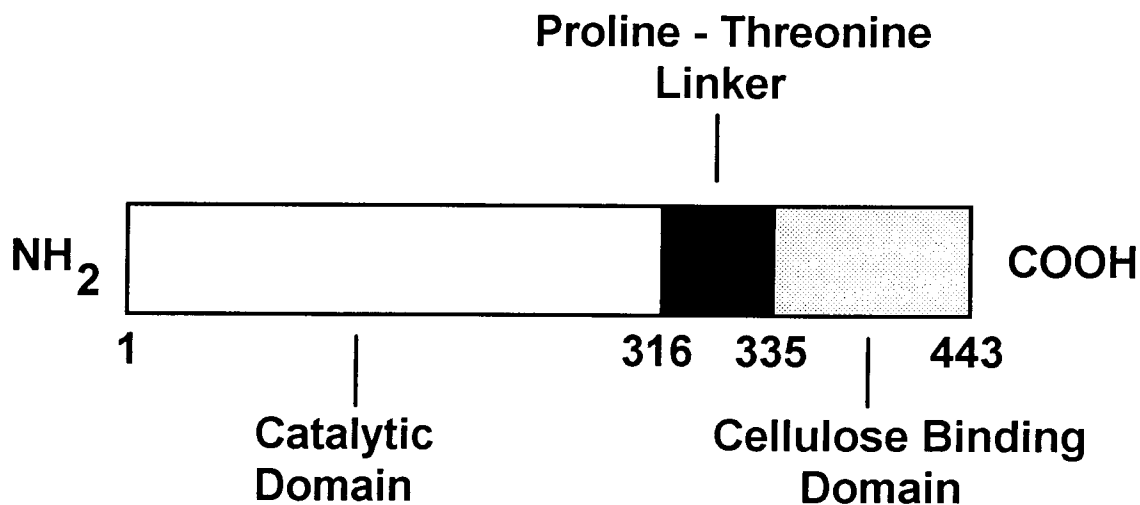


Figure 1.1: Schematic representation of the cellulase exoglucanase from *C. fimi*. The diagram shows the two structurally distinct and independent domains which can be cleaved at the proline-threonine linker.

For example, a genetically engineered β -glucosidase-CBD_{Cex} fusion protein (Ong et al., 1989; Ong et al., 1991) was shown to be as active as the native enzyme and retained more than 40% of the enzyme activity when bound to cellulose. In a cellulose column perfused continuously with substrate, no activity loss was observed over 10 days of operation at 37 °C. In addition, binding to cellulose was stable for prolonged periods of time at temperatures up to at least 70 °C, at ionic strengths from 10 mM to greater than 1 M, and at pH values below 8. Binding could be reversed by distilled water, 1 M NaOH, or 8 M guanidinium HCl.

The CBD technology has been used for the immobilization of enzymes or other proteins, and as an affinity tag for the purification of recombinant proteins using cellulose columns (Kilburn et al., 1992). A genetically engineered Protein A-CBD conjugate has been constructed which is stably bound to paper and dried. The paper strips can then be used to bind antibodies in immunoassays or other diagnostic tests. A conjugate protein was also constructed from CBD and IL-2 with a factor X protease cleavage site in the middle. The conjugate protein can be purified in single step by affinity chromatography on cellulose, and then the IL-2 can be cleaved from the conjugate, either in solution or bound to cellulose. Other proposed applications of the CBD technology include the binding of CBD-conjugated dyes or ink to cellulose-based textiles or paper, and the characterization of cellulose fibre structure using fluorescently labeled CBD.

In the application presented here, the CBD from *C. fimi* exoglucanase (CBD_{Cex}) is chemically conjugated to glucose oxidase using glutaraldehyde. An experimental glucose biosensor is constructed by incorporating a cellulose matrix adjacent to the surface of a platinum electrode, such that the GOx-CBD conjugate can be reversibly immobilized on the electrode. The enzyme is eluted from the cellulose by washing with a suitable elution buffer, and then reloaded using a fresh solution of GOx-CBD conjugate. The enzyme can be loaded and eluted repeatedly in this manner.

1.2 GLUCOSE MONITORING AND CONTROL

1.2.1 Optimization of Bioprocesses

The optimization of the performance of bioprocesses depends on the ability to monitor and control the parameters which describe the bioreactor environment. At present, only a few parameters can be reliably monitored on-line (e.g. temperature, pH, dissolved oxygen tension, stir rate) without the use of highly sophisticated and costly instrumentation. The analysis of fermentation substrates, products, and metabolites is usually achieved by off-line methods (Brooks et al., 1987/88). However, optimal control of a bioprocess requires that measurable parameters be determined as frequently as possible, which in turn requires frequent sampling that increases the risk of contamination (Huang et al., 1991). Furthermore, off-line methods are usually too slow to be used in a closed-loop control system, and it is often difficult to ensure that samples are not significantly degraded or changed during the sampling/analysis procedure. A sensor system based on an *in situ* probe which could provide continuous, real-time analysis would be extremely valuable, particularly for high-density, fed-batch processes. Biosensors have enormous potential (in principle) as *in situ* probes for the analysis of complex fermentation media due to the specificity and selectivity of the biological component of the sensor.

The potential for the development of new feedback control strategies and adaptive control techniques for the optimization of growth rate and protein production in fed-batch processes has motivated research and development of new, reliable, on-line sensors for fermentation monitoring. The economical commercial production of recombinant proteins necessitates the development of engineering strategies for the maximization of the volumetric productivity of expressed products (Hardjito et al., 1993). To do so requires the optimization of gene expression in a high density cell culture. Biochemical engineers have become particularly interested in fed-batch growth techniques because of the

potential to separate the phases of cell growth and cloned-gene expression (Patkar and Seo, 1992) compared to batch or continuous culture. It can be shown that the production of recombinant proteins can be optimized by maximizing the biomass yield on substrate to obtain a high cell density, and then maximizing cell specific productivity through high rates of gene expression. High biomass yield on a given substrate can be obtained by controlling metabolism and minimizing the excretion of inhibitory metabolites through the regulation of substrate level (Smith and Bajpai, 1985). Due to the importance of glucose as the main carbon and energy source for microbial growth in industrial fermentations, it would be desirable to develop a glucose monitoring and control system in order to operate bioprocesses under optimum conditions.

For instance, the specific growth rate of a hybridoma cell line (AFP-27) was found to be directly related to the glucose concentration in continuous culture under glucose-limited conditions (Frame and Hu, 1991). However, in fermentations of the yeast *S. cerevisiae*, cell mass yield has been found to be higher at low glucose concentrations (Patkar and Seo, 1992). At high glucose levels, limitations of the respiratory capacity of certain yeasts results in ethanol production, even under aerobic conditions (Hardjito et al., 1993). Although ethanol produced by the fermentative metabolic pathway can be utilized by cells when glucose is exhausted (diauxic growth), ethanol also inhibits growth and lowers the growth rate. In addition, the fermentation of glucose is inefficient, producing only 2 moles of ATP per mole of glucose (Patkar and Seo, 1992). At low concentrations of glucose in aerobic cultures, glucose is oxidized completely to CO₂ using the respiratory pathway, which produces 16-18 moles of ATP per mole of glucose (Patkar and Seo, 1992). Thus, the increase in cell mass yield at low glucose levels is due to the dominance of the much more efficient respiratory metabolic pathway. Similarly, *E. coli* can be grown to high cell densities by maintaining low glucose concentrations. In a typical batch culture of *E. coli*, glucose ranges from 20 g/l to 0 g/l over a period of 8 hours (Stamm et al., 1992). At high glucose levels, however, depletion of dissolved oxygen due to a high cell

respiration rate, particularly in high cell density cultures, causes a shift to fermentative metabolism. The production of acetate during the fermentative metabolism of glucose limits growth (Smith and Bajpai, 1985). Thus, a fed-batch culture is preferred over batch culture in order to maintain consistently low glucose levels and avoid the effects of fermentative metabolism, thereby achieving high cell density.

Once a high cell concentration has been obtained, the reactor environment can be adjusted to achieve a high protein yield and therefore high production rate. Demain lists a large number of commercially important proteins (e.g. streptomycin, neomycin, penicillin, etc.) which are only expressed during idiophase. These proteins are not expressed during growth because the enzymes responsible for their formation are repressed until the trophophase nears completion (Demain, 1972). In the case of some constitutive promoters, such as CYC1, PGK, and GAPDH, maximum expression is observed during glucose depletion (Hardjito et al., 1993). Patkar and Seo (1992) found that expression of the yeast SUC2 gene was derepressed at glucose levels below 2 g/L, and that there existed an inverse functional relationship between medium glucose concentration and the specific activity of the invertase produced. Some inducible promoters require a high cell density in order for the inducer to accumulate before the gene is derepressed (Demain, 1972). Or, if the inducer is added exogenously, a high cell density may be desired before induction in order to maximize production rate. This may be particularly important for unstable recombinant proteins subject to proteolysis, in which case a high production rate necessitates the minimization of the run time before the product is harvested (Hardjito et al., 1993).

1.2.2 Strategies for Glucose Monitoring and Control

Without a glucose monitoring system to provide continuous, on-line, real-time, glucose analysis of the fermenter medium, efficient control of fed-batch cultures has been

difficult. A number of strategies have been employed to develop feeding schedules for fed-batch culture, such as empirically or mathematically derived models to predict feeding time based on measurable parameters (Smith and Bajpai, 1985). As always, however, certain assumptions must be made in modelling, and an on-line glucose sensor would increase the accuracy of the models by decreasing the number of assumptions necessary. Open-loop control schemes have been developed, using increases in dissolved oxygen or decreases in CO₂ in the reactor off-gases as an indicator of a decrease in the cell respiration rate due to glucose exhaustion. However, cell respiration rate may also decrease if another substrate in the medium becomes limiting, such as ammonium in *E. coli* fermentations.

Some indirect closed-loop strategies have also been investigated. Kole et al., (1986) controlled glucose concentration during a cultivation of *E. coli* based on feedback control of ammonium concentration using an ammonia gas electrode. The ratio of the cellular consumption rates of ammonium and glucose was determined to be 13 moles glucose per mole ammonium, and a corresponding mixture was used to feed the fermenter based on feedback from the ammonium controller. Ammonium and glucose concentrations were maintained at a constant level (15 mM and 8 g/L, respectively) and biomass yield calculated on the basis of glucose or ammonium was increased relative to batch growth. However, acetate production can still be growth inhibiting at a glucose concentration of 8 g/L. In addition, the ammonia electrode required a pH of 11.0 and could not be used *in situ*, requiring a complex hardware system to withdraw and monitor samples from the fermenter in a separate measurement vessel.

Glucose concentration in samples of the medium can be measured directly using off-line enzymatic assays or laboratory glucose analyzers. Numerous enzymatic assays for glucose are commercially available, requiring from 5 to 45 minutes per assay (Sigma, 1993). However, off-line enzymatic assays are not practical for controlling glucose concentration, as the assays are labour intensive and can require up to 1 hour per sample

for the complete procedure of sampling and assay (Patkar and Seo, 1992), thus precluding the use of computerized feedback control systems. Other off-line methods, such as HPLC and gas chromatography, may provide faster assays but are capital intensive and require an experienced operator for instrument set-up and optimization.

Laboratory glucose analyzers, such as the YSI 2300 STAT Glucose and L-Lactate Analyzer (Yellow Springs Instruments, Inc., Yellow Springs, OH, U.S.A.) or the Beckman Glucose Analyzer 2 (Beckman Instruments Inc., Fullerton, CA, U.S.A.) are less expensive and can reduce the assay time to less than 90 seconds, but are difficult to implement on-line. However, Holst et al.(1988) modified a commercially available glucose analyzer (Gambro AB, Lund, Sweden) for use as a glucose monitor during a 3 L cultivation of *E. coli*. The system was completely automated and monitored by computer. Fermenter broth was drawn continuously at 3 mL/min and mixed with metabolic inhibitor to prevent cell-associated changes in glucose concentration during transport to the analyzer. A response time of 6 minutes and a measuring range of 0-5 g/L were reported, and the measured value was updated every 90 seconds. However, the system is complicated, and the sterility of the sampling port and the possibility of influx of metabolic inhibitor into the fermenter were cited as potential problems. Moreover, the consumption of medium by the sampling system could cause a significant decrease in the volume of medium during the course of the fermentation. Recently, Stamm et al. (1992) also reported a modification of the Yellow Springs Instruments YSI 2700 Glucose Analyzer for on-line monitoring of glucose in batch fermentations of *E. coli*. The BIOPEM (Braun, Melsungen, Germany) sampling module was used, which is based on cross-flow membrane filtration of cells from the sample stream, and the filtrate flow rate was 0.5 mL/min. From 4-50 samples could be measured per hour over a linear measuring range of 0.3-25 g/L, with a response time of 4 minutes.

Numerous other automated sampling systems have been published (Mandenius et al., 1984; Romette, 1987; Bradley et al., 1991). In addition, the use of flow injection

analysis (FIA) in conjunction with sampling devices and off-line substrate analyzers has seen rapid development for on-line fermentation monitoring in recent years (Kittsteiner-Eberle et al., 1989; Valero et al., 1990; Huang et al., 1991; Renneberg et al., 1991; Bradley et al., 1991). FIA is characterized by precisely controlled injection of samples into a carrier stream which flows to a detector. The advantages are low sample consumption, dilution of the analyte in the carrier stream (which can be adjusted by varying the flow rate of the carrier), high frequency of analysis, and flexibility and adaptability of the monitoring system due to the typically modular construction. Some of the inherent disadvantages of off-line sample analysis that are often cited, however, include discontinuous measurement, depletion of the medium volume, and increased risk of fermenter contamination. The presence of dead volume in the sampling system also slows response time and allows for changes in the composition of the sample during transport to the detector. In addition, a high degree of automation and extra hardware (e.g. detector(s), pumps, valves, tubing, etc.) is required, which often necessitates a trained or experienced operator to optimize the system.

The advantages and disadvantages of automated sampling systems in contrast with *in situ* probes have been discussed in the literature (Ogbomo et al., 1990; Bradley et al., 1991; Filippini et al., 1991; Lüdi et al., 1992; Cleland and Enfors, 1983). It is generally agreed that *in situ* probes would be the more desirable approach, provided such devices can be made to operate reliably under the conditions and constraints imposed by current bioprocess designs. A sensor system based on an *in situ* biosensor probe has the potential to provide continuous, real-time analysis of complex fermentation media due to the specificity and selectivity of the biological component of the sensor.

1.2.3 *In situ* Enzyme Electrode Probes

Numerous electro-enzymatic biosensor probes have been reviewed and described (Enfors and Molin, 1978; Turner et al., 1987; Mascini and Palleschi, 1989; Guilbault and Luong, 1989; Hendry et al., 1990; Bradley et al., 1991; Moody and Thomas, 1991), and a wide variety of analytes could be monitored using different enzyme-based systems, as shown in Table 1.1. Unfortunately, the practical concerns of using an *in situ* biosensor probe, such as *in situ* sterilizability, long-term stability, adequate measuring range, and membrane fouling, have thus far prevented the widespread application and commercialization of this approach. However, these difficulties are not viewed as insurmountable, and some *in situ* enzyme electrode probes have been used to monitor glucose concentration for limited periods of time during cultivations of Baker's yeast (Bradley et al., 1988, 1989, 1991), *Candida utilis* (Enfors, 1981), and *Escherichia coli* (Cleland and Enfors, 1983, 1984b; Brooks et al., 1987/88).

For fermentation applications, *in situ* enzyme electrode probes in general should have the following characteristics:

1. The measuring range of the sensor must be sufficient to cover the range of analyte concentration encountered in the fermenter, with adequate sensitivity over the working range.
2. The sensor response time must be sufficiently fast to monitor changes in the analyte concentration and permit process control.
3. The sensor must be insensitive to changes in the chemistry of the medium, such as dissolved oxygen tension, pH, and ionic strength.
4. The sensor system must be resistant to electrochemical and enzymatic poisons, inhibitors, interferents, etc. in the analyte medium.
5. The sensor system should allow for re-calibration during fermenter operation. Periodic re-calibration is desirable in order to correct for changes in the

calibration constants of the sensor which may occur during a fermentation due to fouling, poisoning, deactivation, or other internal chemical changes in the probe (Kok and Hogan, 1987/88).

6. Sufficient long-term stability of the enzyme component of the sensor is necessary in order to be useful in a typical fermentation. This may dictate that periodic recalibration of the sensor is required if the enzyme activity diminishes. Alternatively, this may require the capacity for replacement of the enzyme component when the activity has degraded to an unsatisfactory level. This regeneration of the probe must be possible without interrupting the fermentation.

7. *In situ* sterilization of the probe by conventional methods, such as autoclaving, must be possible. Steam sterilization is preferred by industry over other sterilization methods, such as ethanol, chloroform, radiation, etc..

The implementation and commercialization of *in situ* enzyme-based biosensors for bioprocess control has been particularly slowed by problems relating to the *in situ* sterilizability of the probe and the stability of the enzyme component. These problems have been addressed in a variety of ways by other investigators over the past 15 years.

Enfors and Molin (1978), and Enfors and Nilsson (1979) reported an autoclavable enzyme electrode consisting of a potentiometric transducer in a stainless steel housing with a dialysis membrane. The bioreactor and the probe hardware were steam sterilized *in situ*, after which a solution of enzyme was pumped into the enzyme chamber formed by the transducer, the electrode housing, and the dialysis membrane. When the activity of the enzyme had diminished, the enzyme chamber could be perfused with fresh enzyme solution, however the sensor could not be recalibrated using internal standards pumped into the enzyme chamber or the enzyme would be washed out. Furthermore, it is difficult to concentrate the enzyme activity in a region near the surface of the indicating electrode,

leading to excessive H_2O_2 generation throughout the interior of the probe and potential problems due to H_2O_2 accumulation.

Cleland and Enfors (1983) envisaged a probe consisting of a stainless steel housing and a dialysis membrane which could be autoclaved *in situ*. The enzyme would be immobilized on an internal electrode which would then be inserted into the sterilized housing. A sterile barrier between the bioreactor medium and the electrode would be maintained by the dialysis membrane. Cleland and Enfors (1984a, 1984b) also designed an internally buffered enzyme electrode where buffer flowed continuously through the enzyme chamber. The buffer flow across the dialysis membrane provided continuous dialysis of the analyte and permitted variation of the sensor's working range by altering the buffer flow rate. However, the enzyme could not be replaced without dismantling the hardware, which would presumably be difficult to automate.

Bradley et al. (1988, 1989a, 1989b, 1990, 1991) and Brooks et al. (1987/88) reported an autoclavable enzyme electrode with provisions for internal calibration and rapid replacement of the enzyme. The stainless steel sensor housing and dialysis membrane were sterilized *in situ*, after which the internal electrode was inserted. The internal electrode consisted of a shaft with graphite discs for electrodes. The enzyme was immobilized on the graphite discs. A flow of buffer through the enzyme chamber could be maintained if desired, and the sensor could be calibrated internally by pumping calibration standards into the enzyme chamber. Rapid enzyme replacement was performed when required by removing the internal electrode and exchanging the graphite discs. However, it was necessary to carry out the process of enzyme replacement manually.

Bühler and Ingold (1976) designed a mechanically retractable probe that could be isolated from the fermenter completely by a ball valve. The probe could be cleaned, recalibrated, modified, or replaced entirely, without compromising the fermentation, and then re-sterilized with steam before re-introduction to the fermenter. Kok and Hogan (1987/88) described an *in situ* electrode calibrator, which isolated the probe tip from the

fermenter broth using two half-cylinders forced together around the probe pneumatically to form a small chamber. The external surface of the sensor membrane could be cleaned by washing or spraying with a jet of cleaning solution, and calibration solutions could be injected into the chamber to recalibrate the sensor. The probe tip was then re-sterilized with steam before re-exposing to the fermenter medium.

In the probe designs described above, the combined functions of enzyme replacement and recalibration of the sensor cannot be performed without operator intervention. Thus, an operator must be standing by during a long fermentation run to manually replace the enzyme component periodically and then recalibrate the sensor. The regenerable biosensor probe developed in this thesis incorporates the essential characteristics of the probes described above, but the hardware system is relatively simple and the enzyme component can be replaced when necessary using computer-controlled pumps and valves. This enables automated, *in situ* replacement of the enzyme component periodically during a long fermentation, without interrupting the fermentation or dismantling the sensor. Furthermore, a single "generic" probe body can, in principle, be used to implement a variety of different electro-enzymatic sensors, based on different enzymes and/or transducers. The design and principle of operation of the proposed sensor system is described in Chapter 2.

CHAPTER 2

BACKGROUND AND THEORY

2.1. INTRODUCTION

In general, the design and operation of enzyme-based biosensors capitalizes on biochemical reactions involving the species of interest, (i.e., the analyte) which are catalyzed by naturally occurring biological molecules called enzymes. Usually, the analyte is a substrate or co-substrate of the enzyme reaction. In the case of enzyme electrodes, the sensor operation is based on the electrochemical determination of reactant(s) or product(s) associated with the enzyme reaction. The advantage of incorporating the enzyme component in the biosensor is that the natural specificity of the enzyme for the analyte is imparted to the sensor, thus the biosensor can be used for analyte determination in typically complex biological solutions. In addition, enzymes are able to catalyze reactions faster than many non-biological catalysts in the temperature and pH range normally encountered in biological environments (Bailey and Ollis, 1986). The combination of the chemical signal amplification due to enzyme catalysis and the high sensitivity inherent to electrochemical detectors results in a highly sensitive enzymatic sensor.

2.2. ENZYME ELECTRODE COMPONENTS

A schematic diagram of a typical glucose sensitive enzyme electrode is shown in Figure 2.1. The approach used here is based on the amperometric detection of hydrogen peroxide produced as a by-product of the enzymatic oxidation of glucose by glucose oxidase. A potentiostat is used to maintain the necessary bias potential for the electrochemical oxidation of hydrogen peroxide at a noble metal indicating electrode, and

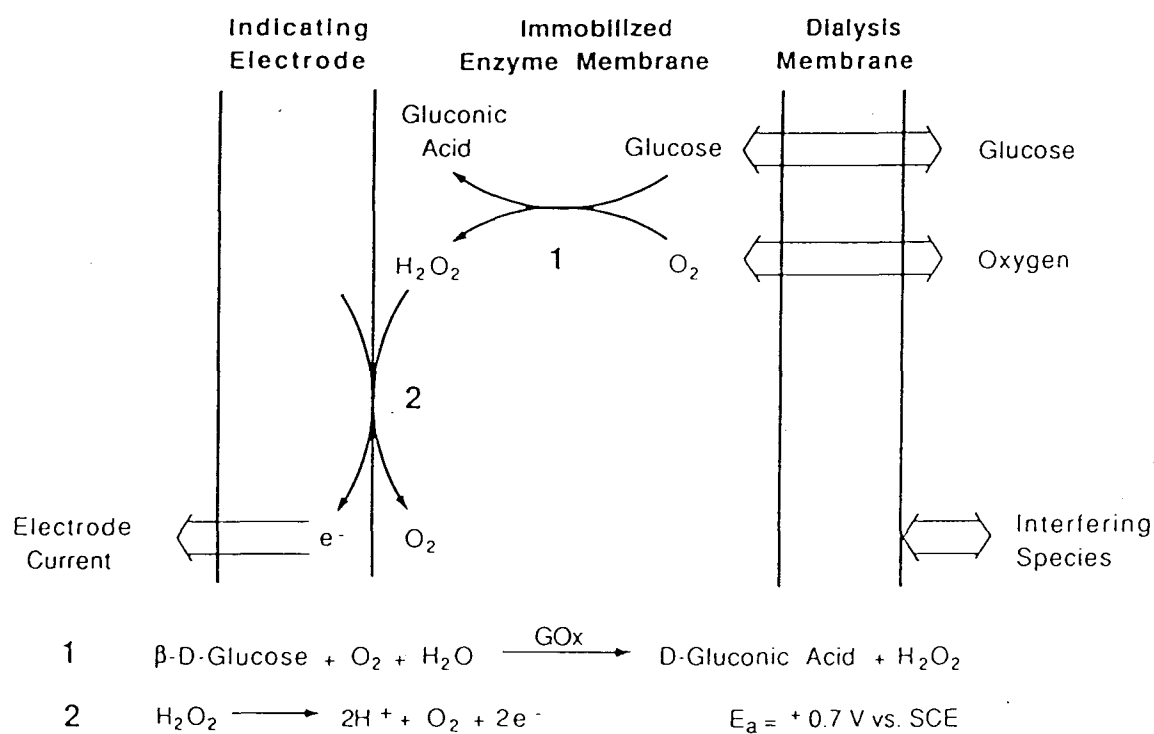


Figure 2.1: Schematic diagram of a glucose sensitive enzyme electrode. The basic components of the sensor hardware and the principle biochemical and electrochemical reactions are shown.

also converts the glucose-dependent electrode current into a useable output voltage. The enzyme is immobilized in a gel or thin film, (the enzyme membrane) in close proximity to the surface of the indicating electrode, which is typically platinum, gold, or carbon. In this case, the indicating electrode is platinum. One or more dialysis or covering membranes are normally used over the enzyme membrane. Glucose and oxygen diffuse into the enzyme layer and react with the enzyme to produce gluconic acid and hydrogen peroxide. Some of the hydrogen peroxide diffuses to the electrode where it is oxidized electrochemically, liberating oxygen, protons, and electrons. Thus, the current measured at the indicating electrode is related to the concentration of the analyte in the bulk solution.

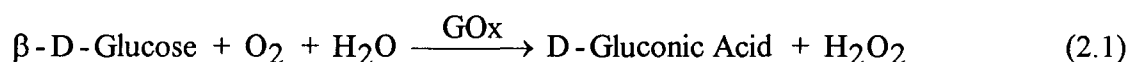
The outer membrane of the sensor is very important, as it represents the interface between the biosensor and the analyte medium. The purpose of the dialysis membrane is to allow the diffusion of glucose, oxygen and electrolytes into the enzyme layer while excluding potential interfering species which may be present in the analyte medium, such as cells, proteins, enzyme inhibitors, or electrochemical interferents. The dialysis membrane also provides a significant mass transfer resistance which increases the linearity of response and the working range of the sensor, although at the expense of sensitivity. Selectively permeable membranes can be used to increase the mass transfer of oxygen with respect to glucose, thereby minimizing the possibility of oxygen limitation of the biosensor. A covering membrane may also be used to protect the physical integrity of the enzyme membrane.

2.3. BIOCHEMICAL CONSIDERATIONS

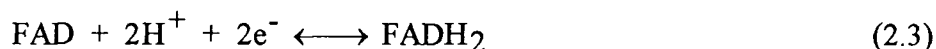
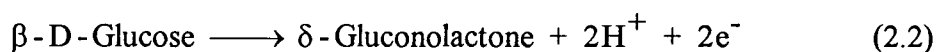
The enzyme glucose oxidase (β -D-glucose:oxygen 1-oxido-reductase, EC 1.1.3.4) belongs to a class of enzymes called flavoprotein oxidases. Most studies are performed using the enzyme from *Aspergillus niger*, although the enzyme from *Penicillium*

amagasakiense or *Penicillium notatum* has been used. Glucose oxidase from *A. niger* is a dimer with two tightly bound FAD molecules per dimer. The tertiary structure of glucose oxidase from *A. niger* was recently reported by Hecht et al. (1993). Molecular weights between 155 and 186 kD have been reported for this enzyme by different sources, but a value in the range of 155 kD is most common. The physical properties and the enzyme kinetics of glucose oxidase have been studied extensively and can be found in standard texts on enzymology (Bright and Porter, 1975; Dixon and Webb, 1964).

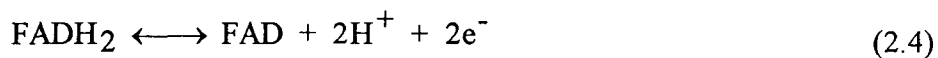
The glucose oxidase catalyzed reaction of glucose is often presented in a single step:



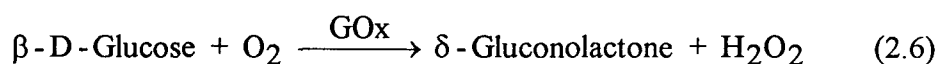
The reaction shown above is actually a net reaction which consists of two redox steps and a non-enzymic hydrolysis step. The electron transfer path is from the electron donor (glucose) to the coenzyme flavin adenine dinucleotide (FAD), and then to an electron acceptor. The first redox step involves the oxidation of glucose by glucose oxidase and the reduction of the coenzyme FAD:



The second redox step involves the reduction of FADH₂ and the transfer of electrons to the electron acceptor:



In this case, oxygen plays the role of electron acceptor. The summation of the two redox steps yields:



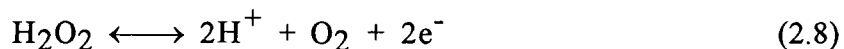
The δ -gluconolactone undergoes a spontaneous hydrolysis reaction given by:



The sum of Equations 2.6 and 2.7 gives the overall net reaction given in Equation 2.1.

2.4. ELECTROCHEMICAL CONSIDERATIONS

Some of the hydrogen peroxide produced by the enzymatic oxidation of glucose in the enzyme layer diffuses to the surface of the indicating electrode and is oxidized electrochemically according to the reaction:



The standard electromotive force (emf) of the half-cell reaction in Equation 2.8 is $E^\circ = +0.695 \text{ V}$ versus the standard hydrogen electrode (SHE) at pH 0. At pH 7, the

standard emf is shifted by approximately -0.410 V. At an electrode potential that is slightly more positive of the standard emf, the reaction becomes spontaneous, although it may be kinetically limited. To ensure that the electron transfer at the anode occurs at the maximum rate, i.e., that the electrochemical reaction is diffusion limited rather than kinetically limited, an electrode bias potential of +0.94 V versus SHE is normally applied. Under diffusion limited conditions, the current measured at the indicating electrode will be proportional to the concentration of hydrogen peroxide.

The saturated calomel electrode (SCE) or the silver/silver chloride (Ag/AgCl) electrode are typically used as reference electrodes as the SHE reference is rather inconvenient. However, the standard emf of each these half-cell reactions is different. The emf of the SHE is taken to be 0 V by convention. The half-cell reactions are given below.:



Thus, the normal operating electrode bias potential for most biosensor applications using the principle of operation above is approximately +0.7 V versus saturated calomel or Ag/AgCl reference electrodes. A comprehensive treatment of electrochemical considerations can be found in standard texts on electrochemistry (Bard and Faulkner, 1980; Sawyer and Roberts, 1974).

2.5. MODELLING CONSIDERATIONS

In this thesis, all of the experimental results were empirical and no attempt at modelling was undertaken. However, the study of modelling theory is worthwhile for a clearer understanding of the behaviour of electro-enzymatic biosensors and the processes that determine biosensor performance. Due to the small physical dimensions and other geometric considerations of enzyme electrodes, it is generally not possible to measure concentrations and fluxes of substrates and products within the membrane layers of these sensors. For this reason, mathematical modelling has become an important tool to analyze and improve the performance of enzyme electrodes. Ideally, a successful mathematical model should predict the measuring range, sensitivity, response time, and detection limit of a given sensor configuration. The model can then be used to evaluate variations in parameters such as membrane thickness and immobilized enzyme activity (enzyme loading) with the aim of improving the analytical characteristics of the sensor. Trial and error experiments to improve these sensor characteristics have produced what often seem like conflicting results (Fortier et al., 1990; Foulds and Lowe, 1986). Hence, the combination of modelling and experimental research can lead to a more directed development effort.

Theoretical studies of immobilized enzyme electrodes are complicated by the non-linear nature of the enzyme kinetics and the mass transport processes. The overall mechanism is categorized as a diffusion-reaction problem, which is described by a set of non-linear, partial differential equations that can be solved analytically or numerically. The overall process may be diffusion controlled or kinetically controlled. Most published models are one layer models and consider only the immobilized enzyme layer, although real sensors almost always employ one or more additional membrane layers which increase the mass transport resistance. Consideration of the effects of covering membranes in

terms of diffusion retardation and modification of the effective permeabilities of substrate and co-substrate is presented in Section 2.5.5.

A general model applicable to all sensor arrangements cannot normally be formulated due to the number of special cases that can exist. Furthermore, it is necessary to weigh the advantages of a complex model with high integrity that accounts for many of the physical phenomena, against the convenience and simplicity of a more approximate yet qualitative model (Schulmeister, 1990). The intended application of the model must be held in mind throughout its development. Once a basic model has been well developed, the features of more complex sensor systems can be incorporated into the model.

The type and complexity of the model to be used also depends on whether the principle of measurement is transient or steady-state. When the transient response of the sensor to a step change is followed, the result is very rapid and very sensitive, and the model can also be used to estimate the time to approach steady-state. However, the modelling is much more difficult because of the system of differential equations which must be solved. If the response is allowed to reach steady-state, then the time derivatives of the differential equations are zero and a system of algebraic equations results.

The models presented here will be limited to monoenzyme electrodes, specifically the glucose oxidase electrodes for glucose determination. The co-substrate is oxygen. Mediated enzyme electrodes and other modified enzyme electrodes are not considered. Amperometric electrodes are of primary interest, however the same reaction rate and diffusion equations are employed to describe amperometric and potentiometric systems but different initial and boundary conditions for the solution of the resulting partial differential equations are used. For potentiometric electrode sensors, the concentrations of substrate and product at the electrode surface are permitted to vary, but the flux of both substrate and product must be zero. For amperometric sensors, the flux of the electroactive species to be determined is non-zero at the electrode surface, due to the electrochemical reaction which occurs (Janata, 1989; Leyboldt and Gough, 1984).

Similarly, the mode of operation of the amperometric sensor can be based on detection of co-substrate (oxygen) or product (hydrogen peroxide); the observations and results are qualitatively similar (Leypoldt and Gough, 1984).

2.5.1. Assumptions and Approximations

The following are typical assumptions and approximations made in the modelling literature involving enzyme electrodes for glucose:

1. At the boundaries of a given membrane, the Dirichlet condition applies. That is, the boundary values for all substances are equal to the concentration values on the opposite side of the interface (Schulmeister, 1990). This is generally true if the partition coefficient is equal to one. See assumption number 2.

2. No partitioning of reactants and products occurs between the membrane and the solution. However, this may not always be true. For example, Maresse et al. (1987) found that the partition coefficient for potassium ferrocyanide was greater than one for albumin-glutaraldehyde membranes.

3. Reactions occurring on the external surface of the membrane are unimportant in comparison with the reactions occurring within the membrane. The contribution from the reactions at the external surface only becomes important in the limit where the reactions are extremely fast compared to the rate of diffusion (Schulmeister, 1990).

4. The bulk solution is assumed to be perfectly stirred and acts as an infinite reservoir of substrate if the volume is great enough (Schulmeister, 1990; Jochum and Kowalski, 1982). Thus, the bulk solution concentration of substrate is assumed to be constant.

5. The concentration gradients within the enzyme layer can be assumed to be linear (Leypoldt and Gough, 1984). In actual fact, the concentration gradients are curvi-

linear, however, for the purposes of numerical analysis, the gradients may be approximated as linear if a sufficiently small step size is used.

6. The diffusion process can be reduced to one spatial dimension. Thus, a planar electrode is approximated as semi-infinite and edge effects are ignored (Janata, 1989). Cylindrosymmetrical electrodes can be reduced from two spatial dimensions (axial and radial) to one spatial dimension if the ratio of the diameter of the sensor surface to the thickness of the enzyme membrane is large (Schulmeister, 1990).

7. No depletion layer exists at the membrane/solution boundary if the solution is stirred rapidly. However, there exists a stagnant boundary layer even under stirring. This thin layer (10^{-3} - 10^{-1} mm depending on viscosity and stir rate) (Schulmeister, 1990) is often ignored since the diffusion in solution is rapid compared to diffusion in the membrane. Nevertheless, a shallow depletion layer can exist within the stagnant boundary layer.

8. The immobilized enzyme is uniformly distributed in a homogeneous membrane. Thus the mass transport and kinetic parameters are constant at all points in the membrane. Membrane homogeneity is important to the model for simplicity and is assumed in all the published models. A heterogeneous membrane would be extremely complex to model because of the variation of parameters at every point in the membrane. However, the validity of the assumption of homogeneity of the immobilized enzyme membrane is an important issue with some uncertainty.

9. The long-time processes of enzyme inactivation can be ignored (Schulmeister, 1990). This is a reliable assumption over the time period of a single measurement and when enzyme loading is high.

10. The rates of protonation reactions are assumed instantaneous. This is a safe assumption on the time scale of the other processes in the overall mechanism (Janata, 1989).

11. The electrochemical double-layer which exists within the membrane at the electrode surface is ignored. The electron transfer processes at the electrode surface are also considered to be fast compared to the membrane processes.

2.5.2. Diffusion Equations

The enzyme electrode is often considered as a series of resistances (Janata, 1989):

1) The resistance to charge transfer at the working or indicating electrode; 2) the resistance to mass transport; and 3) the resistance to charge transfer at the auxiliary or counter electrode. Normally, the counter electrode area is much larger than the indicating electrode area, so the resistance to charge transfer at the counter electrode is negligible. Furthermore, the electron transfer reaction at the indicating electrode is considered to be fast compared to the processes which occur in the membrane, so the resistance at the indicating electrode is generally neglected as well. The mass transport resistance can be subdivided into: 1) The external mass transport resistance, which occurs at the solution/membrane interface; and 2) the internal mass transport resistance, which occurs within the membrane (Cronenberg and van den Huevel, 1991, Hall, 1991). Furthermore, the process of mass transport occurs by the three mechanisms of diffusion, migration, and convection, and can be described by the Nernst-Planck equation. For a species i :

$$J_i = -D_i \frac{dC_i}{dx} - z_i F U_i \frac{d\phi}{dx} + C_i (v_x) \quad (2.12)$$

The first term is the diffusion term and is usually the only current limiting term. The second term is for migration and is considered negligible, if there exists an excess of inert electrolyte, or constant, if the electric field in the membrane is constant at a given potential. The third term is the convection term and is also considered constant when the

electrode is rotating or vibrating, or it is assumed negligible in the membrane layer (Schulmeister, 1990).

Mass transfer in the bulk solution is generally considered to be quite fast compared to mass transfer in the membrane because of the higher diffusion coefficients in the solution and because of stirring. Thus, only the internal mass transfer resistance is usually considered. Within the membrane, the Nernst-Planck equation reduces to Fick's law:

$$J_{d,i}(x,t) = -D_{m,i} \frac{\partial c_i(x,t)}{\partial x} \quad (2.13)$$

Normally, $x = 0$ at the electrode surface and $x = L$ at the membrane/solution interface, where L is the thickness of the enzyme membrane.

2.5.3. Enzyme Reaction-Rate Equations

Let the enzyme reaction rate be given by $R(S,O)$ for substrate, S , and oxygen, O . Most commonly, the published models assume Michaelis-Menten enzyme kinetics, described by the rate equation:

$$V = \frac{V_{\max} S}{K_m + S} \quad (2.14)$$

where V is the enzyme reaction rate, V_{\max} is the maximum reaction rate, and K_m is the Michaelis constant for the enzyme (Bailey and Ollis, 1986). In the special case that oxygen is present in excess and the glucose concentration is low, the reaction can be considered first-order and the reaction rate can be modelled linearly (Bailey and Ollis,

1986). This assumption holds when the substrate concentration is much less than the Michaelis constant, that is, $S^0 \ll K_m$. Therefore Equation 2.1 reduces to:

$$V = kS = R(S) \quad (2.15)$$

$$\text{where } k = \frac{V_{\max}}{K_m}$$

One-substrate models have been successful in simulating the calibration curves for two-substrate enzyme electrodes when the co-substrate concentration is always close to the saturation value, such that the substrate is the limiting reagent in the reaction. However, the response at lower co-substrate concentrations demonstrates unusual behaviour that cannot be predicted by the one-substrate models (Leypoldt and Gough, 1984). The characteristic, two-substrate rate expression used is the non-linear, Ping-Pong reaction rate equation (Schulmeister, 1990; Leypoldt and Gough, 1984; Ylilammi and Lehtinen, 1988; Bailey and Ollis, 1986):

$$R(S, O) = \frac{V_{\max}(S)(O)}{(O)(S + K_s) + K_o S} \quad (2.16)$$

$$\text{or, } R(S, O) = \frac{V_{\max}}{1 + \frac{K_s}{S} + \frac{K_o}{O}} \quad (2.17)$$

The concentration of oxygen remains a parameter in the rate expression, and the oxygen concentration will be included in the glucose-dependent current, i_g . The values of K_s and K_o for glucose oxidase are typically 0.11 M and 5×10^{-4} M, depending on the data source (Linek et al., 1980). In the case where the substrate concentration is low and oxygen is present in excess, then $K_s/S \gg K_o/O$ and Equation 2.1 becomes:

$$R(S) = \frac{V_{\max}}{K_s} S = kS \quad (2.18)$$

$$\text{if } k = \frac{V_{\max}}{K_s} \quad (2.19)$$

The Ping-Pong rate expression reduces to the first-order reaction rate equation once again.

If Michaelis-Menten kinetics are assumed for the enzyme reaction rate, then the typical kinetic parameters which must be determined are the maximum rate, V_{\max} , and the Michaelis constant, K_m , for the substrate. However, the kinetic parameters for the immobilized enzyme are not necessarily the same as for the soluble enzyme. For that matter, the use of Michaelis-Menten kinetics for the immobilized enzyme may be invalid, since the Michaelis-Menten model is defined for a homogeneous and mobile (i.e., soluble) system. However, the Michaelis-Menten model fits the experimental data well and is used for its simplicity. In the case of an amperometric enzyme electrode, the sensor current is often taken to be representative of the enzyme rate since the electron transfer at the electrode is relatively fast and the electrochemical reaction can be ignored. The parameter V is replaced by I in the Michaelis-Menten equation (Equation 2.14) and the sensor current and substrate concentration data are used to determine the enzyme kinetic parameters. The Michaelis-Menten equation becomes:

$$R(S) = I = \frac{I_{\max} S}{K'_m + S} \quad (2.20)$$

However, the kinetic parameters that are determined must be denoted as "apparent" kinetic parameters, I_{\max} and K'_m , because any unresolved mass transfer resistances are

included in the apparent kinetic parameters (Leypoldt and Gough, 1984). I_{\max} comprises terms that include the amount of enzyme activity immobilized in a given sensor configuration. The parameter K_m' includes the characteristic Michaelis constant of the enzyme as well as any unresolved mass transport resistances of the given sensor configuration (e.g. choice of covering membrane system, immobilization method, and sensor geometry).

However, the kinetic parameters need not necessarily be known explicitly. The approach suggested by Leypoldt and Gough (1984) and supported by Schulmeister (1990) is to determine the mass transfer properties of each substrate without reaction using a membrane covered disk electrode. Then, measuring known substrate concentrations using a given sensor and drawing a calibration curve, the unknown kinetic parameters can be determined by fitting an appropriate model to the calibration curve using a non-linear least-squares fit. The parameters determined can be used repeatedly for the given sensor, as long as the calibration curve is unchanged. The method is useful for characterizing individual electrodes, since the immobilized enzyme membranes cannot be reproduced with very high precision and it becomes difficult to analyze their exact dynamics using general values for parameters.

It should be noted that if the substrate concentration is high, that is, S/K_m is large, then Michaelis-Menten kinetics predict that the reaction rate becomes zero-order:

$$R = V_{\max} \quad (2.21)$$

The reaction rate is independent of the substrate concentration and becomes a function of the number of active sites of immobilized enzyme (Tran-Minh and Broun, 1975). Thus, the enzyme electrode is not useful if the substrate concentration in the interior of the enzyme membrane greatly exceeds K_m because the sensor signal essentially becomes independent of bulk solution substrate concentration S^0 in this regime.

2.5.4. The General Modelling Approach

The total rate of change of concentration of reactants and products in the enzyme layer is represented as the sum of the diffusion term and the reaction term:

$$\frac{\partial c_i(x,t)}{\partial t} = \frac{\partial J_{d,i}(x,t)}{\partial x} \pm R(S,O) = -D_{m,i} \frac{\partial^2 c_i(x,t)}{\partial x^2} \pm R(S,O) \quad (2.22)$$

The following system of equations results:

$$\frac{\partial c_s(x,t)}{\partial t} = -D_{m,s} \frac{\partial^2 c_s(x,t)}{\partial x^2} - kS \quad (2.23)$$

$$\frac{\partial c_p(x,t)}{\partial t} = -D_{m,p} \frac{\partial^2 c_p(x,t)}{\partial x^2} + kS \quad (2.24)$$

$$\frac{\partial c_o(x,t)}{\partial t} = -D_{m,o} \frac{\partial^2 c_o(x,t)}{\partial x^2} - kS \quad (2.25)$$

where S is for substrate (glucose), P is for product (hydrogen peroxide) and O is for oxygen. This system of equations can be solved using the appropriate initial and boundary conditions. At time $t = 0$, the bulk solution concentration of substrate is S^0 and the product concentration, P^0 , is zero. In the membrane, substrate and product concentrations are also zero. The membrane is assumed to be saturated with oxygen. At time $t > 0$, the sensor is immersed in the analyte solution. Substrate molecules diffuse into the enzyme layer and react with the enzyme. Product molecules diffuse throughout the enzyme layer. Since amperometric electrodes are operated with an applied potential on the diffusion-limiting plateau, all of the electroactive species reaching the electrode are

reacted and the surface concentration is effectively zero. These conditions can be expressed as follows:

At the solution/membrane interface and for all time t :

$$C_s(L,t) = S^0 \quad (2.26)$$

$$C_p(L,t) = 0 = P^0 \quad (2.27)$$

$$C_o(L,t) = C_o^* = O^0 \quad (2.28)$$

For all x such that $0 \leq x \leq L$ and time $t = 0$:

$$C_s(x,0) = 0 \quad (2.29)$$

$$C_p(x,0) = 0 \quad (2.30)$$

$$C_o(x,0) = \alpha_o C_o^* \quad (2.31)$$

For an amperometric, product sensitive electrode, at all time t :

$$C_p(0,t) = 0 \quad (2.32)$$

$$\frac{\partial c_s(0,t)}{\partial x} = 0 \quad (2.33)$$

$$\frac{\partial c_o(0,t)}{\partial x} = 0 \quad (2.34)$$

The conditions for oxygen detection mode are qualitatively similar.

The goal of the model is to determine the glucose dependent current, i_g . In the product sensitive case, the number of ion equivalents, n_p , reaching a unit area of the electrode is:

$$n_p = -D_p \frac{dP}{dx} \quad (2.35)$$

The resulting anodic current is:

$$i_g(t) = z F A D_{m,p} \frac{\partial c_p(0,t)}{\partial x} \quad (2.36)$$

where z is the number of charge equivalents per mole, F is the Faraday constant, and A is the electrode area. The sensor current can be obtained by solving the system of partial differential equations for the product flux at the electrode surface and substituting into Equation 2.36. The details of the numerical solution will not be presented here, but the resulting product flux is a function of the concentration of substrate in the bulk solution, S^0 . Hence, the anodic current is also a function of bulk solution substrate concentration.

2.5.5. Multi-layer Modelling

Linear one-layer models are able to describe quite well the dynamic behaviour of real arrangements and are often sufficient, but multi-layer models are necessary for greater accuracy (Schulmeister, 1990). A multi-layer model may be suitable in the following situations:

1. The bulk solution cannot be considered well-stirred. A two-compartment model is often used in this case, where the bulk solution is considered to be one compartment and the enzyme membrane layer is the second compartment (Jochum and Kowalski, 1982).
2. A front membrane, such as a dialysis membrane, is employed to stabilize the enzyme membrane.

3. The sensor uses selective layers which are permeable to the desired substance(s) but impermeable to others. Selective layers can increase selectivity, enhance the diffusion of oxygen over glucose, or provide protection for the metal surface of the electrode or the enzyme (Schulmeister, 1987).

4. The model includes the effects of the boundary layer at the membrane/solution interface and the internal electrolyte layer at the electrode surface.

The usual system of reaction-diffusion equations and initial and boundary conditions is used. In the model by Schulmeister (1987), a number of layers, l , are imagined, where $i = 1$ to l and each layer i has width d_i . The mathematical problem is that the boundary conditions at the interface of each layer are unknown. Schulmeister proposes a boundary function for substrate, S , and product, P , at each interface that is defined as:

$$S_i^*(t) = S_i(d_i, t) = S_{i+1}(0, t) \quad (2.38)$$

$$P_i^*(t) = P_i(d_i, t) = P_{i+1}(0, t) \quad \text{for } i = 1 \text{ to } l - 1 \text{ and } t > 0 \quad (2.39)$$

Conservation of mass at each interface requires that:

$$D_{s,i} \left(\frac{\partial S_i}{\partial t} \right) = D_{s,i+1} \left(\frac{\partial S_{i+1}}{\partial t} \right) \quad (2.40)$$

$$D_{p,i} \left(\frac{\partial P_i}{\partial t} \right) = D_{p,i+1} \left(\frac{\partial P_{i+1}}{\partial t} \right) \quad (2.41)$$

The conservation of mass equations are used to solve for the boundary function at each i and t . Thus for each interval of time, the concentration profiles must be approximated for all i successively, because the values of $S_i^*(t)$ and $P_i^*(t)$ are needed for

the next time step. The multi-layer model was fitted to current-time data obtained from a commercial glucose analyzer with a three-layer membrane arrangement. The three-layer model yielded very good fits and could be implemented on a personal computer (Schulmeister, 1987).

2.6. PRINCIPLE OF OPERATION

Figure 2.2 is a schematic diagram of a biosensor based on CBD-immobilized enzymes. The basic design consists of a platinum electrode, a porous cellulose matrix, and a protective dialysis membrane, all incorporated into a stainless steel probe for insertion into the bioreactor. Inlet and outlet tubes in the probe body allow for perfusion of the cellulose matrix with the enzyme-CBD conjugate solution and the elution buffer. The internal electrode can be raised to permit complete perfusion of the cellulose matrix and then lowered into contact with the immobilization matrix to facilitate substrate monitoring.

The concept is similar to that employed in the commercial CO₂ electrode from Ingold (Ingold, 1990). In this work, a prototype glucose biosensor is built from a modified Ingold CO₂ probe. For operation as a glucose sensor, the probe requires a glucose-permeable outer membrane, a cellulose matrix, and a custom - built internal electrode assembly with three electrodes for amperometric operation. The cellulose matrix for immobilization of the enzyme-CBD conjugate is enclosed in the enzyme chamber formed by the probe body, the dialysis membrane, and the internal electrode unit. The internal electrode unit can be raised and lowered via a threaded shaft. When necessary, the internal electrode unit is raised and the enzyme is eluted by perfusing the cellulose matrix with a suitable elution buffer (e.g. distilled water, sodium hydroxide, or guanidine hydrochloride), followed by perfusion with soluble GOx-CBD conjugate to replace the immobilized enzyme. For glucose monitoring, the internal electrode is lowered such that the cellulose matrix is sandwiched between the dialysis membrane and the

platinum indicating electrode. The enzyme chamber is filled with electrolyte which equilibrates with the electrolyte of the external analyte solution.

Figure 2.3 outlines the principle of operation of the sensor system for continuous fermentation monitoring. The entire probe, exclusive of the enzyme, is sterilized *in situ* during steam sterilization of the fermenter and contents. Following sterilization, the enzyme is loaded into the sensor by perfusion of the cellulose matrix with soluble GOx-CBD conjugate, resulting in immobilization of the enzyme (behind the sterile barrier provided by the dialysis membrane) via attachment of the CBD. The sensor is calibrated during the addition of glucose to the fermenter. Periodically during the fermentation, the sensor calibration can be checked by off-line analysis of samples of the broth, or by pumping internal calibration standards through the enzyme chamber.

Bradley and Schmid (1991) have reported that the relationship between the sensor response to internal calibrant and to external glucose concentration was constant for a given sensor configuration. Thus, response to internal calibration standards can be measured and compared to the external calibration response, and if the results of the internal calibration check do not compare well then the sensor calibration constants may be updated.

If the internal calibration check indicates that the sensor performance has deteriorated to an unacceptable degree due to deactivation of the enzyme, then the enzyme can be eluted by perfusion of the cellulose matrix with elution buffer. The sensor is reloaded with fresh GOx-CBD conjugate as before, the sensor is re-calibrated using the internal calibration standards, and fermentation monitoring continues. The sensor calibration can be verified, if desired, by comparison of the sensor output with off-line glucose analysis of a sample of the fermenter broth.

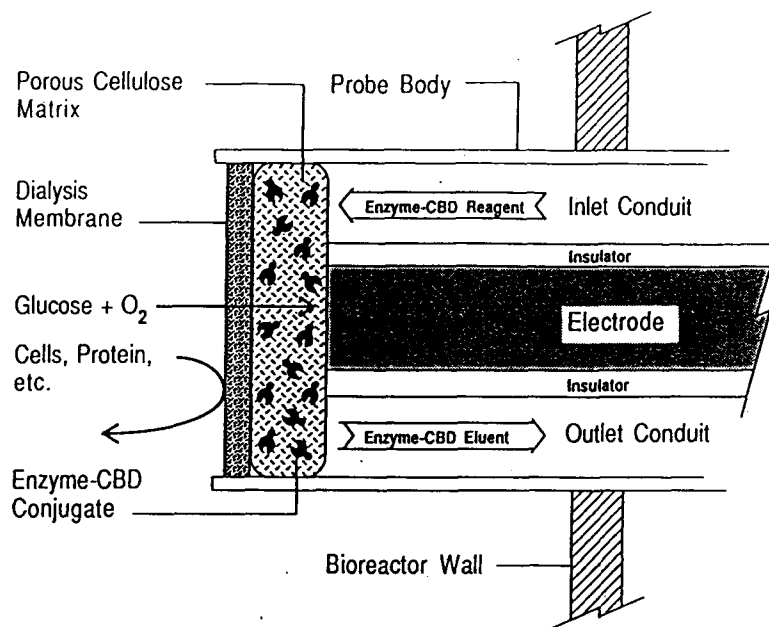


Figure 2.2 Schematic diagram of a biosensor based on CBD-immobilized enzymes.

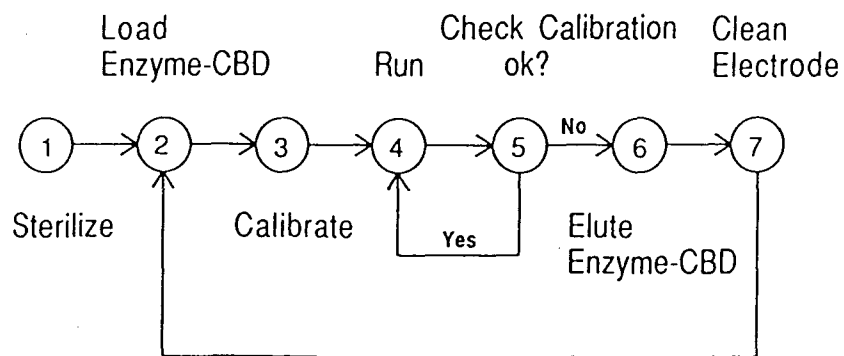


Figure 2.3 Process flow diagram demonstrating the principle of operation of a fermentation monitoring system using the renewable biosensor probe.

Before the cellulose matrix is reloaded with fresh enzyme-CBD conjugate, the sensor could also be perfused with electrode/membrane cleaning solutions and the electrode could be cycled and anodized in order to regenerate the platinum surface if necessary. It would also be possible to clean the external surface of the membrane at this point, without breaching the sterility of the fermentation, by mechanically isolating the probe tip from the fermentation broth and washing or spraying with a jet of cleaning solution, as described by Kok and Hogan (1987/88). The probe tip would then be re-sterilized with steam before re-exposing to the fermenter medium. To continue fermentation monitoring, the sensor is reloaded with enzyme-CBD conjugate. These electrode and membrane cleaning and regeneration processes may or may not be necessary, depending on the resistance of the system to fouling during the course of a typical fermentation.

The proposed sensor system described here addresses the sterilizability and stability problems of electro-enzymatic sensors, but differs from sensor systems described by other researchers in that the complete process of diagnosis and regeneration could potentially be performed under computer control and without interrupting the fermentation. This includes automated, *in situ*, replacement of the enzyme component. The proposed system allows for:

1. conventional autoclaving of the electrode housing exclusive of the enzyme,
2. periodic internal calibration verification,
3. long term sensor operation by replacing the enzyme when necessary, *in situ*, and without interrupting the fermentation,
4. recalibration following enzyme replacement using internal standards, and
5. the possibility of cleaning the membrane and the electrode during the enzyme replacement cycle, if necessary.

The prototype glucose biosensor described in this thesis has been developed with all of the above design characteristics in mind, but the development of the protocol for internal calibration and the equipment for membrane and electrode cleaning were beyond the scope of this project. The automation of the various protocols is discussed, however the sensor functions described are performed manually in this work. The chapters which follow describe the synthesis and characterization of the GOx-CBD conjugate protein, the demonstration of the concept of a regenerable glucose biosensor using the GOx-CBD conjugate, and the construction and testing of an experimental glucose biosensor prototype which demonstrates the potential of this technology for on-line bioprocess monitoring and control..

CHAPTER 3

SYNTHESIS AND CHARACTERIZATION OF THE GLUCOSE OXIDASE - [CELLULOSE BINDING DOMAIN] CONJUGATE

3.1. INTRODUCTION

The first stage of the prototype development involved the conjugation of the enzyme glucose oxidase (GOx) with the cellulose binding domain from the cellulase exoglucanase (CBD_{Cex}) from *Cellulomonas fimi*. In this work, a chemically conjugated GOx-CBD protein was synthesized using the bi-functional cross-linking agent glutaraldehyde. The synthesis and characterization of the GOx-CBD conjugate is described.

3.2. MATERIALS AND METHODS

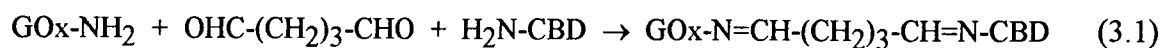
3.2.1. Enzymes and Chemicals

Glucose oxidase (EC 1.1.3.4) was Type X from *A. niger* (Sigma Chemical Co., St Louis, MO) and was used without further purification. The cellulose binding domain from *C. fimi* exoglucanase (CBD_{Cex}) was harvested from recombinant *E. coli* and purified according to methods described elsewhere (Ong et al., 1993). CBD_{Cex} antiserum was produced in rabbits (Whittle et al., 1982). Grade 1 glutaraldehyde, 25% aqueous solution (Sigma Chemical Co.) was used as received for the GOx-CBD conjugation. The synthesis, purification, and storage of the GOx-CBD conjugate was carried out in 50 mM potassium phosphate buffer, pH 7. Cellulose powder (Avicel, type PH101, FMC International Food & Pharmaceutical Products, Cork, Ireland), washed with distilled water

and phosphate buffer, was used for purification of the GOx-CBD conjugates. All other chemicals were analytical grade and used as received.

3.2.2. Enzyme-CBD Conjugation

A 10 mg/mL solution of glucose oxidase in 50 mM phosphate buffer, pH 7, was first activated with glutaraldehyde using a 50-fold excess of glutaraldehyde for each amino group (lysine residue or N-terminus) on the enzyme (Gibson and Woodward, 1992). 40 μ L of glutaraldehyde (25% aqueous solution) was added per mL of GOx solution. After incubation overnight at 4 $^{\circ}$ C, the excess glutaraldehyde was removed by dialysis versus phosphate buffer using Spectra/Por 2 dialysis tubing, MWCO 12-14 kD (Spectrum Medical Industries Inc., Los Angeles, CA, U.S.A.). Dialysis was performed for 24 hours versus 0.25 L of 50 mM phosphate buffer per mL of activated GOx solution. The dialysis buffer was changed after 12 hours. CBD_{Cex} was added in a 1:1 molar ratio based on glucose oxidase and incubated overnight at 4 $^{\circ}$ C. 0.693 mL of 11.2 mg/mL CBD_{Cex} stock solution was added per mL of activated GOx solution. The CBD binds to the activated GOx either via the single lysine residue present or via the N-terminus of the CBD polypeptide (Coutinho et al., 1992; Hansen and Mikkelsen, 1991) according to the net reaction:



Excess CBD was removed by buffer exchange with 50 mM phosphate buffer in an Amicon stirred cell using an Amicon PM30 (non-cellulose) membrane (Amicon Canada Ltd., Oakville, Ontario). Buffer exchange was performed until the absorbance (A_{280}) of the filtrate versus phosphate buffer approached zero. The GOx-CBD conjugate was then purified in a single step by binding to Avicel, using at least 150 mg of Avicel per mL of

activated GOx solution. The conjugate was eluted from Avicel by washing twice with 0.1 M NaCl in 50 mM phosphate buffer, followed by ten washes with 5 mM phosphate buffer, and then one wash with de-ionized, distilled water. The final wash was saved and made up to 50 mM in potassium phosphate using 0.5 M phosphate buffer. The purified GOx-CBD conjugate was stored in 50 mM phosphate buffer at 4 °C. For longer term storage, the conjugate was stored bound to Avicel in 50 mM phosphate buffer at 4 °C and eluted when required. Batches of 1 mL and 10 mL volumes of GOx-CBD conjugate were prepared using this protocol.

3.2.3. Total Protein and Enzyme Activity Assays

Total protein and enzyme activity assays were performed to determine the specific activity (i.e., units of activity/mass of protein) of a conjugate sample. Total protein assays were also performed on conjugate samples before and after binding the conjugate to cellulose, and the amount of protein bound was determined from the difference.

Total protein was assayed using the Bio-Rad protein assay (Bio-Rad Laboratories, Richmond, CA, U.S.A.). Samples were assayed in triplicate on a 96 well plate using the Molecular Devices Vmax kinetic microplate reader (Menlo Park, California). The results were compared to a standard curve determined simultaneously with GOx standards ranging from 0 to 1200 µg/mL. For each assay, 160 µL of sample and 16 µL of dye reagent concentrate were used, and the absorbance was measured at 595 nm after a minimum 15 minute incubation period.

GOx activity was assayed using a modified Sigma GOx activity assay. This colorimetric, kinetic assay is based on the rate of oxidation of o-dianisidine in the presence of peroxidase and hydrogen peroxide produced from the oxidation of β-D-glucose by glucose oxidase. The red colour resulting from the oxidation of o-dianisidine was measured spectrophotometrically at 490 nm. Samples were assayed in triplicate on a 96

well plate using the kinetic microplate reader. For each assay, 240 μL of dye-buffer solution (66 $\mu\text{g/mL}$ o-dianisidine in 50 mM phosphate buffer, pH 7. *Caution: o-dianisidine is a known carcinogen.), 10 μL of peroxidase solution (60 Purpurogallin units/mL H_2O), and 10 μL of sample were added to each well. At time zero, 50 μL of glucose reagent (0.1 g glucose/mL H_2O) was added to each well using a multi-channel pipette and mixed quickly. The increase in absorbance was measured over four minutes and the maximum rate was used for calculation. The results were compared to a standard curve determined simultaneously with GOx standards ranging from 0 to 2.5 U/mL¹. The activity assay was performed in 50 mM phosphate buffer, pH 7, at ambient temperature.

3.2.4 Gel Electrophoresis and Immunoblotting

Gel electrophoresis and Western blotting of the GOx-CBD conjugate were performed according to the protocols described by Harlow and Lane (1988). A homogeneous, 7.5% polyacrylamide gel was used, suitable for a molecular weight range of 45-200 kD. Bands containing CBD_{Cex} were identified by a Western blot using rabbit anti-CBD_{Cex} for the primary antibody (1:1000 dilution). The secondary antibody was horseradish peroxidase-labelled anti-rabbit antibody (1:10 000 dilution). The blot was developed using ECL Western blotting detection reagents (Amersham International plc, Amersham, UK) and exposed onto autoradiography film.

3.3. RESULTS AND DISCUSSION

Figure 3.1 shows the results of gel electrophoresis (SDS-PAGE) of the GOx-CBD conjugate and Western blotting using primary antibody against CBD_{Cex}. The GOx

¹ One unit is defined as the glucose oxidase activity which oxidizes 1 μmole of $\beta\text{-D-}$ glucose per minute at pH 5.1 and 35°C.

control in lane 2 shows a band between 68 kD and 97 kD, due to the subdivision of GOx, Mr 155 kD, (Wilson and Turner, 1992) into two equal subunits. The CBD_{Cex} control, Mr 11 kD, (Ong et al., 1993) was not resolved on this gel but was carried to the anode in the dye front. The raw GOx-CBD conjugate before purification is shown in lane 4. Uncoupled GOx was present in the raw GOx-CBD conjugate, but not after purification of the sample by binding to cellulose, as shown in lane 3. SDS-PAGE of a sample of purified GOx-CBD conjugate both before (lane 6) and after (lane 5) binding to cellulose does not demonstrate any significant change due to binding to cellulose. The GOx-CBD conjugation product appears in bands at 200 kD and higher. The high molecular weight of the product is attributed to cross-linking of glucose oxidase by glutaraldehyde reagent in the activation step of the conjugation protocol.

The cross-linking of glucose oxidase may result in a GOx-CBD conjugation ratio greater than unity. This feature of the conjugate protein could be advantageous in that a higher enzymic activity could be loaded onto a fixed number of CBD binding sites on a given cellulose matrix. On the other hand, the cross-linking of the glucose oxidase may cause a change in the conformation of the protein which could reduce the enzymic activity or change the enzyme specificity. It may be possible to tailor the GOx-CBD conjugation ratio by modifying the conjugation protocol in order to increase, reduce, or eliminate this cross-linking.

Two experimental protocols were tested in an attempt to reduce cross-linking and ensure a 1:1 conjugation ratio. In these protocols, the CBD was activated first, in either the soluble form or bound to cellulose, followed by the addition of GOx to the activated CBD, but an active conjugate was not obtained. Other conjugation protocols and immobilization methods may still be investigated. For example, glucose oxidase has been immobilized using the carbohydrate moieties of the enzyme to prevent covalent bonding of glutaraldehyde to lysine residues in the active site of the enzyme (Pieters and Bardeletti, 1992)

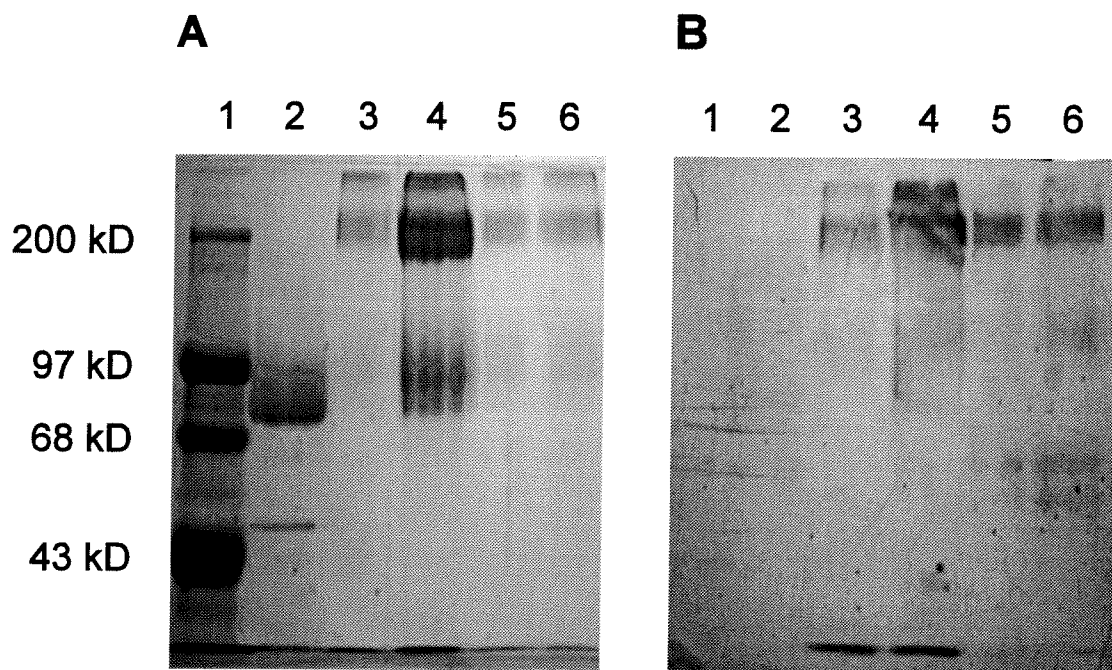


Figure 3.1: **A.** Gel electrophoresis (SDS-PAGE) of the GOx-CBD conjugate. A 7.5% polyacrylamide gel and Coomassie staining were used. Lane designations are: 1, size markers; 2, GOx control; 3, raw conjugate after binding to cellulose; 4, raw conjugate before binding to cellulose; 5, purified conjugate after binding to cellulose; 6, purified conjugate before binding to cellulose. **B.** Western blot of the gel in A. Primary antibody was rabbit - α CBD_{Cex}.

In the conjugation protocol, distilled water was used for eluting the purified GOx-CBD conjugate from Avicel. The use of 8 M guanidine HCl and 1 M NaOH for elution, as suggested by Kilburn et al. (1992), caused irreversible loss of enzyme activity. Using distilled water for elution, the soluble conjugation product was found to retain greater than 60% of the activity of the original, unconjugated enzyme. In addition, the GOx-CBD conjugate retained the binding affinity of the CBD for cellulose, and exhibited GOx activity when bound to cellulose comparable to that of GOx immobilized by other techniques (Harrison et al., 1988). The conjugate could be adsorbed and desorbed from cellulose repeatedly, and could also be dehydrated for storage at room temperature, then reconstituted with PBS, pH 7.4, without a significant loss of activity. Non-specific binding of unconjugated GOx to Avicel or regenerated cellulose was found to be insignificant. The specific GOx activities of various samples of soluble GOx-CBD conjugate are shown in Table 3.1 to illustrate the typical stability of the conjugate over time. In glucose biosensor experiments using the GOx-CBD conjugate, it was found that the conjugate retained sufficient activity to be useful after up to 2 months in storage (when stored bound to Avicel).

Further characterization of the GOx-CBD conjugate will follow the optimization of the conjugation protocol. A potential alternative to chemical conjugation would be to develop an appropriate genetic construct that yields an active GOx-CBD fusion protein. Apropos of this, the gene encoding the glucose oxidase protein of *Aspergillus niger* has been cloned and expressed in yeast (Frederick et al., 1990; DeBaetselier et al., 1991). The main advantages of a genetically engineered conjugate would be greater uniformity and homogeneity of the conjugate reagent, as well as considerable simplification of large-scale conjugate production. A possible disadvantage, however, might be that the size and GOx-CBD ratio of the resulting conjugates could not be as easily tailored when compared to the chemical conjugation method, which may limit the efficacy of the GOx-CBD reagent.

Further characterization and optimization of the chemically conjugated reagent should reveal the feasibility of this approach.

Table 3.1: Specific activity of various samples of soluble GOx-CBD conjugate. The specific activity was calculated from the results of GOx activity and total protein assays. The relative activity was determined compared to unconjugated GOx.

Sample	Time in Storage	Conditions	Specific Activity (U/mg)	Relative Activity
Unconjugated GOx	0	Freshly prepared in 50 mM phosphate buffer, pH 7	118	100%
GOx-CBD Conjugate Batch #2	3 weeks	Purified on Avicel; eluted by distilled water after 1 week in storage	68	58%
GOx-CBD Conjugate Batch #3a	5 weeks	Unpurified	91	77%
GOx-CBD Conjugate Batch #3b	6 weeks	Unpurified	72	61%
GOx-CBD Conjugate Batch #3a	9 weeks	Purified on Avicel; eluted by distilled water after 7 weeks in storage	30	25%

CHAPTER 4

DEMONSTRATION OF THE FEASIBILITY OF A REGENERABLE

GLUCOSE BIOSENSOR

4.1. INTRODUCTION

In this chapter, the feasibility of a regenerable glucose biosensor based on the reversible immobilization of the enzyme using CBD technology is demonstrated. The GOx-CBD conjugate was used in an experimental glucose biosensor constructed from a platinum rotating disk electrode (RDE) with a cellulose matrix for enzyme immobilization via the CBD. Using glucose standards, the biosensor is calibrated repeatedly in PBS during multiple cycles of loading and elution of the GOx-CBD conjugate in order to simulate the periodic regeneration of a glucose biosensor during a fermentation.

4.2. MATERIALS AND METHODS

4.2.1. Instrumentation

Electrochemical data were obtained using a Pine AFRDE4 bi-potentiostat and a Pine AFMSRX analytical rotator (Pine Instrument Co., Grove City, PA, U.S.A.). A Pine AFMDI1980 0.5 cm diameter platinum rotating disk electrode (RDE) was used for the experimental indicating electrode. A platinum counter electrode was fabricated in-house from 1.0 mm diameter platinum wire (Aldrich, Milwaukee, WI, U.S.A.) bound in flint glass tubing (5 mm outside diameter) with epoxy (Chemgrip, Norton Co., Wayne, NJ, U.S.A.). A 25 mm X 25 mm, 52 mesh platinum wire gauze (Aldrich) was crimped onto the platinum wire to increase the surface area of the counter electrode. The reference electrode was a saturated calomel electrode (SCE) (Fisher Scientific, Ottawa, Ontario,

Canada, No. 13-620-52). A Kipp & Zonen Model BD112 strip chart recorder (Kipp & Zonen, Delft/Holland) was used for recording sensor output, and a Kipp & Zonen Model BD91 XY recorder was used for recording cyclic voltammograms. The platinum working electrode (RDE) was prepared by polishing with 0.05 μm alumina and rinsing with distilled water. Immediately before each experiment, the working electrode was cycled in quiescent 0.5 M H_2SO_4 from -0.26 V to +1.2 V at 100 mV/s for 10 minutes, anodized at +1.8 V for 10 minutes, then cycled again until a stable cyclic voltammogram was obtained.

4.2.2. Experimental Glucose Biosensor Preparation

The rotating disk electrode was modified using a retainer such that different cellulose matrices could be held in place over the platinum disk. The retainer was either a Teflon ring or a rubber ring (formed by cutting a transverse slice off the end of a piece of Tygon tubing) sized to fit tightly over the RDE. Three different cellulose-based membranes were used during the experimental biosensor trials: 1) Whatman No. 1 qualitative filter paper (Whatman International Ltd., Maidstone, England), 2) Spectra/Por 2 regenerated cellulose dialysis membrane, MWCO 12-14 kD (Spectrum Medical Industries Inc., Los Angeles, CA, U.S.A.), and 3) nitrocellulose protein transfer membrane with 0.45 μm pores (Schleicher & Schuell, Keene, NH, U.S.A.). The GOx-CBD conjugate was loaded by immersing the electrode assembly in a solution of GOx-CBD conjugate, followed by a single wash with 50 mM phosphate buffer.

The RDE was rotated at 500 rpm and potentiostated at +0.7 V versus SCE in a 250 mL beaker with 100 mL of electrolyte. The electrolyte used in all biosensor experiments was phosphate buffered saline (PBS), pH 7.4, $\mu = 0.2$ M (0.1 M NaCl, 5 mM NaH_2PO_4 , 30 mM Na_2HPO_4 , preserved with 1 mM EDTA, and 5 mM sodium benzoate). The sensor was calibrated in PBS by recording the steady-state RDE current in

response to a series of aliquots of glucose standard (0.1 M glucose in PBS). The sensor response to decreasing concentrations of glucose was recorded by removing aliquots of the cell electrolyte and replacing with fresh, glucose-free PBS. Elution of the GOx-CBD conjugate was achieved by immersing the electrode assembly in the elution buffer, followed by a series of washes with 50 mM phosphate buffer only before reloading fresh GOx-CBD conjugate. Three different elution buffers were used : 1) distilled, deionized water, 2) 1 M NaOH, and 3) 8 M guanidine hydrochloride (99+%(Cl) from Sigma Chemical Co., St. Louis, MO, U.S.A.), prepared in 50 mM phosphate buffer and filtered through Whatman qualitative filter paper. All chemicals were analytical grade and used as received.

The experimental system was intended to simulate what will eventually be an automated process. In the prototype system, the appropriate reagent solutions will be perfused through the cellulose matrix enclosed in the enzyme chamber of the probe via the internal tubing of the Ingold CO₂ probe body. In a future stage of the prototype development the system will be automated using computer controlled pumps and valves for the reagents.

4.3. RESULTS AND DISCUSSION

An experimental glucose biosensor was assembled using an RDE system in order to investigate the feasibility of loading, eluting, and reloading the enzyme-CBD conjugate on a platinum electrode with an immobilized cellulose matrix. The RDE system was advantageous during the first stages of development because experimental parameters could be easily manipulated. In addition, the rotation of the RDE created well-defined hydrodynamic conditions at the surface of the electrode which contributed to a stable, reproducible sensor signal, as well as reproducible conditions for loading/eluting the GOx-CBD conjugate. In the experimental system, this was essential for evaluating and

comparing different procedural modifications and conditions. In order to enable easy access to the cellulose matrix/enzyme membrane, no covering dialysis membrane was used in the work reported here. Within the scope of the present feasibility investigation, the analyte medium was limited to well-defined solutions of PBS and glucose, and the use of a covering membrane was not imperative. However, a suitable covering dialysis membrane will be required for monitoring glucose in fermentation broths, and a number of candidate materials are currently being evaluated.

Figure 4.1 shows a typical calibration curve obtained using the experimental glucose biosensor. Relatively large electrode currents in response to glucose were obtained, indicating that a substantial amount of enzyme had been immobilized (see below). The sensor was calibrated using increasing and decreasing concentrations of glucose in order to demonstrate the reversibility of the sensor, a necessary characteristic for fermentation monitoring. To investigate the possibility of desorption of the enzyme-CBD conjugate during the experiment, the background signal was monitored using a bare, enzyme-free, platinum electrode, and the electrolyte in the electrochemical cell was assayed for GOx activity following the experiment. No GOx activity could be detected, indicating that the enzyme was sufficiently strongly bound to the cellulose matrix.

Different response time, signal magnitude, and durability was observed for each cellulose matrix used (see Table 4.1). The response time was measured as the time required for the sensor signal to reach steady-state following the injection of an aliquot of glucose standard into the electrolyte. The relative signal attenuation due to the cellulose matrix was determined by injecting an aliquot of H_2O_2 into the electrolyte and recording the magnitude of the sensor current for each cellulose matrix. The filter paper matrix was found to have the fastest response time (15-50 seconds) and the highest signal magnitude but disintegrated over time when subjected to the shear stress encountered at high rpm on the RDE. The regenerated cellulose matrix was more durable, but the response time was much slower (2.5-5 minutes) and the signal was severely attenuated, indicative of the

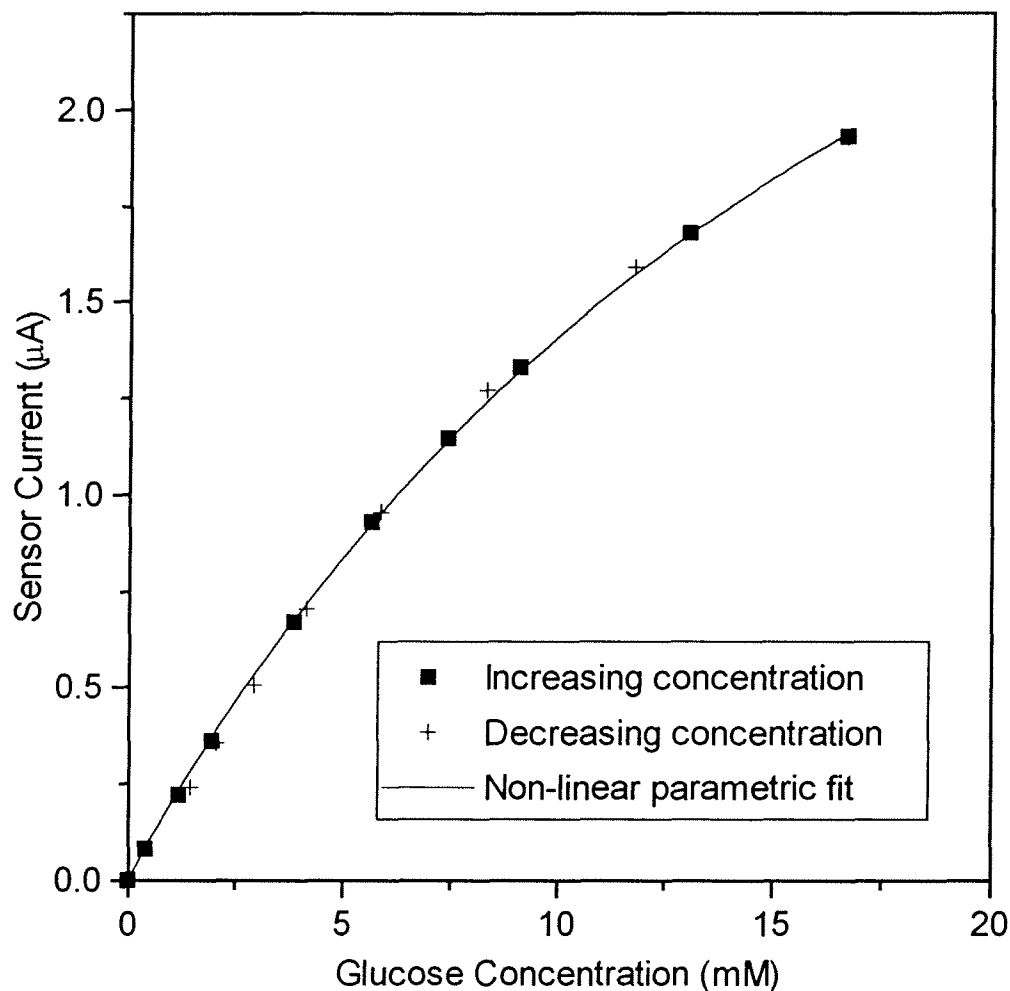


Figure 4.1: Typical calibration data for the experimental glucose biosensor. The GOx-CBD conjugate was bound to a nitrocellulose matrix on the Pt RDE. The RDE was rotated at 500 rpm and potentiostated at +0.7 V versus SCE. Data points represent increasing and decreasing changes in glucose concentration. Solid line represents a non-linear parametric fit of the calibration data (concentration changes in the increasing direction) using the Michaelis-Menten model for enzyme kinetics. Apparent kinetic parameters were $I_{\max} = 4.4 \mu\text{A}$, $K_m' = 21.3 \text{ mM}$.

substantially larger mass transport resistance of the regenerated cellulose when compared to the filter paper. The nitrocellulose matrix with the 0.45 μm pore size was equally as durable as the regenerated cellulose matrix when exposed to the 8 M guanidine elution buffer, but hardened and cracked when using 1 M NaOH as the elution buffer. Nevertheless, the response time when using the nitrocellulose matrix was 20-50 seconds and the signal attenuation was not as severe as that of the regenerated cellulose. For the best combination of response time, signal magnitude, and durability, the nitrocellulose matrix was used in conjunction with the 8 M guanidine elution buffer for the glucose biosensor experiments using the modified RDE.

Table 4.1: Properties of the cellulose matrices used in the experimental glucose biosensor system. The cellulose matrix was held on the Pt RDE by a retaining ring. For the glucose response time, the cellulose matrix was loaded with GOx-CBD conjugate.

Cellulose Matrix	Sensor Current in Response to 50 μL of 0.03% H_2O_2 in PBS (μA)	Response Time Following Glucose Standard Injection
Filter Paper	0.188	15-50 sec
Regenerated Cellulose	0.050	2.5-5 min
Nitrocellulose	0.110	20-50 sec

Figure 4.2 shows calibration curves obtained during five complete cycles of enzyme loading, elution, and replacement. The GOx-CBD conjugate sample was divided into equal aliquots before the experiment, and a fresh aliquot was used for each loading cycle. Total protein assays of the aliquots following the experiment showed approximately 20% variation in the amount of protein loaded. The sensor was calibrated following each GOx-CBD conjugate loading procedure (Load #1 - Load #5). After each calibration curve, the cellulose membrane was washed with the elution buffer and tested

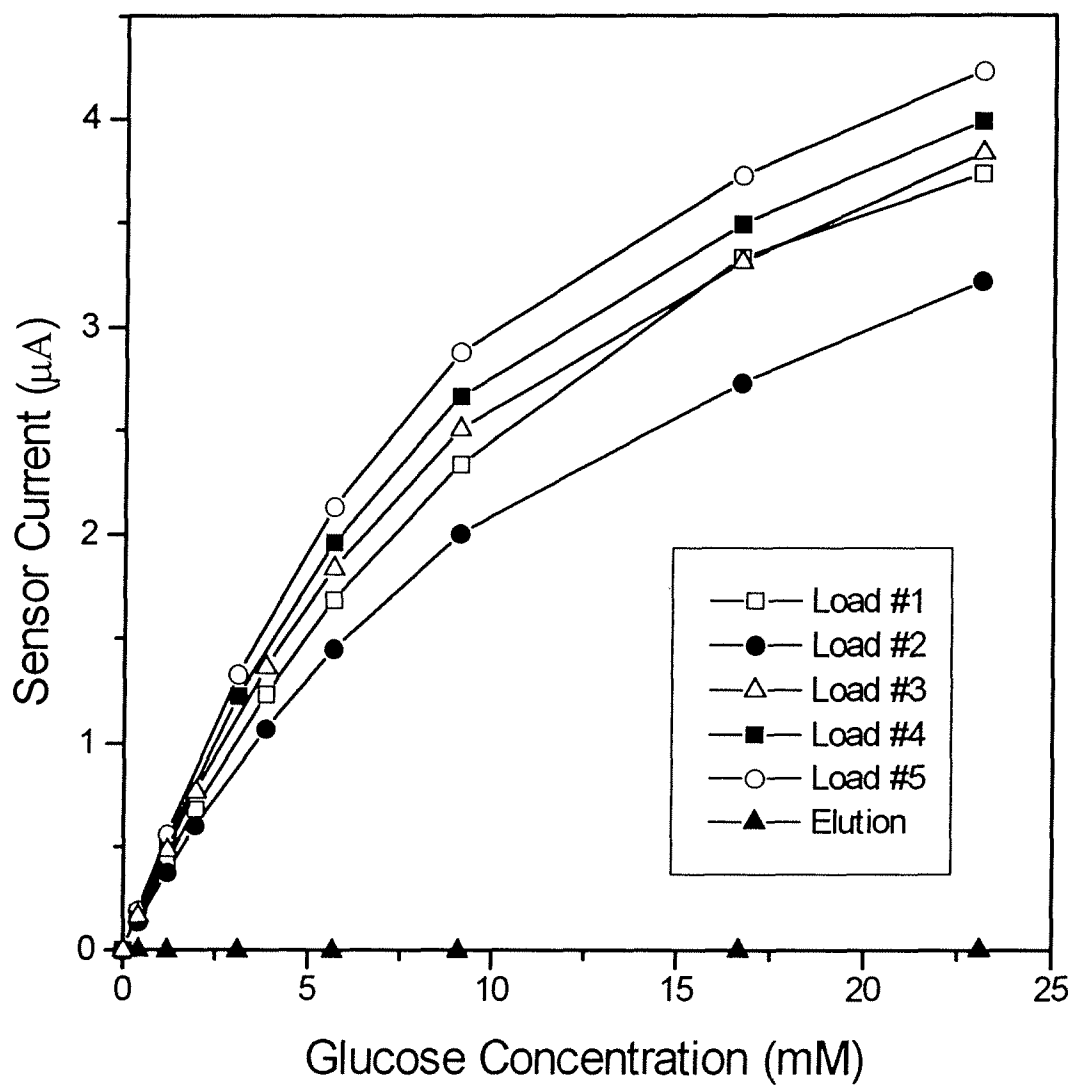


Figure 4.2: Calibration data for multiple cycles of loading and elution of the GOx-CBD conjugate. See Figure 4.1 for experimental conditions. The GOx-CBD conjugate sample was divided into equal aliquots before the experiment, and a fresh aliquot was used for each loading cycle. The elution buffer was 8 M guanidine in 50 mM phosphate buffer. A typical glucose response curve following elution of the GOx-CBD conjugate is shown.

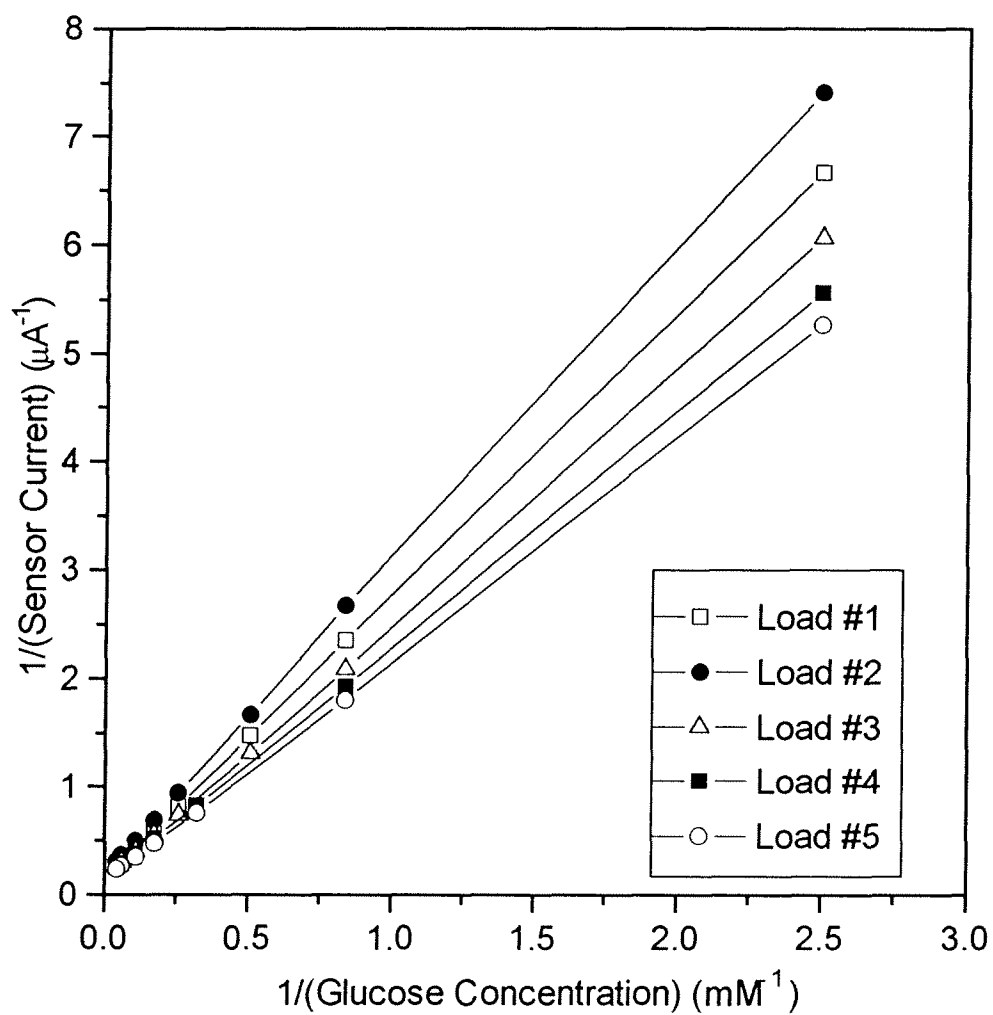


Figure 4.3: Lineweaver-Burk plot of the calibration data in Figure 4.2.

for glucose response to confirm that the enzyme had been completely eluted. The elution buffer used was 8 M guanidine, as the NaOH elution buffer was found to degrade the nitrocellulose membrane and distilled water did not elute 100% of the attached enzyme, resulting in a residual, glucose-dependent current after elution. A typical calibration curve following the elution step is included in Figure 4.2, demonstrating that the sensor does not respond to glucose after elution of the enzyme with 8 M guanidine. The elution procedure was found to be effective in clearing all active enzyme from the cellulose matrix, however the possibility exists that some denatured enzyme may have remained attached. No attempt was made to quantify residual denatured enzyme that remained bound to the cellulose matrix following the elution procedure. The absence of a clear, sequence-dependent trend in the calibration curves reported in Figure 4.2 suggests that very little enzyme remained attached. The differences in the calibration curves following each loading step are not unlike the typical unit-to-unit variations found between amperometric, enzyme-based biosensors fabricated by other methods, and are attributed to differences in the amount of enzyme activity loaded. For a given experiment, the specific activity of the GOx-CBD conjugate sample and the protein loading data could be used to calculate the amount of enzyme activity loaded in each loading cycle. Results were typically in the range of 0.5-3 units.

The shape of the calibration curves suggested that the Michaelis-Menten equation for enzyme kinetics might be useful as an experimental model. In the case of an amperometric enzyme electrode, the sensor current can be taken to be representative of the enzyme rate, since the electron transfer at the electrode is relatively fast, and the sensor current and substrate concentration data are used to determine the kinetic parameters of the Michaelis-Menten equation, as described in Chapter 2. The use of Michaelis-Menten kinetics for the immobilized enzyme may be invalid, since the Michaelis-Menten model is defined for a homogeneous and mobile (i.e., soluble) system of single-substrate enzyme. Nevertheless, the Michaelis-Menten model is useful for its simplicity,

and was found to fit the experimental data very well, as shown in Figure 4.1. This observation was supported by the linearity of a Lineweaver-Burk plot of the data from the multiple cycle experiment (Figure 4.3) and the correlation coefficients from linear regression analysis of the Lineweaver-Burk data (Table 4.2).

Table 4.2: Apparent enzyme kinetic data derived from the calibration data of Figure 4.2.

	Linear Regression of the Lineweaver-Burk Plot (Figure 4.3) of the Calibration Data in Figure 4.2			Non-linear Parametric Fit of the Calibration Data in Figure 4.2 Using the Michaelis-Menten Equation		
	I_{\max} (μA)	K_m' (mM)	r^2	I_{\max} (μA)	K_m' (mM)	Chi^2
Load #1	7.0	18.3	0.9999	6.4	15.7	0.0010
Load #2	5.2	15.1	0.9999	5.3	15.2	0.0004
Load #3	7.6	18.0	0.9998	5.9	12.8	0.0008
Load #4	7.4	15.9	0.9999	6.0	11.8	0.0009
Load #5	8.5	17.4	0.9998	6.3	11.2	0.0016
Mean	7.14	16.9	-	6.0	13.3	-
Standard Deviation	1.2	1.4	-	0.4	2.0	-
Coefficient of Variation	17%	8%	-	7%	15%	-

The kinetic parameters determined for the immobilized enzyme are not necessarily the same as for the soluble enzyme. The kinetic parameters determined for the immobilized enzyme will include unresolved mass transport resistances due to the immobilization matrix and the configuration of the sensor system (e.g. covering membrane, sensor geometry, etc.) and, hence, must be denoted as "apparent" kinetic

parameters. The maximum sensor current, I_{\max} , is analogous to the maximum reaction velocity, V_{\max} , and is useful as an indicator of the amount of enzyme loaded or the amount of immobilized enzyme activity. The apparent Michaelis constant, K_m' , is intrinsic to the enzyme and also the sensor configuration used. Table 4.2 shows the apparent enzyme kinetic data determined from the Lineweaver-Burk plot in Figure 4.3 and from a non-linear parametric fit of the data in Figure 4.2 using the Michaelis-Menten equation. Kinetic data determined by the non-linear parametric fit is deemed to be more accurate, as the slope (K_m'/I_{\max}) of the Lineweaver-Burk plot is strongly determined by the substrate and current values which lie far from the origin, but which are the least accurately measured (Bailey & Ollis, 1986). Using these values of I_{\max} and K_m' , an accurate empirical model for the calibration curve can be obtained, which enables operation of the sensor over a working range much greater than the linear range normally reported in biosensor literature.

It is interesting to note that the coefficients of variation of the apparent kinetic parameters for the five cycles of enzyme loading were roughly 15% or less (see Table 4.2). Complete characterization of the GOx-CBD conjugate and the sensor system may prove that one or both of these parameters will be consistent for a given conjugate sample and sensor configuration. Using the analogy of a straight line, the sensor can be calibrated using only a single point if one of the parameters of the line is known (i.e., the intercept or the slope). Using the Michaelis-Menten function, the sensor system could potentially be calibrated using a single point if one of the values of K_m' or I_{\max} can be determined reliably. Failing this, the sensor could possibly be calibrated using 2 or 3 points to double check the accuracy of the calibration curve based on the expected values of K_m' or I_{\max} . In the proposed prototype biosensor, this calibration check could potentially be performed using internal calibration standards which are pumped into the enzyme chamber of the probe body. Bradley and Schmid (1991) have reported that the relationship between the sensor response to internal calibrant and to external glucose concentration was constant

for a given sensor configuration. The feasibility of these proposed calibration protocols can be investigated following the complete characterization of the biosensor design.

CHAPTER 5

DESIGN AND CHARACTERIZATION OF THE

EXPERIMENTAL GLUCOSE BIOSENSOR PROTOTYPE

5.1. INTRODUCTION

In this chapter, the development and characterization of an experimental glucose biosensor prototype is described. The prototype is based on a modified Ingold CO₂ probe and uses cellulose binding domain technology for the reversible immobilization of the enzyme. A cellulose matrix is incorporated into the "enzyme chamber" of the probe body, and the GOx-CBD conjugate described in Chapter 3 is loaded and eluted from the cellulose matrix by pumping the appropriate loading or eluting buffer through the enzyme chamber via inlet and outlet tubes in the probe body. The construction of the prototype and modifications of the Ingold CO₂ probe are detailed. The prototype is characterized in pilot-scale experiments in the absence of cells, and a glucose-permeable outer membrane is developed for use in a real microbial fermentation. Finally, the prototype glucose sensor is used in a 20 L fermenter to monitor glucose consumption during a fed-batch cultivation of *E. coli*.

5.2. MATERIALS AND METHODS

5.2.1. Prototype Design and Construction

A diagram of the stainless steel Ingold CO₂ probe that was used as the basis for the prototype glucose biosensor is shown in Figure 5.1 (Ingold, 1990). The Ingold probe was designed to withstand temperatures from 20 - 125 °C and pressures from 0 - 2 bars. In its original configuration, the CO₂-permeable membrane was silicone rubber reinforced

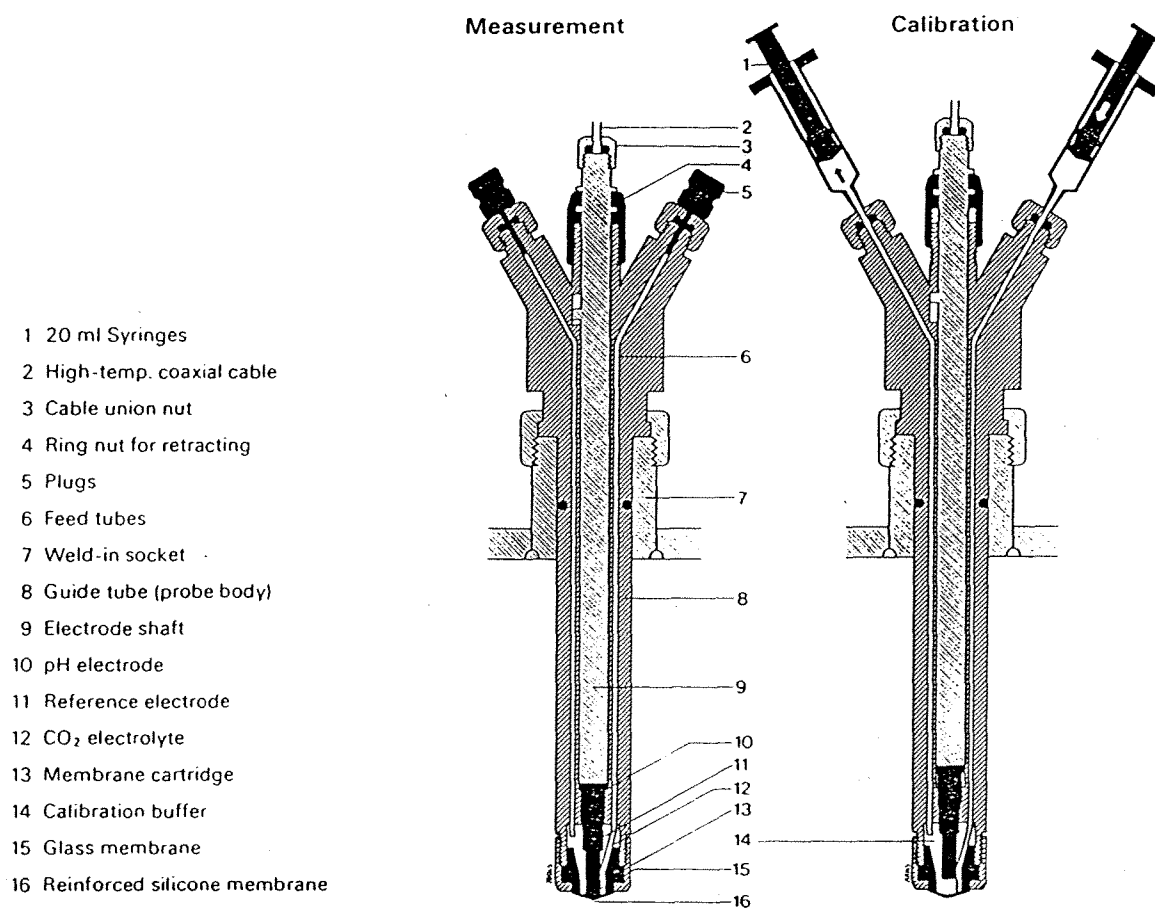


Figure 5.1: Construction of the Ingold CO₂ probe. Reprinted from the Ingold product catalogue with permission from Ingold Electrodes Inc..

with a stainless steel mesh and a nylon net, mounted on a sterilizable plastic membrane cartridge with a stainless steel sleeve and a silicone rubber washer. The internal electrode was a glass pH electrode. The pH electrode was attached to a threaded shaft and could be raised from, and lowered to, the silicone membrane by turning a knurled knob at the end of the shaft. The probe body contained inlet and outlet tubes used for injecting electrolyte and pH calibration standards into the electrolyte chamber and was equipped with the necessary fittings for insertion into the 25 mm side-ports of Chemap fermenters.

The basic hardware of the Ingold CO₂ probe had many of the features of the proposed glucose biosensor hardware described in the schematic diagram of Figure 2.2, made available in a convenient, fermenter compatible package. Several modifications were performed to convert the Ingold probe to the prototype glucose biosensor:

1. A cellulose matrix was incorporated into the electrolyte chamber.
2. The silicone membrane was replaced with a glucose-permeable membrane.
3. The internal pH electrode was replaced with a custom designed electrode assembly with three electrodes for amperometric operation.
4. To fit the new internal electrode unit into the probe body, a custom designed adapter was required to mount the electrode assembly onto the threaded shaft used for raising and lowering the internal pH electrode.
5. The syringes used for injecting electrolyte and pH electrode calibrant into the CO₂ probe were replaced with tubing, valves, and a peristaltic pump.

Cellulose matrix:

The characterization of different cellulose matrices is described in Chapter 4. The cellulose matrix used in the experimental prototype was a disk of Whatman No. 1 qualitative filter paper (Whatman International Ltd., Maidstone, England) cut to

approximately 7 mm in diameter. The cellulose matrix was sandwiched between the internal electrode and the glucose-permeable outer membrane.

Glucose-permeable outer membrane:

The original silicone membrane of the CO₂ probe was removed by separating the steel sleeve from the plastic membrane cartridge and dissolving the silicone with Silicone Sealant Remover (Dow Corning Canada Inc., Mississauga, Ontario, Canada). The new glucose-permeable membrane was draped over the membrane cartridge and secured using steel wire and/or Silastic medical adhesive (Dow Corning Corporation, Medical Products, Midland, MI, U.S.A.). The steel sleeve was placed over the membrane and cartridge and sealed in place with Silastic adhesive.

A number of different membranes were tested as glucose-permeable outer membranes. Candidate membranes were chosen on the basis of structure, strength, molecular weight cut-off, availability, and ease of use. Non-cellulose membranes were chosen where possible to prevent conjugate binding to surfaces other than the intended cellulose matrix and thereby simplify the system of experimental variables:

1. Spectra/Por 2 dialysis tubing from regenerated cellulose, MWCO 12-14 kD, cut lengthwise to form a flat sheet (Spectrum Medical Industries, Inc., Los Angeles, CA, U.S.A.),
2. Amicon PM10 (MWCO 10 kD) and PM30 (MWCO 30 kD) non-cellulose ultrafiltration membranes with support backing (Amicon Canada Ltd., Oakville, Ontario, Canada),
3. Filtron Omega 10 (MWCO 10 kD) polysulfone ultrafiltration membrane with support backing (Filtron Technology Corporation, Northborough, MA, U.S.A.), and
4. A custom designed perfluorosulfonic acid (Nafion) membrane (Aldrich Chemical Company, Inc., Milwaukee, WI, U.S.A.) cast on a 0.2 µm Metrice GA-8 (cellulose triacetate) membrane filter (Gelman Instrument Co., Ann Arbor, MI, U.S.A.).

One coat of 250 μL of 0.5% Nafion (in 50/50 isopropyl alcohol in water) was solution cast on a 25 mm diameter membrane filter with a 50 μm stainless steel mesh for rigid support. The membrane filter and stainless steel mesh were secured onto the membrane cartridge with steel wire before casting the Nafion membrane. The Nafion solution was allowed to dry in air for at least 1 hour before the stainless steel sleeve was placed over the membrane cartridge and sealed with Silastic adhesive. The stainless steel mesh faced the interior of the membrane cartridge such that the Nafion coated membrane filter was on the exterior and would be in direct contact with the fermentation broth. Using this arrangement, a smooth Nafion coating could be cast on the outer surface which would likely behave in a more well-defined manner in a stirred solution than the steel mesh. The steel mesh would also provide structural support for the membrane during the high pressure steam sterilization of the fermenter.

Internal electrode assembly:

The internal electrode assembly designed and built in-house is shown in Figure 5.2. The three-electrode unit had an outside diameter of 6 mm and consisted of a Pt indicating electrode, Pt counter electrode, and Ag/AgCl reference electrode. The Pt indicating electrode was a 1.0 mm diameter platinum wire (Aldrich, Milwaukee, WI, U.S.A.) in a glass shroud made from 4 mm O.D. flint glass tubing. One end of the glass tubing was partially closed by melting the glass over a Bunsen burner, such that the inside diameter was just greater than 1 mm. The platinum wire was then bonded into the glass using Chemgrip epoxy (Norton Co., Wayne NJ, U.S.A.) to form a seal. The glass-shrouded platinum wire was ground and sanded with successively finer grades of sandpaper, followed by polishing to a mirror finish with 0.3 μm and 0.05 μm alumina, leaving exposed a circular platinum disk with a surface area of 0.785 mm^2 .

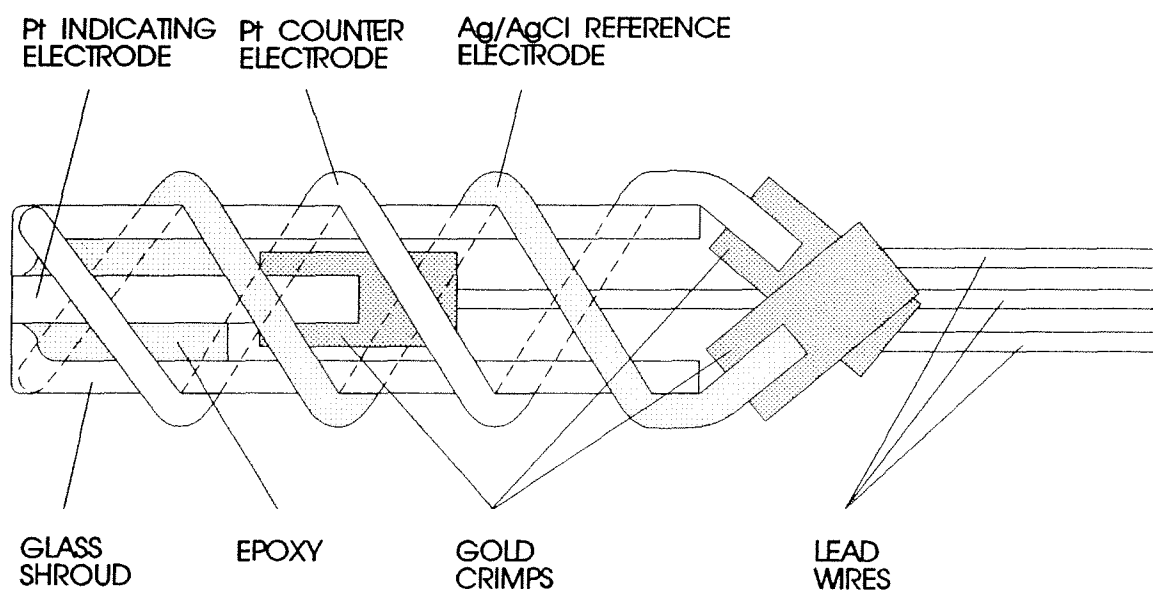


Figure 5.2: Diagram of the internal electrode assembly. The glass-shrouded platinum indicating electrode, platinum counter electrode, and silver-silver chloride reference electrode are shown. The outside diameter of the three-electrode unit was 6 mm.

The counter electrode and reference electrode were 1.0 mm diameter Pt and Ag wire, respectively (Aldrich, Milwaukee, WI, U.S.A.), tightly coiled around the glass shrouded indicating electrode. The surface area of the counter electrode was much greater than the surface area of the indicating electrode to ensure that the area of the counter electrode was not charge transfer limiting. The Ag/AgCl reference electrode was fabricated by anodizing the Ag wire in the presence of Cl^- , based on the method of Sawyer and Roberts (1974). The Ag wire was potentiostated at +0.2 V versus SCE for 8 hours, using a Pt wire counter electrode and an electrochemical cell containing 0.1 M KCl.

Modem cable was used for the electrode leads, because the shielding of the individual wires in the modem cable allowed the reference electrode lead to be shielded from the other electrode leads. The electrode leads were attached to the electrode wires using gold crimps and soldered.

Immediately before use, the bare Pt indicating electrode was cycled in quiescent 0.5 M H_2SO_4 from -0.26 V to +1.2 V at 100 mV/s for 10 minutes, anodized at +1.8 V for 10 minutes, then cycled again until a stable cyclic voltammogram was obtained. For some experiments, described below, the indicating electrode was coated with cellulose acetate using a modification of the method described by Wang and Hutchins (1985). A 7.5 μL drop of 2.5% cellulose acetate (BDH Ltd., Poole, England) in a 1:1 solution of acetone and cyclohexanone (stirred for 12 hours) was applied to the indicating electrode and allowed to dry overnight. The indicating electrode was cycled and anodized immediately before coating with cellulose acetate.

Mounting adapter for the internal electrode unit:

The stainless steel adapter used to mount the internal electrode unit to the electrode shaft of the probe body is shown in Figure 5.3. The flange on the adapter was

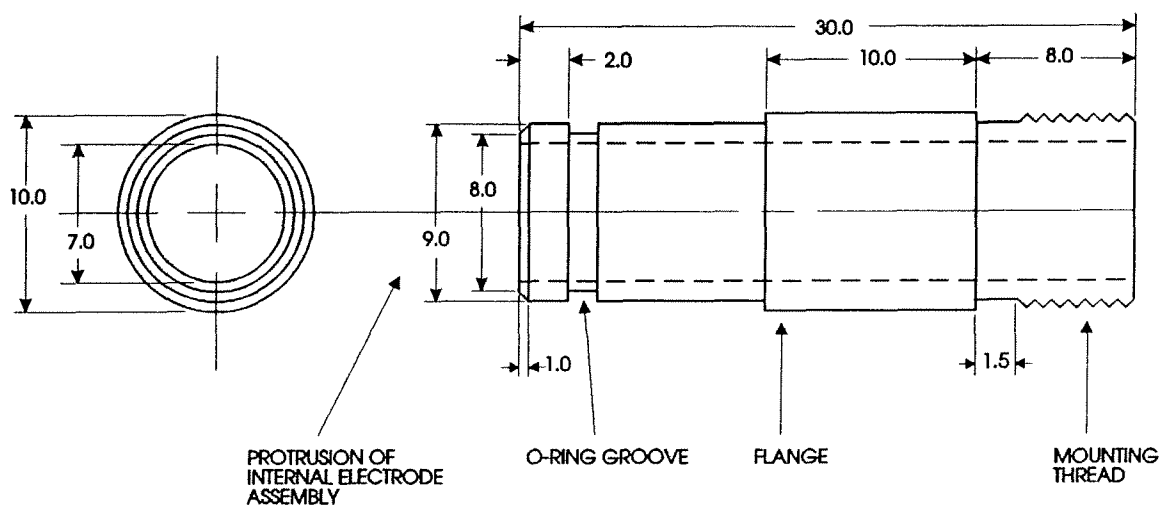


Figure 5.3: Stainless steel adapter for mounting the internal electrode unit. The threaded end mounts onto the electrode shaft of the probe body; the three-electrode unit protrudes from the opposite end. The electrode lead wires were routed through the inside of the adapter and the electrode shaft to the opening at the top of the probe body. The flange on the adapter prevented over-insertion of the electrode unit by stopping against a steel shoulder inside the probe body. Drawing not to scale.

designed to meet a shoulder inside the probe body to prevent the electrode shaft from being inserted too far into the probe body. An O-ring was used between the adapter and the inside wall of the probe body to maintain a sealed internal chamber. An insulating wrap of black electrical tape was used between the electrodes and the adapter. Silastic adhesive was used to bond the internal electrode unit into the adapter and provide a liquid seal. The distance from the tip of the internal electrode unit to the flange on the adapter was set at 35 mm, such that the indicating electrode would contact the outer membrane when fully lowered. It was also necessary to bore the minimum inside diameter of the probe body from 8.13 mm to 9.55 mm.

Reagent flow system:

A Gilson Minipuls 3 peristaltic pump (Gilson Medical Electronics, Middleton, WI, U.S.A.) was used to pump the appropriate reagent solutions through silicone tubing into the probe body. A combination of three-way valves, shown in Figure 5.4, was used to select the reagent to be pumped. The three reagent reservoirs contained 1) the internal electrolyte and washing buffer, 2) glucose standard, for internal calibration, and 3) the elution buffer. The internal electrolyte and washing buffer was PBS (0.1 M NaCl, 5 mM NaH_2PO_4 , and 30 mM Na_2HPO_4 , pH 7.4, $\mu = 0.2$ M, preserved with 1 mM EDTA and 5 mM sodium benzoate). The elution buffer was PBS with 8 M guanidine hydrochloride. At this stage of the prototype development, pump control and valve switching was performed manually.

The protocols used for loading and eluting the GOx-CBD conjugate are listed below. Flow rate was calibrated against pump speed, and the volumes of the different segments of the flow system shown in Figure 5.4 were determined by measuring the time required for a fluid to pass through the different segments at a given flow rate. The time required to wash all unbound GOx-CBD conjugate out of the enzyme chamber after the

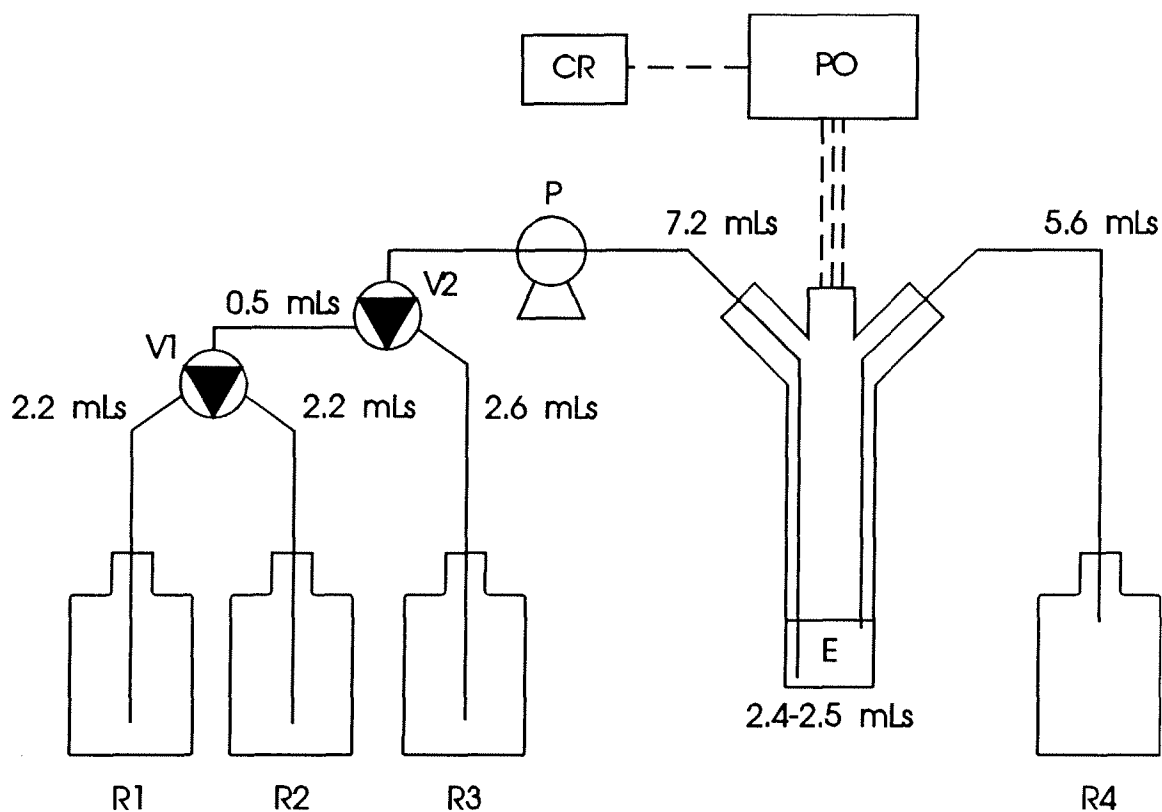


Figure 5.4: Schematic diagram of the biosensor prototype showing the reagent flow system and instrumentation. R1, internal electrolyte and wash buffer reservoir (PBS); R2, internal calibrant reservoir (not used); R3, elution buffer reservoir (8 M guanidine in PBS); R4, waste reservoir; V1 and V2, three-way valves; P, peristaltic pump; E, enzyme chamber; PO, potentiostat; CR, chart recorder. The volume of the each segment of the flow lines and the enzyme chamber are shown. The volume of the enzyme chamber depended on the position of the internal electrode unit (i.e., raised or lowered). Solid and dashed lines represent flow lines and electrical connections, respectively.

enzyme loading cycle was determined by collecting fractions of the effluent from the probe while washing the enzyme chamber with PBS. The presence of protein in the fractions was determined by measuring the absorbance at 280 nm versus fresh PBS. The time required to wash all traces of the guanidine elution buffer out of the enzyme chamber after the enzyme elution cycle was determined using the Pt indicating electrode as a detector for guanidine at the normal operating potential of +0.7 V versus Ag/AgCl. The enzyme chamber was washed with PBS until the sensor signal returned to baseline.

Enzyme loading protocol:

1. Raise the internal electrode assembly.
2. Pump GOx-CBD conjugate solution for 1.0 minute at 4.0 rpm (i.e., 2.2 mls/min)
3. Pump PBS for 4.5 minutes at 4.0 rpm.
4. Stop flow for 1.0 minute. At this point the bolus of GOx-CBD conjugate has filled the enzyme chamber.
5. Pump PBS for 7.5 minutes at 4.0 rpm to wash unbound conjugate from the enzyme chamber.
6. Lower the internal electrode assembly.

The GOx-CBD conjugate was pumped into the flow system by removing the inlet tubing from the PBS reservoir and inserting into a reservoir of conjugate. The soluble conjugate solution prepared for use in the enzyme chamber of the prototype biosensor was made 0.1 M in NaCl to approximate the composition of the PBS electrolyte and satisfy the requirements of the Ag/AgCl reference electrode. Once a bolus of the GOx-CBD conjugate was loaded into the flow system, the tubing inlet was rinsed with distilled water and re-inserted into the PBS reservoir. PBS was pumped through the flow system to push the bolus of GOx-CBD conjugate into the enzyme chamber. The total time required for the loading protocol was 14.0 minutes.

Enzyme elution protocol:

1. Raise the internal electrode assembly.
2. Pump guanidine elution buffer for 2.5 minutes at 4.0 rpm.
3. Pump PBS for 2.0 minutes at 4.0 rpm.
4. Pump PBS for 5.5 minutes at 48.0 rpm (maximum pump rotation speed)
5. Lower the internal electrode assembly.

Separate tubing inlets were used for the guanidine elution buffer and the PBS wash buffer, controlled by a three-way valve. The total time required for the elution protocol was 10.0 minutes.

Dummy electrode:

In addition to the modifications described above, a stainless steel plug, or "dummy electrode", shown in Figure 5.5, was fabricated so that the probe body could be steam sterilized in a fermenter with the internal electrode assembly removed. The internal electrode assembly as constructed could not be autoclaved or the Chemgrip epoxy would become brittle and crack. A dummy electrode was required as a plug when the internal electrode assembly was removed, in case failure of the probe membrane during steam sterilization released superheated steam through the electrode shaft.

5.2.2. Prototype Characterization Experiments

Prototype characterization experiments were performed in the absence of cells in a 150 mL beaker and a Chemap Type SG 3.5 L fermenter (Chemap AG, Switzerland). Experiments in the 150 mL beaker were performed using 100 mL of PBS for electrolyte and the probe was inserted to the 70 mL mark on the 150 mL beaker for every experiment. The electrolyte was stirred by a magnetic stir bar and an air-driven magnetic

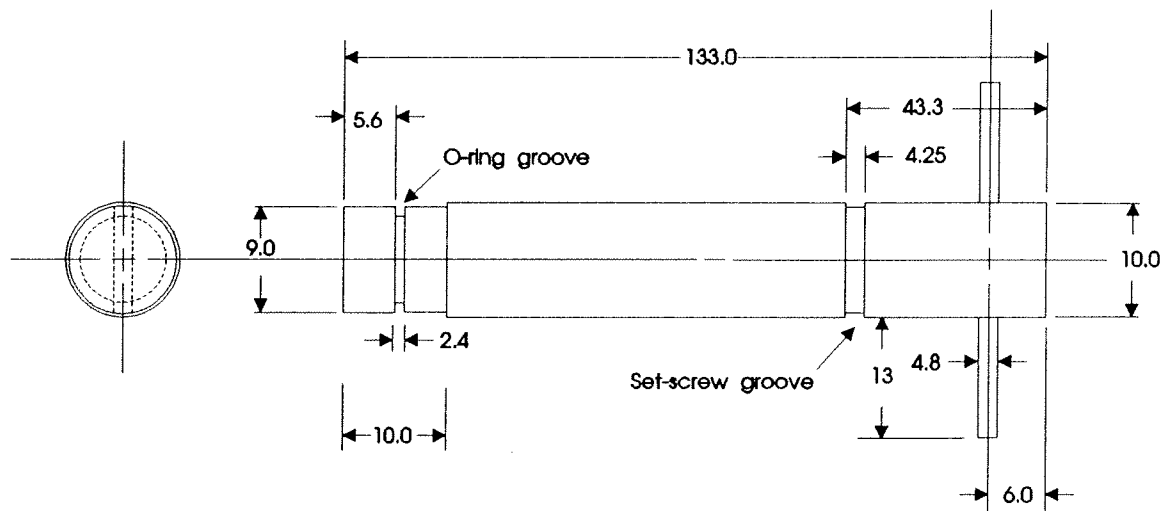


Figure 5.5: Stainless steel dummy electrode. The dummy electrode was used to replace the three-electrode unit during the steam sterilization process. Drawing not to scale.

stirring module from a Hewlett-Packard spectrophotometer (HP 89055A, Hewlett-Packard Canada Ltd., Mississauga, Ontario, Canada). A regulator was used to control air flow, and the air pressure was adjusted to 9 psig for each experiment. The indicating electrode was potentiostated at +0.7 V versus Ag/AgCl using a Pine AFRDE4 bi-potentiostat (Pine Instrument Co., Grove City, PA, U.S.A.) and the sensor output was recorded on a Kipp & Zonen Model BD112 strip chart recorder (Kipp & Zonen, Delft/Holland). The probe was calibrated using aliquots of 0.1 M glucose standard prepared in PBS.

To test the performance of a given sensor configuration in complex medium, the sensor was first calibrated in PBS. Residual glucose in the membrane and the enzyme chamber was removed by pumping PBS internally and washing the probe externally in fresh PBS until a stable baseline was obtained. The electrolyte in the 150 mL beaker was then replaced with fresh Luria Broth (10g/L tryptone (E. Merck, Darmstadt, Germany), 8 g/L yeast extract (Merck), and 5 g/L NaCl, pH 7.2) and recalibrated. Antifoam C (Sigma Chemical Co.) was added at a concentration of 1.6 mL/L to investigate the effect on the sensor signal.

Experiments to characterize the effect of medium dissolved oxygen tension, pH, temperature, stir rate, and air flow rate were performed in the 3.5 L fermenter using the Chemap Type 3000 base unit and Type FZ3000 control unit. The fermenter had three 25 mm side-ports and the standard blade stirrer was installed. An Ingold InFit 764-50 sterilizable pH electrode (Ingold Electrodes Inc., Wilmington, MA, U.S.A.) and an Ingold sterilizable O₂ electrode (No. 401814-06, 25 mm O.D.) were used in two of the fermenter side-ports. The third side-port was used for the glucose biosensor prototype. The biosensor system used the same potentiostat, chart recorder, and reagent flow system as described above. The fermenter was filled with 1.75 L of PBS and aliquots of 1 M glucose standard in PBS were used for calibration. For the pH sensitivity experiments, the

fermenter was filled with 1.75 L of unbuffered saline (0.1 M NaCl) and the pH was adjusted using HCl or NaOH.

5.2.3. Glucose Monitoring During Fed-Batch Cultivation of *E. coli*:

Organisms:

A strain of *E. coli* JM101/pTUgEO7K3 was used for the cultivation. The organism contained the plasmid for the production of CBD_{Cex} and was stored in 10% DMSO at -70 °C. The plasmid consisted of the *tac* promoter and the leader sequence of *C. fimi* exoglucanase (Cex), followed by the structural gene for CBD_{Cex}. The resistance marker was kanamycin and the inducer was IPTG (E. Ong, unpublished results). The inducer was not added in this experiment.

Media:

Minimal medium M-9 was prepared with the following composition (g/L): Na₂HPO₄, 11.76; KH₂PO₄, 5.88; NaCl, 0.5; NH₄Cl, 1.0; MgSO₄, 0.49; CaCl₂, 0.01; thiamine, 1.685; kanamycin, 0.025; and the following trace metals (mg/L): Al₂(SO₄)₃·7H₂O, 0.040; CoCl₂·6H₂O, 0.032; CuSO₄·5H₂O, 0.008; H₃BO₃, 0.004; MnCl₂·4H₂O, 0.080; NiCl₂·6H₂O, 0.004; Na₂MoO₄·2H₂O, 0.020; ZnSO₄·7H₂O, 0.020. The starting glucose concentration was 2.40 g/L. Medium for the inoculum was prepared as follows (g/L): Na₂HPO₄, 6.00; KH₂PO₄, 3.00; NaCl, 0.5; NH₄Cl, 1.0; MgSO₄, 0.49; CaCl₂, 0.01; thiamine, 3.37; kanamycin, 0.05; glucose, 2.80 g/L.

Cultivation:

The cultivation was performed in a 20 L Chemap Type SG fermenter with the standard blade stirrer and three 25 mm side-ports. The fermenter working volume was 8 L. A 500 mL inoculum was prepared in shake flask culture. One side-port was used for the Ingold InFit 764-50 pH electrode. A second side-port was used for an optical density

monitor (Cerex MAX Cellmass Sensor Probe, Cerex Corporation, Ijamsville, MD, U.S.A.). The third side-port was used for the glucose biosensor prototype. A 19 mm diameter Ingold sterilizable O₂ probe (No. 40180-03) was inserted through a port in the fermenter head plate. For the purpose of monitoring glucose concentration with the glucose biosensor prototype, it was unnecessary to use aseptic techniques during the fermentation.

The Chemap 3000 Series base unit and controller were used. Initially, the air flow rate was set at 6 L/min and stir rate was controlled between 50 and 700 rpm in order to maintain the dissolved oxygen setpoint at 95% of air saturation. As the fermentation reached higher cell density, it was necessary to increase the air flow rate to 7.5 L/min and decrease the dissolved oxygen setpoint to 80%. Temperature was controlled at 37 °C. Medium pH was uncontrolled.

Analyses:

Samples were withdrawn from the fermenter at different intervals using the sampling/harvesting valve. Glucose concentration in each sample was analyzed using the Beckman Glucose Analyzer 2 (Beckman Instruments Inc., Fullerton, CA, U.S.A.) after centrifuging the sample at 14,000 rpm for 2 minutes. The absorbance of each sample at 600 nm (versus distilled water) was also measured using a Varian DMS 200 UV-VIS spectrophotometer (Varian Pty. Limited, Mulgrave, Victoria, Australia). In addition, the Genesis Control Series software package (Iconics, Foxborough, MA, U.S.A.) was used to log temperature, pH, dissolved oxygen tension, stir rate, and optical density from the on-line sensors every five minutes during the course of the fermentation.

5.3. RESULTS AND DISCUSSION

In all experiments reported here, the operation of the pump and valves and the raising and lowering of the internal electrode assembly was performed manually in order to

simulate the automated process. It was beyond the scope of this thesis to produce a fully automated prototype; however, in subsequent development phases of the prototype an automated version of the system described here can be realized by interfacing the pump with a personal computer. In addition, the valves can be actuated by computer controlled electric or pneumatic actuators, and the operation of raising and lowering the internal electrode assembly, which is accomplished by turning a knurled knob on a threaded shaft, can be driven by a computer-controlled stepper motor. The sensor output can be monitored by a personal computer rather than a chart recorder, such that the data can be used in computer algorithms for sensor calibration, self-diagnosis, and regeneration, as well as feedback control algorithms for bioprocess control.

5.3.1. Prototype Characterization:

In general, the performance of the experimental prototype fulfilled expectations and was consistent with the results of the preliminary experimental studies described in Chapter 4. The response of the prototype could be calibrated with respect to glucose concentration up to at least 23 mM (the maximum concentration tested) in medium without cells. The sensor signal was relatively stable and noise-free, demonstrating less than 5% variation per hour and signal noise less than 1% of the sensor current. The GOx-CBD conjugate could be loaded and eluted successfully using the inlet and outlet tubing of the modified Ingold probe body and the loading and elution protocols described above. After elution of the enzyme, the sensor response to glucose was less than or equal to the baseline signal, confirming that the enzyme had indeed been eluted.

The Whatman qualitative filter paper, characterized in Chapter 4, proved to be a satisfactory cellulose matrix for the biosensor prototype. The low mass transfer resistance of the filter paper compared to the other cellulose matrices tested was advantageous in terms of fast sensor response time and low signal attenuation due to the matrix. The filter

paper also had a high porosity and cellulose surface area for binding the GOx-CBD conjugate, and was anticipated to be more easily perfused with the reagent solutions than the regenerated cellulose dialysis membrane or the nitrocellulose protein transfer membrane. Structural stability of the filter paper was not a problem, as in the RDE experiments, due to the absence of shear stress from stirring or rotation. Cotton batten was also tested as a potential cellulose matrix, but the relatively uniform thickness and incompressibility of the filter paper was preferred for experimental reproducibility.

Characteristics of the glucose-permeable outer membrane:

Table 5.1 lists the characteristics of a number of different membranes tested as possible glucose-permeable outer membranes for the prototype. Four properties were determined to be essential for the outer membrane:

1. The membrane must be autoclavable.
2. The membrane must be sufficiently permeable to glucose and oxygen so that the sensor response time is fast enough to follow changes in the glucose concentration in the medium. For example, a high cell-density cultivation of *E. coli* with an optical density of 40 (measured at 600 nm versus distilled water) can consume 2.5 g of glucose from 1 L of medium in approximately 10 minutes (D. Hasenwinkle and E. Jervis, unpublished results). A sensor response time of less than five minutes was considered adequate for the present work, although faster response times would certainly be advantageous.
3. The membrane must be impermeable to electroactive species which will contribute to a high background signal, as well as to medium components which will inhibit or denature the enzyme or poison the platinum surface of the indicating electrode over the course of a fermentation run.
4. The membrane itself must be resistant to fouling by protein or microbial adsorption (for example) over the course of a fermentation run.

Table 5.1: Characteristics of different membranes tested as potential outer membranes for the glucose biosensor prototype.

Dialysis Membrane	MWCO (kD)	Steam sterilizable?	Performance rating in complex medium	Response time (min)
None	-	-	-	5
Spectra/Por 2	12-14	Yes	-	12
PM30	30	No	Poor	6
PM10	10	No	Fair	25
Omega 10	10	No	-	∞^1
Nafion	-	Yes	Fair	10
Nafion(autoclaved) ²	-	Yes	Fair	3
Nafion (autoclaved)/ Cellulose Acetate ^{2,3}	-	Yes	Excellent	5

¹ The sensor did not respond to glucose in the concentration range from 0-23 mM with this membrane.

² The membrane cartridge with the Nafion membrane was submerged in PBS and autoclaved before testing.

³ This notation refers to the combination of a Nafion membrane on the membrane cartridge (the glucose-permeable outer membrane of the sensor) and a cellulose acetate coating on the surface of the indicating electrode.

No off-the-shelf membrane tested could satisfy all of the required conditions listed above. A custom membrane was designed using a solution of perfluorosulfonic acid (Nafion) cast on a 0.2 μm cellulose triacetate membrane filter with a 50 μm stainless steel mesh. Nafion has been used with good results as a dialysis membrane material on GOx/Pt electrodes for the determination of glucose in whole blood (Harrison et al., 1988). The permselectivity of Nafion is due to the rejection of anionic species by the negatively-

charged perfluorinated ionomer membrane, as well as the specific morphology of the membrane. The sterilizability of the Nafion membrane is discussed below. The 0.2 μm membrane filter acted as a support for casting the Nafion membrane, and also ensured that a sterile barrier was maintained in case of failure of the Nafion coating. The stainless steel mesh provided rigid support.

A cellulose acetate coating for the indicating electrode was also developed, to be used in conjunction with a glucose-permeable outer membrane. It was anticipated that the background signal in complex media would be high, due to the presence of electroactive species in the media that can be oxidized at a potential of +0.7 V. Furthermore, the indicating electrode is susceptible to poisoning by components of the analyte medium. This is particularly true in biological media, which contain proteins and other components (e.g., ascorbate ion) that may adsorb to the Pt surface, thereby attenuating the electrocatalytic activity of the electrode surface. Dilution of the analyte using an internal buffer flow through the enzyme chamber can decrease the background signal and slow the process of electrode fouling, but the internal buffer flow also causes a decrease in sensor sensitivity. Another approach is to coat the indicating electrode surface with an inert film, such as cellulose acetate, that rejects interfering electroactive species and prevents surface adsorption. Cellulose acetate films coated on the surface of platinum electrochemical detectors in liquid chromatography systems have been shown to prevent electrode fouling from protein adsorption and eliminate some electroactive interferences, while at the same time permitting rapid diffusion of H_2O_2 (Sittampalam and Wilson, 1983; Wang and Hutchins, 1985). Detector response time was not significantly different with the addition of the cellulose acetate coating (Wang and Hutchins, 1985). Cellulose acetate films have also been shown to protect the Pt electrode component of glucose sensors for medical applications (Yamasaki, 1984). The most significant drawback of the coating is the attenuation of the electrode signal resulting in a loss of sensitivity (Sittampalam and Wilson, 1983; Wang and Hutchins, 1985; Kuhn et al., 1989). However, controlled base

hydrolysis of the cellulose acetate film is known to increase the porosity of the film by removing acetate functional groups, and has been shown to decrease the electrode signal attenuation as a result of the cellulose acetate film (Wang and Hutchins, 1985). An additional advantage of the cellulose acetate coating is that the cellulose polymer will bind the GOx-CBD conjugate, thereby increasing the amount of enzyme activity that can be loaded. It was also found that the conjugate could be eluted from cellulose acetate using the 8 M guanidine elution buffer and that the coating was not degraded by the guanidine.

A 2.5% solution of cellulose acetate in acetone and cyclohexanone (1:1) was used for coating the indicating electrode in some of the prototype biosensor experiments with the Nafion membrane.¹ Experiments were performed to investigate the signal attenuation due to the cellulose acetate coating. Identical Pt electrodes were coated with different concentrations of cellulose acetate and the electrode response in PBS was compared using aliquots of hydrogen peroxide. Base hydrolysis of some electrodes was performed in 0.07 M KOH. The results revealed that the least signal attenuation was obtained using a 2.5% cellulose acetate coating, without performing base hydrolysis (see Figure 5.6). The use of lower concentrations of cellulose acetate or longer periods of base hydrolysis were not tested as the membrane might become too fragile. The Pt electrode with the 2.5% cellulose acetate coating was also compared to a bare Pt electrode in Luria broth (data not shown). The electrode with the cellulose acetate coating showed a lower electrode current in response to aliquots of hydrogen peroxide than the bare Pt electrode, but the background current and signal-to-noise ratio of the cellulose acetate coated electrode was also lower. Both electrodes demonstrated signal attenuation in Luria broth compared to PBS.

¹ The use of the custom-designed Nafion membrane (described above) as the glucose-permeable outer membrane of the sensor in conjunction with a cellulose acetate coating on the surface of the indicating electrode is denoted as "Nafion/cellulose acetate".

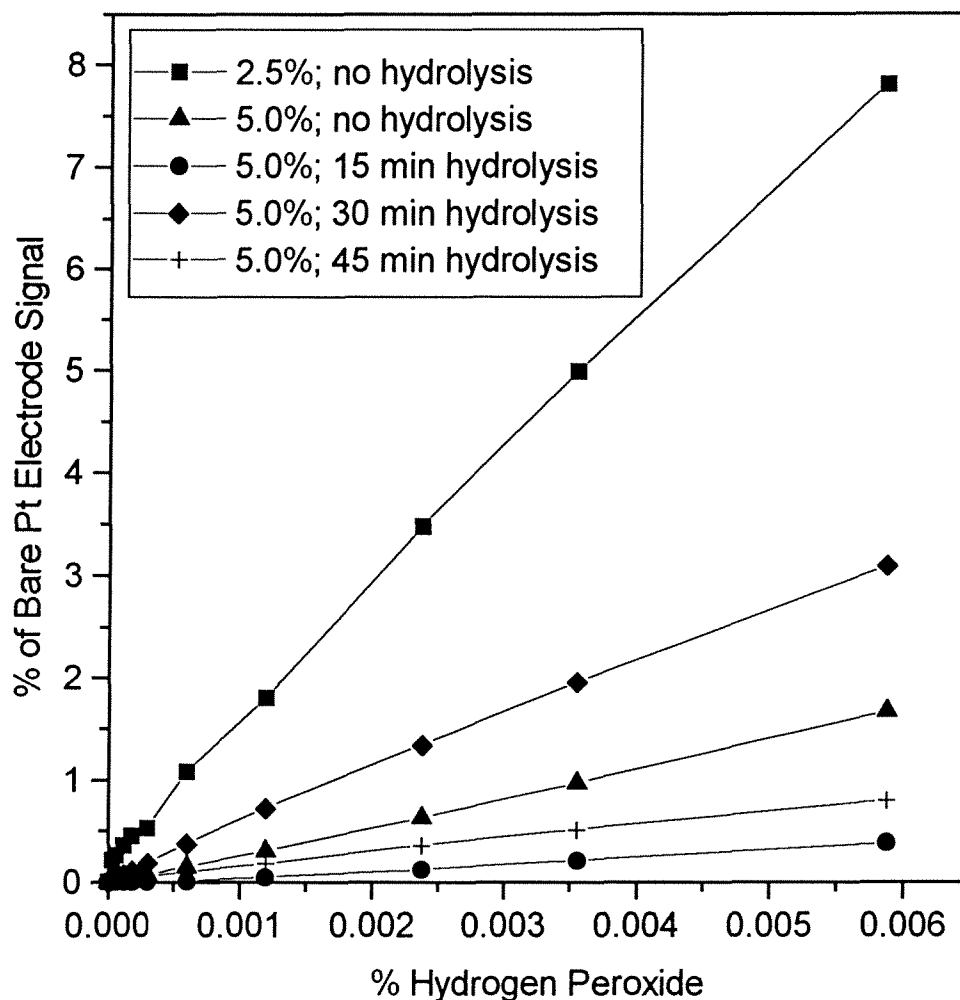


Figure 5.6: Comparison of the response of different cellulose acetate coated Pt electrodes to hydrogen peroxide. Different concentrations of cellulose acetate in a 1:1 solution of acetone and cyclohexanone were used. Base hydrolysis was performed in 0.07 M KOH. Each electrode was potentiostated at +0.7 V vs SCE in PBS and the electrode current was reported relative to a bare Pt electrode.

Performance in complex media:

By far, the most demanding conditions in which the candidate membranes will be used are the conditions of a real fermenter run, due to the presence of cells, cellular metabolites, proteins, and other medium components. Not only must the membrane be autoclavable and enable a fast sensor response time, but the membrane must contribute to stable sensor operation over the course of the entire fermentation. The potential of each membrane to perform satisfactorily in the fermentation environment was evaluated in 150 mL beaker experiments using Luria broth as a complex medium for testing. The prototype sensor with a given membrane was first calibrated in PBS and the response time to the addition of aliquots of glucose was noted (Table 5.1). The electrolyte was then immediately changed to Luria broth and the sensor was recalibrated in order to assess the performance of the given membrane in complex medium. The time between obtaining the two calibration curves was minimized to lessen the possible effect of enzyme deactivation on the sensitivity of the second calibration curve. The addition of Antifoam C to the Luria broth was found to have no effect on the sensor signal at steady state.

In order to compare the results of a series of experiments using different membranes on the same graph, the sensor calibration curve established in PBS for each sensor configuration was normalized with respect to the maximum sensor current (i.e., at 23 mM glucose) to give a maximum dimensionless sensor current of 1. The calibration curve in Luria broth from a given experiment was then expressed relative to the calibration curve in PBS by normalization with the same value, since the only experimental variable changed was the electrolyte/medium.

It can be seen from the results in Figure 5.7 that, in all cases, significant signal attenuation and sensitivity loss was observed in complex medium compared to defined medium (i.e., PBS). This phenomenon has been reported for other enzyme electrodes, as

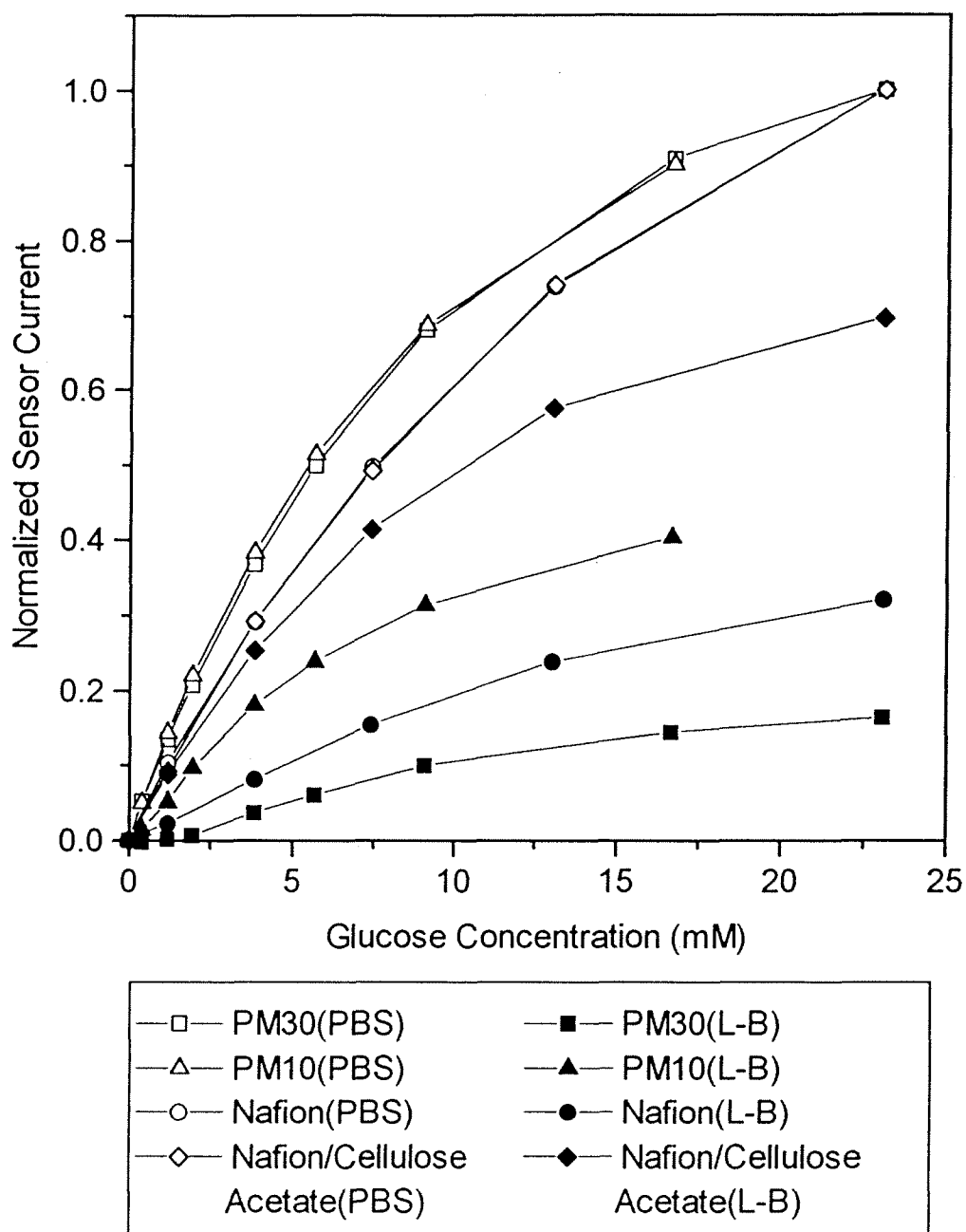


Figure 5.7: Normalized calibration data for the prototype biosensor in PBS and Luria broth (L-B) using different membranes. For each membrane, the prototype was first calibrated in PBS and then recalibrated immediately afterwards in Luria broth. The Nafion membrane used had been autoclaved previously.

well as ion-selective electrodes, mass spectrometers, and gas chromatographs, (Cleland and Enfors, 1983; Merten et al., 1986; Locher et al., 1992). Although not completely understood, the observations are attributed to effects of the analyte matrix. A number of possible explanations have been forwarded, however the phenomenon may be due to more than one chemical effect, or a symbiosis of several different effects:

1. It is the activity and not the concentration of the analyte that is measured by chemical sensors. The equality of concentration and activity is true only at infinite dilution. The presence of additional molecular species, as in fermentation media, may reduce the activity of the analyte (Merten et al, 1986).

2. Low-molecular weight molecules may complex with macromolecules in biological media, thereby reducing the chemical activity with respect to concentration (Merten et al, 1986), the mass transfer through the sensor membrane, or the affinity of the enzyme for the substrate.

3. Proteins, lipids, and other hydrophobic components of biological media may occupy a non-aqueous compartment of the solution which is not accessible to the analyte. Thus the volume occupied by the analyte is lower than the total volume (Merten et al., 1986). This does not necessarily explain the observed signal attenuation and loss of sensitivity, but may explain the poor correlation in analytical results obtained by different techniques (Bradley et al., 1989a).

4. Changes in the composition of the liquid phase may change the properties of mass transfer through membranes significantly (Locher et al., 1992). For example, the partitioning coefficient of the membrane/solution interface may differ depending on the solution. Protein or microbial adsorption to the membrane may increase the mass transfer resistance of the membrane.

5. In the case of enzyme electrodes, components of the medium may inhibit or denature the enzyme or poison the electrode, causing a decrease in the measured sensor signal or a loss of sensitivity. For example, competitive inhibition of glucose oxidase by

D-glucal (a substrate analog) and/or halide ions (Cl^- , Br^- , I^-) has been reported by Rogers and Brandt (1971). (However, published results by Cleland and Enfors (1983) for a glucose oxidase electrode have not shown any effect by chloride ion at concentrations up to 0.26 M NaCl. The immobilization of the enzyme was thought to prevent the inhibitory effect of Cl^- ion.) In addition, other components of the medium, such as ascorbate, are known to adsorb to platinum surfaces, forming a monolayer which blocks electrochemical reactions at the surface, thereby attenuating the sensor signal and eventually poisoning the electrode.

6. In the case of oxidase enzyme-based systems, the analyte matrix may affect the activity or concentration of dissolved oxygen, which is required as the electron acceptor for the reduced form of the enzyme cofactor FADH_2 . The solubility of oxygen, for example, is reduced by high concentrations of ionic species.

Figure 5.8 shows the equilibration time of the prototype sensor when inserted into Luria broth, before the addition of glucose. All of the membranes tested, except the Nafion/cellulose acetate combination, demonstrated an initial current response peak which then decayed to a stable background. Although the mechanism for this behaviour is not clear, the initial peak in response was attributed to the oxidation of electroactive species in the medium, and the subsequent decay of the peak was thought to be a result of membrane fouling and/or electrode poisoning by adsorption of proteins or other species in the medium. The absence of the initial response peak in the case of the Nafion/cellulose acetate combination membrane may have been due to the protective cellulose acetate coating on the indicating electrode and the permselective properties of the Nafion membrane. The Nafion/cellulose acetate combination membrane also established the lowest background signal compared to the other membranes investigated, indicating a high rejection of interfering species, as expected.

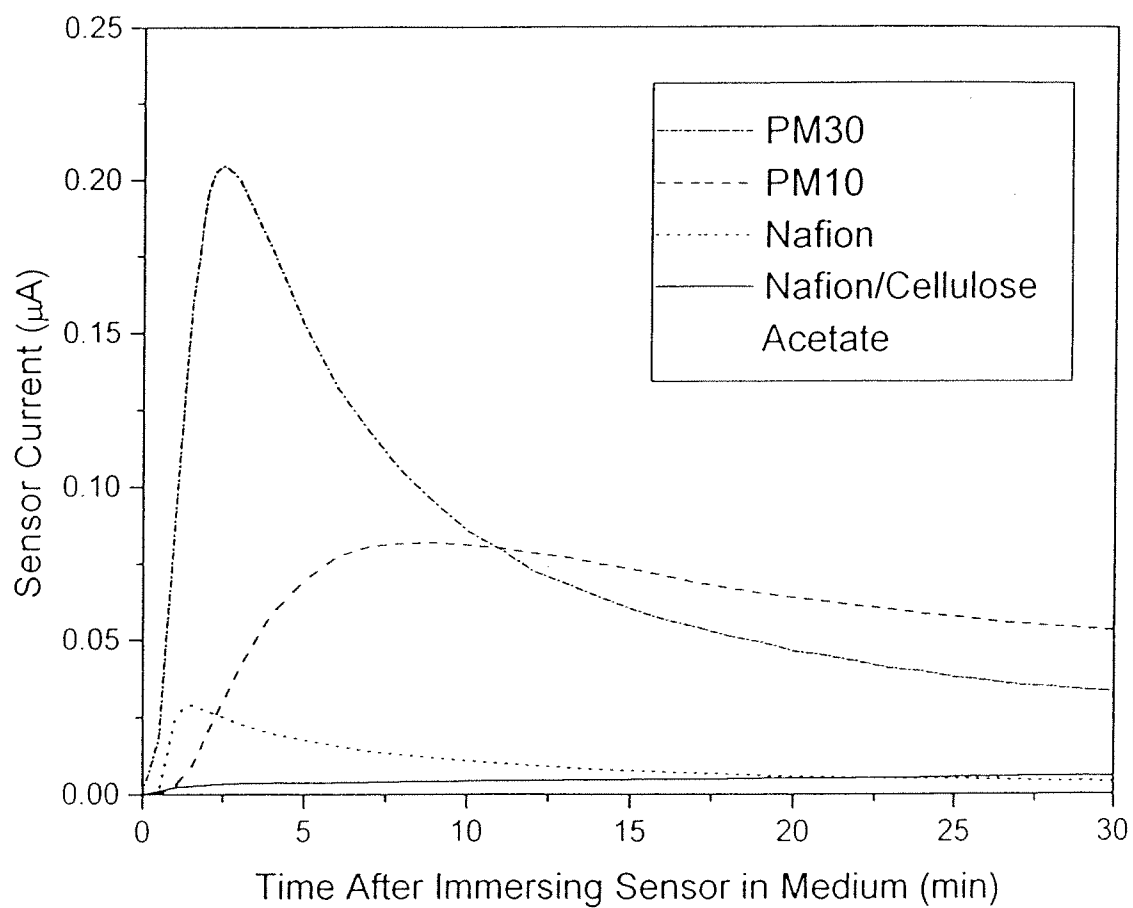


Figure 5.8: Sensor equilibration time after insertion in Luria broth using different membranes. Equilibration time was the time for the sensor signal to reach a stable baseline before the addition of glucose.

These characteristics, in addition to the relatively fast sensor response time and low signal attenuation and sensitivity loss in Luria broth (refer to Figure 5.7), pointed to the Nafion/cellulose acetate membrane system as the best choice (among the membranes investigated here) for use in the biosensor prototype during glucose monitoring of a real fermentation. The sterilizability of the Nafion membrane was established by autoclaving the membrane cartridge while submerged in PBS. After autoclaving the membrane and recalibrating the sensor in PBS, the sensor response time was found to have decreased from 10 minutes to 3 minutes. This may have been due to the dissolution of a small fraction of the Nafion coating during the high temperature process of autoclaving (Moore and Martin, 1986), resulting in a decrease in mass transfer resistance in the membrane and a faster sensor response time. Most importantly, however, Figure 5.9 demonstrates that the performance of the autoclaved Nafion membrane in complex medium was not significantly affected.

Effect of temperature and pH:

Using the Chemap fermenter control unit and the 3.5 L fermenter, a number of fermenter operating parameters could be varied to investigate the effects on the sensor signal at steady state. The effect of temperature was investigated over the range of normal operating temperatures for industrial fermentations (see Figure 5.10). A direct relationship between the sensor signal and temperature was expected due to temperature-dependent increases in the reaction rate constant and the diffusion coefficient, as predicted by Arrhenius' law and the Stokes-Einstein equation, respectively. However, the decrease in medium dissolved oxygen concentration at higher temperatures (as a result of lowered oxygen solubility) may also have reduced the sensor signal due to limitation of the enzyme kinetics. At temperatures greater than 40 °C, the enzyme glucose oxidase is reported to be unstable (Nakamura et al., 1976). Fortier et al. (1990) have investigated the effect of temperatures greater than 40 °C for glucose oxidase immobilized in polypyrrole on a Pt

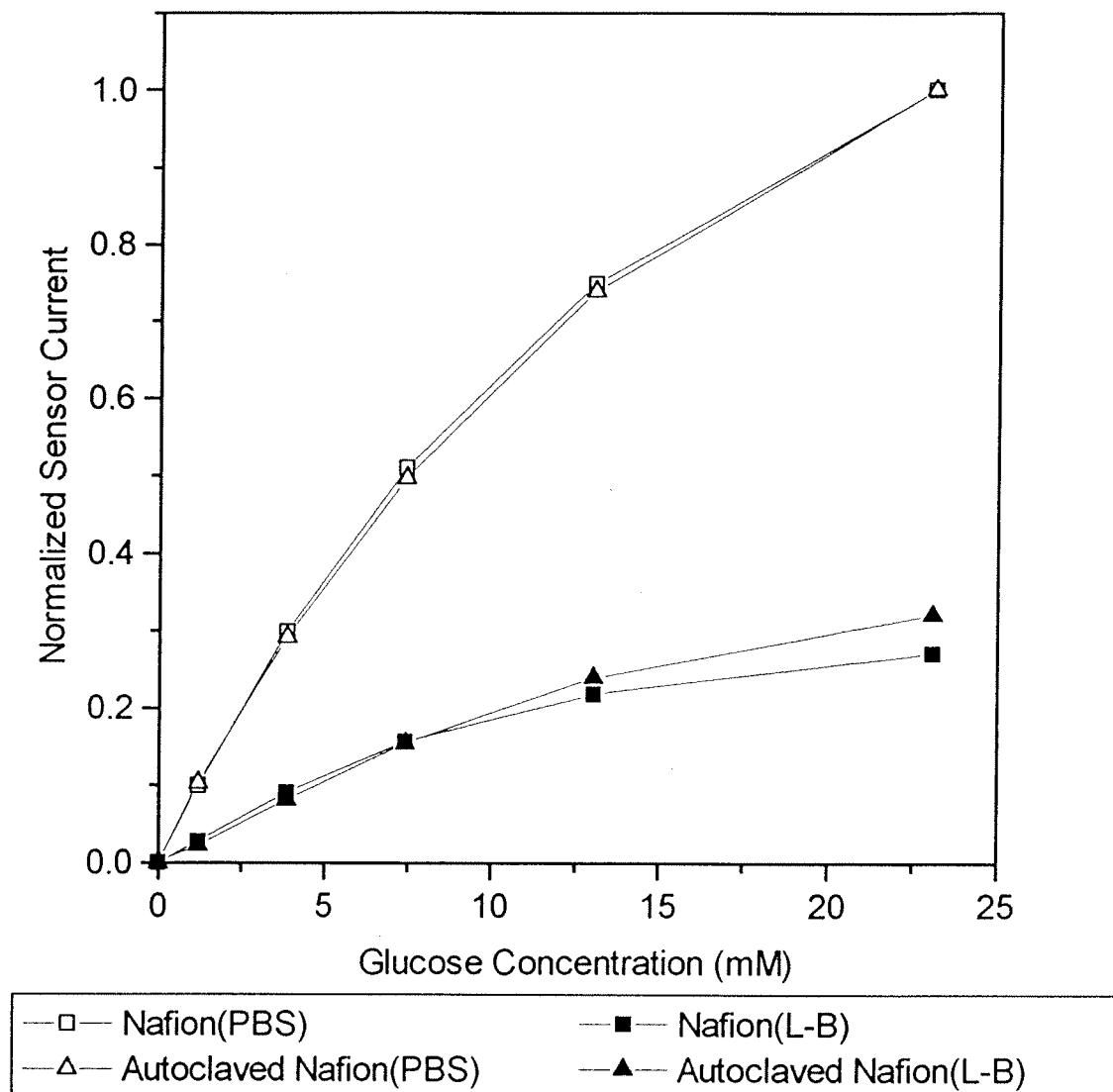


Figure 5.9: Normalized calibration data for the prototype sensor in PBS and Luria broth (L-B) using the Nafion membrane before and after autoclaving. The prototype was first calibrated in PBS and then recalibrated immediately afterwards in Luria broth using a pristine Nafion membrane. The experiment was then repeated after the membrane cartridge had been removed, autoclaved while submerged in PBS in a media bottle, and replaced.

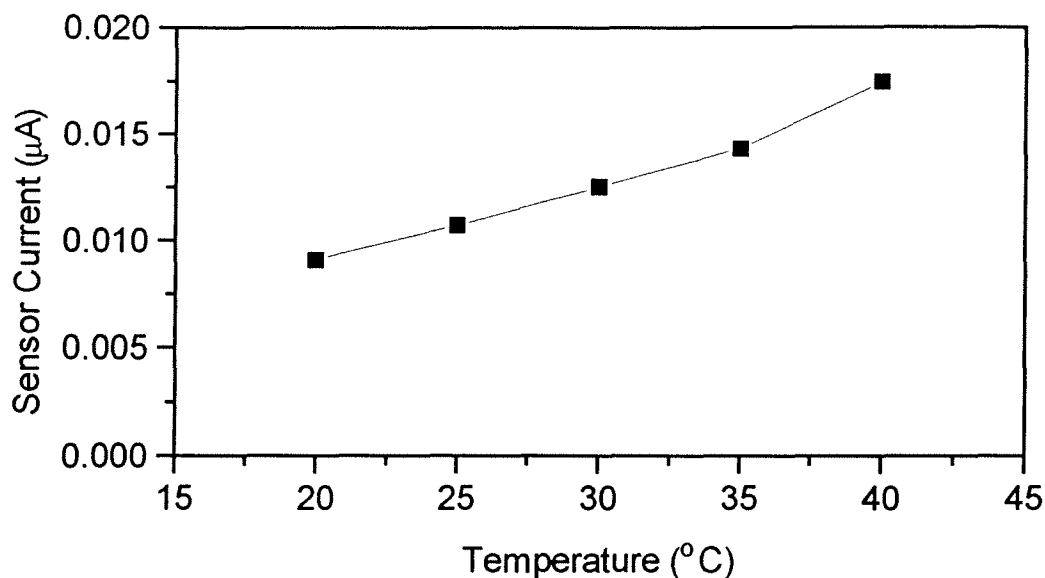


Figure 5.10: Effect of temperature on the sensor signal at steady-state. Temperature was controlled using the Chemap fermenter control unit. Fermenter parameters were: medium, PBS; glucose concentration, 14 mM; pH, 7.4; stir rate, 150 rpm; air flow rate, 0 L/min; dissolved oxygen tension, >98% of air saturation. The Nafion/cellulose acetate membrane system was used.

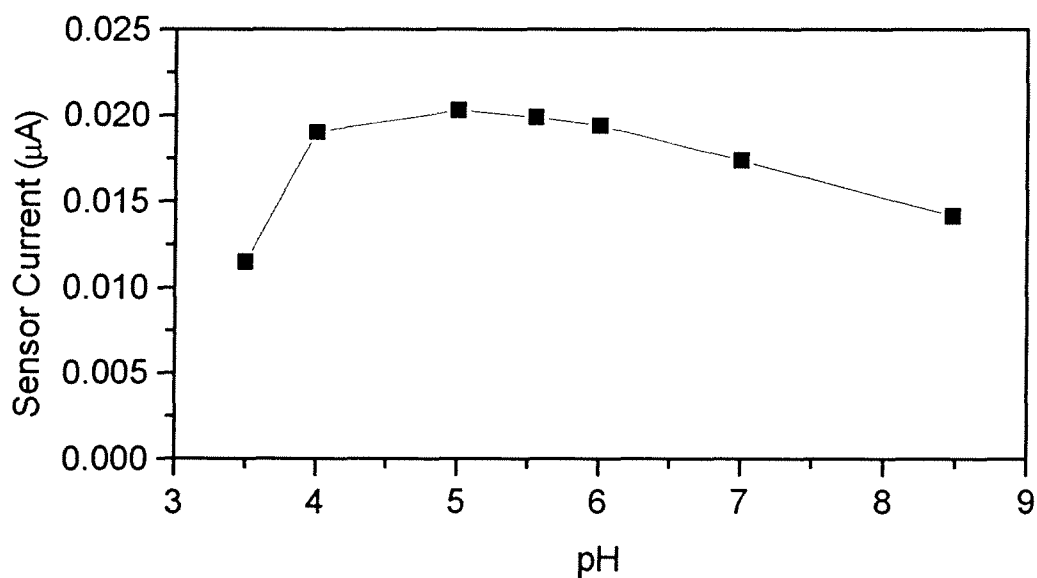


Figure 5.11: Effect of medium pH on the sensor signal at steady-state. Medium pH was adjusted manually using HCl and NaOH. Fermenter parameters were: medium, 0.1 M NaCl in distilled, deionized water; glucose concentration, 14 mM; temperature, 37 °C; stir rate, 150 rpm; air flow rate, 0 L/min; dissolved oxygen tension, >98% of air saturation. The Nafion/cellulose acetate membrane system was used.

electrode and reported a decrease in sensor current, due to temperature-induced denaturation of the enzyme. However, the effect was found to be reversible up to a temperature of 50 °C.

The effect of medium pH on the steady-state sensor signal is shown in Figure 5.11, which demonstrates a maximum at pH 5. The pH sensitivity of the sensor is largely due to the pH dependence of the enzyme activity itself. Fortier et al. (1990) have reported similar results, with a maximum observed at pH 6. Studies of the reaction rate of soluble glucose oxidase from pH 3-8 have found an optimum pH of 5.5-5.6 when oxygen is the electron acceptor for the reduced form of the FAD (Wilson and Turner, 1992). Glucose oxidase has been reported to be stable over the range from pH 3-10 (Bright and Porter, 1975). However, in this study the sensor signal was seriously reduced at pH values below 3.5, and at pH values greater than 8 the binding of the CBD might be disrupted (Kilburn et al., 1992).

Effect of medium dissolved oxygen tension, stir rate, and air flow rate:

The effect of medium dissolved oxygen tension was investigated in the 3.5 L fermenter by sparging the fermenter simultaneously with nitrogen and air and adjusting the flow rates of the two gases to control the medium dissolved oxygen at various levels. A direct relationship was observed between dissolved oxygen level and the steady-state sensor signal (see Figure 5.12). The requirement for oxygen as the electron acceptor to turn over the reduced form of the flavin group of glucose oxidase during the oxidation of glucose has been discussed in Chapter 2. At high dissolved oxygen concentrations, where the enzyme kinetics are glucose limited, variations in the dissolved oxygen level are not critical. The effect of medium dissolved oxygen on the sensor output becomes important in fermentations where the dissolved oxygen level experiences large fluctuations. From Figure 5.12, it can be seen that a constant dissolved oxygen concentration would have to be maintained in order to eliminate the dissolved oxygen dependence of the sensor output.

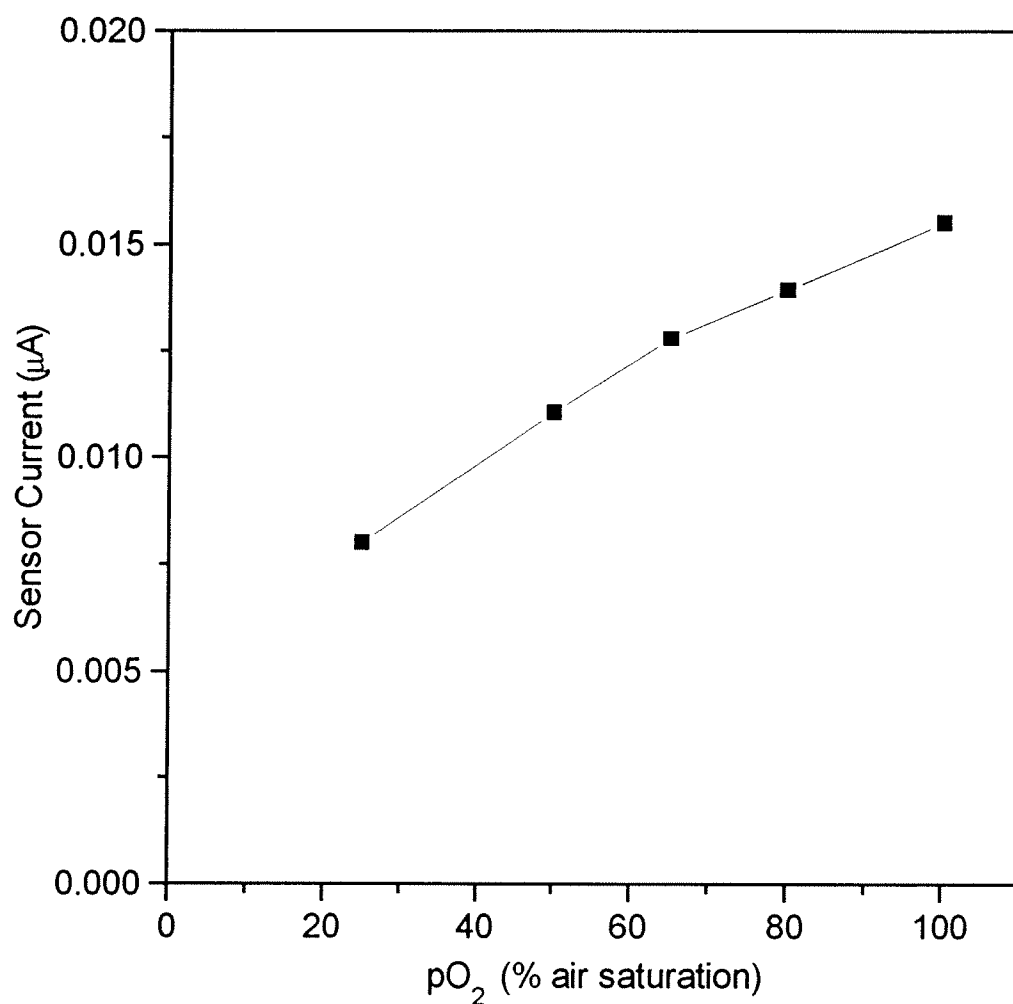


Figure 5.12: Effect of medium dissolved oxygen tension on the sensor signal at steady-state. The fermenter was sparged simultaneously with nitrogen and air and the flow rates of the two gases were adjusted to control the medium dissolved oxygen at different levels. Fermenter parameters were: medium, PBS; glucose concentration, 14 mM; pH, 7.4; temperature, 37 °C; stir rate, 150 rpm. The Nafion/cellulose acetate membrane system was used.

Dissolved oxygen control during a fermentation is easily accomplished using currently available technology for feedback control of aeration and stir rate. The effect of variation of stir rate and air flow rate on the steady-state sensor signal was investigated in the 3.5 L fermenter. The sensor prototype was found to be insensitive to stir rate over the range from 300 to 500 rpm. A 3% change in the steady-state signal was observed over the range from 25 to 200 rpm, indicating that the sensor signal was limited to a small extent by external mass transfer resistance in this range. At zero stir rate, the sensor signal began to increase, which was attributed to H₂O₂ accumulation in the enzyme chamber. Experiments with aeration demonstrated a 1-2% decrease in the steady-state signal with the initialization of air flow, but no further change was observed over the range of air flow rates from 3 to 7 L/min. It should be noted that these observations were recorded for the prototype sensor using the Nafion/cellulose acetate membrane system. The results are dependent on the sensor configuration and the mass transfer properties of the membrane system, however, and as part of the process of optimization of the prototype, the sensor response should be re-characterized following each design change.

Cleland and Enfors (1983) reported an enzyme electrode for which the relationship between sensor signal and medium dissolved oxygen level could be mathematically described by the linear relationship:

$$I = k_e * DOT + I_0 \quad (5.1)$$

where k_e is an electrode constant independent of glucose and I_0 is a glucose dependent constant. Thus, software compensation could potentially be used to correct the sensor output for the effect of variations in dissolved oxygen during the course of the fermentation. The linear model presented by Cleland and Enfors is not appropriate for the data presented in Figure 5.12, but an appropriate empirical model could presumably be determined for the sensor described in this work. However, accurate characterization of the sensor response under varying conditions is essential for this approach.

As the medium dissolved oxygen was exhausted, a significant decrease in the sensor response was observed and the signal approached zero (data not shown). This may have been due to depletion of dissolved oxygen in the enzyme chamber by enzymatic consumption and/or mass transfer into the fermenter medium through the sensor membrane. Glucose oxidase electrodes which depend on oxygen as the electron acceptor cannot be used in anaerobic environments unless oxygen is provided by some internal source within the probe body (e.g., an oxygenated buffer flow stream), or substitute electron acceptors, such as ferrocene derivatives (Cass et al., 1984), are used in place of oxygen to mediate the electron transfer from the enzyme to the electrode. A number of approaches have been reported to address the performance of oxidase enzyme electrodes in anaerobic or oxygen-limited media. Unfortunately, the complete consideration of these methods is beyond the scope of this discussion, and the reader is referred to the available literature (Romette et al., 1979; Cleland and Enfors, 1983; Rishpon et al., 1990; Stoecker and Yacynych, 1990; Sansen et al., 1992).

5.3.2. Glucose Monitoring During Fed-Batch Cultivation of *E. coli*

Cultivation of *E. coli* was performed in a 20 L fermenter for the purpose of monitoring glucose concentration with the glucose biosensor prototype. The probe body was sterilized *in situ* but the internal electrode assembly was removed to prevent degradation of the Chemgrip epoxy used to bond the indicating electrode into the glass shroud. If this had occurred, liquid leakage into the glass shroud around the indicating electrode would have caused undesirable variations in the electrode current due to the exposure of electrochemically active internal materials contacting the Pt electrode. Other high-temperature adhesives must be investigated to replace the Chemgrip epoxy in the internal electrode assembly if the electrode is to remain inserted in the probe body during sterilization (although this may not be essential).

The Nafion/cellulose acetate membrane system was used, but it was discovered that the Nafion coated membrane filter stretched during sterilization in the fermenter. This was likely due to the pressure difference which existed across the membrane (i.e., between the interior of the fermenter and the enzyme chamber of the probe) during the sterilization cycle in the fermenter, thus it may be necessary to design a more rigid support for the membrane to prevent stretching. Alternatively, a pressure equalization manifold could be engineered which would connect the enzyme chamber to the interior of the fermenter (or some other appropriately pressurized vessel) during the sterilization cycle to equalize the pressure on either side of the membrane. For the purpose of this experiment, however, the membrane cartridge was replaced with a spare and the probe was re-inserted into the fermenter.

The GOx-CBD conjugate was loaded using the enzyme loading protocol described above, and the sensor was calibrated before inoculation by adding a known amount of glucose to the medium in a series of aliquots. The sensor calibration curve was determined by comparing the steady-state sensor signal after each aliquot to the calculated glucose concentration in the fermenter. The Michaelis-Menten equation was fitted to the sensor calibration curve and used as a conversion function to calculate the medium glucose concentration from the measured sensor signal during the fermentation. The sensor response time was five minutes or less.

After 8 hours, the enzyme was eluted and reloaded *in situ*. The internal electrode unit was lowered into contact with the cellulose matrix after elution of the enzyme to measure the background signal. During this phase (i.e., the second enzyme loading of the prototype) the background signal was used as the baseline for recalibration of the sensor after reloading fresh GOx-CBD conjugate. Ideally, the sensor would be recalibrated at this point using internal calibration standards pumped into the enzyme chamber, however, the protocol for internal calibration has not yet been developed. The sensor was recalibrated by adding four aliquots of glucose to the fermenter, and the steady-state

sensor signal was compared to the results of off-line glucose analysis of medium samples (taken once the sensor signal had reached steady-state). This method is not ideal, as the inaccuracies of the off-line glucose analyzer are incorporated into the calibration curve. In addition, the medium glucose concentration is changing during the calibration due to cellular metabolism. However, the sensor response time in this experiment was relatively fast, and it was found that steady-state sensor signals could be obtained within a sufficiently short period of time to obtain a useful calibration.

The time course of the fermenter variables monitored during the fermentation is shown in Figure 5.13. The fermentation run was carried out for a total of 16.5 consecutive hours. Furthermore, the experiment was not terminated due to failure or deterioration of the probe. The longest experiment reported in the literature (to this author's knowledge) involving glucose monitoring during a fermentation with an *in situ* enzyme electrode probe is 12 hours (Cleland and Enfors, 1983). Most of the experimental results reported in the literature ranged from 36 minutes to 5 hours of operation (Bradley et al., 1988,1989,1991; Cleland and Enfors, 1983, 1984). The longevity of this experiment is attributed to the stability of the biosensor prototype provided by the Nafion/cellulose acetate membrane system and the capacity for *in situ* enzyme replacement.

Figure 5.14 shows the output from the prototype sensor and the results of the off-line glucose analyses over the course of the experiment. These results demonstrate the effect of the analyte matrix on the sensor response and the importance of sensor calibration under appropriate conditions. From Figure 5.14, it is obvious that the sensor output correlated more closely with the results of the off-line analyses after recalibration of the sensor in the fermenter broth with cells, compared to the initial calibration of the sensor in fresh medium without cells. After reloading the enzyme and recalibrating the sensor, the profile of the sensor output followed the profile of the off-line analyses with substantially greater fidelity than the preceding phase, correctly indicating the exhaustion

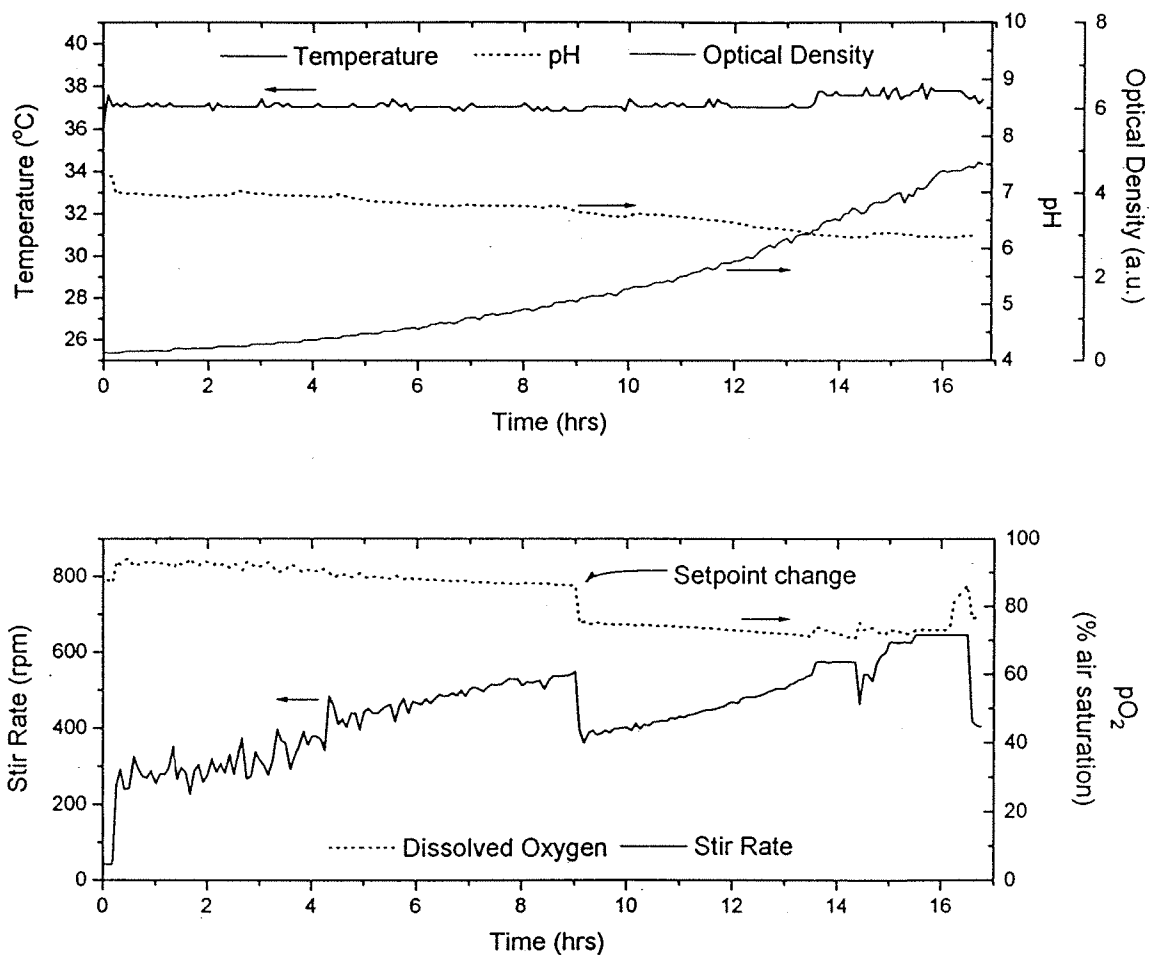


Figure 5.13: Time-course of the fermenter variables during fed-batch cultivation of *E. coli* in a 20 L fermenter. The fermenter was inoculated at time zero. Fermenter variables were recorded every 5 minutes using the Genesis Control Series software package and on-line sensors. The dissolved oxygen setpoint was changed from 95% of air saturation to 80% as the cells reached higher density.

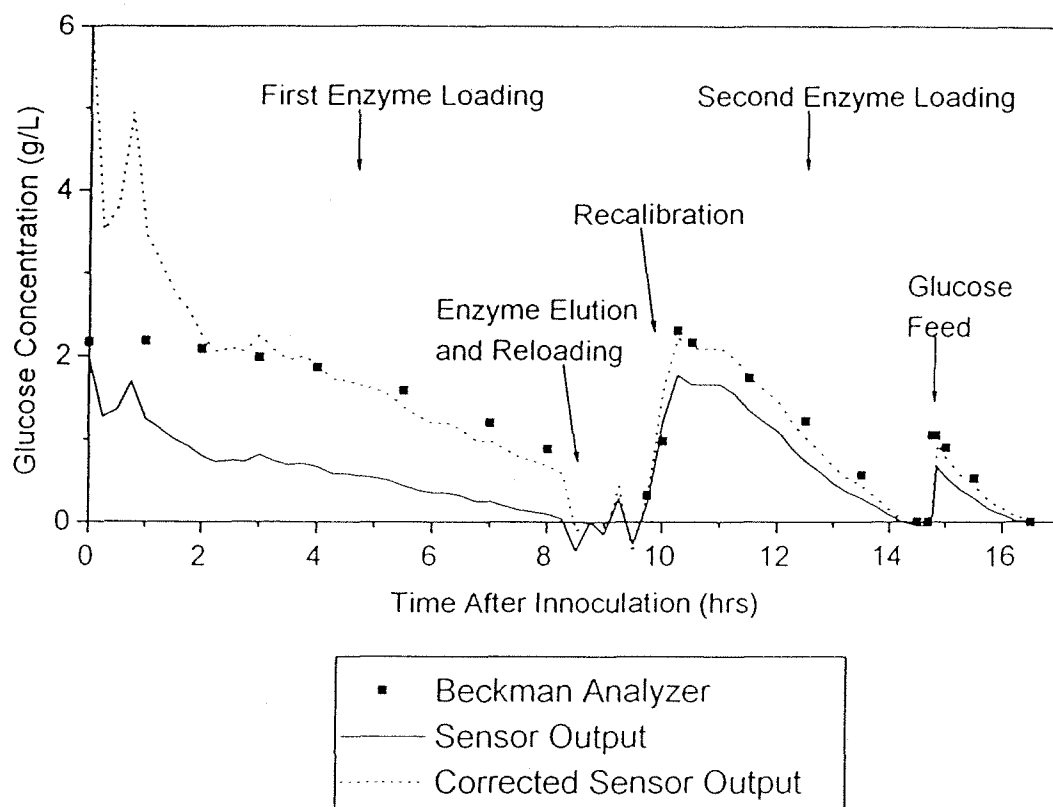


Figure 5.14: Medium glucose concentration measured by the prototype glucose sensor and the Beckman off-line glucose analyzer during fed-batch cultivation of *E. coli* in minimal medium (M-9) in a 20 L fermenter. The sensor current was converted to glucose concentration using the Michaelis-Menten type conversion function in Equation 5.2. The corrected and uncorrected sensor calibration constants for the first and second enzyme loadings are shown in Table 5.2.

of the medium glucose and accurately following the infusion of glucose (and without significant delay). The improved correlation was expected, since the inaccuracies of the off-line analyzer and the unresolved effects of the analyte matrix were included in the sensor calibration constants after recalibration. Innoculation of the fermenter following the initial calibration in fresh medium changed the composition of the sample matrix, therefore calibration of the sensor would have best been performed after inoculation and after measurement of the background (i.e., prior to loading the enzyme). Ideally, on-line calibration could be performed without disturbing the fermentation by using a series of internal calibration standards in a scheme similar to that proposed by Bradley and Schmid (1992). Alternatively, the sensor could be calibrated by adding glucose to the medium in aliquots after inoculation and determining the substrate concentration after each aliquot by calculation or by using the off-line glucose analyzer (in the same manner as calibration was performed following the second enzyme loading in this experiment).

The glucose concentrations determined by the prototype sensor were consistently lower than the results obtained from the off-line glucose analyzer. This behaviour may have been due to effects of the analyte matrix and/or systematic differences between the two analytical methods. These observations are consistent with similar comparisons published in the literature (Merten et al., 1986; Bradley et al., 1989a; Locher et al., 1992). An empirical model was formulated for the sensor calibration curve which was used to experiment with corrections to the sensor calibration constants in an attempt to fit the sensor output more closely to the off-line glucose analyzer results. The Michaelis-Menten function used for the conversion of the measured sensor current (μA) to glucose concentration (g/L) was obtained by manipulation of Equation 2.20. An additional parameter, I_0 , was included to represent the value of the sensor baseline current which is normally subtracted from the measured sensor current before conversion, giving:

$$S = \frac{(I - I_0) K_m'}{I_{\max} - (I - I_0)} \quad (5.2)$$

where S is the glucose concentration (g/L), I is the measured sensor current (μA), I_0 is the sensor baseline (μA), I_{\max} is the maximum sensor current (μA), and K_m' is the apparent Michaelis constant (g/L). Using numerical analysis and several initial values for the parameters I_0 , I_{\max} , and K_m' , the corrected sensor output shown in Figure 5.14 was determined. The corrected and uncorrected sensor calibration constants for the first and second enzyme loadings are shown in Table 5.2.

Table 5.2: Prototype sensor calibration constants for the first and second enzyme loadings.

Parameter	Load #1		Load #2	
	Uncorrected	Corrected	Uncorrected	Corrected
I_0 (μA)	0.014	0.0068	0.0068	0.0068
I_{\max} (μA)	0.047	0.040	0.0127	0.0135
K_m' (mM)	8.6	9.99	6.44	10.10
Correlation Coefficient	0.9797	0.9710	0.9856	0.9917

The results were found to be reasonable. The calibration constants for the first enzyme loading could be corrected significantly by adjusting the baseline to account for the change in the analyte matrix after inoculation. The value used for the sensor baseline was the background signal determined during the fermentation (measured by lowering the internal electrode unit into contact with the cellulose matrix after elution of the enzyme and recording the sensor current). This value was taken to be relatively constant throughout the experiment, making the assumption that the membrane system effectively

rejected interfering species and resisted fouling during the course of the fermentation. The apparent Michaelis constant was found to be nearly identical for the first and second enzyme loading, which is consistent with the results of Chapter 4 for multiple cycles of enzyme loading and elution using the modified rotating disk electrode. The values of I_{\max} , which can be taken to be representative of the amount of enzyme loaded, were not changed significantly by the correction procedure.

It can be seen from Figure 5.14 that, after applying the corrected sensor calibration constants, the sensor output matches the results profile from the off-line analyses much more accurately. The transient fluctuations in the sensor output observed at the beginning of the experiment are not normally observed in the medium glucose concentration and are presumed to be a result of some initial instability in the local environment of the probe (e.g., due to entrapped bubbles), although the actual cause in this case could not be determined. In any case, the perturbation was temporary and did not recur. Once the perturbation subsided, the correlation between the corrected sensor output and the off-line results was excellent.

Although the correlation coefficients reported in Table 5.2 do not show any significant change, the cross-correlation plots in Figure 5.15 demonstrate that the relationship between the sensor output and the off-line results was shifted closer to the line of direct proportionality after correction of the calibration constants. Part B of Figure 5.15 also demonstrates that the sensor output and the off-line results correlated when the glucose concentration varied in a non-sequential manner. The cross-correlation plots in Figure 5.15 are consistent with results reported in the literature for the comparison of different analytical methods for glucose analysis (Bradley et al., 1989a).

The approach used above assumes that the off-line glucose analyzer was precise and accurate and that the sensor output was in error. According to Locher et al. (1992), the accuracy of the measured value of a single sensor can normally be validated by comparison with alternative measurement methods. Unfortunately, different measuring

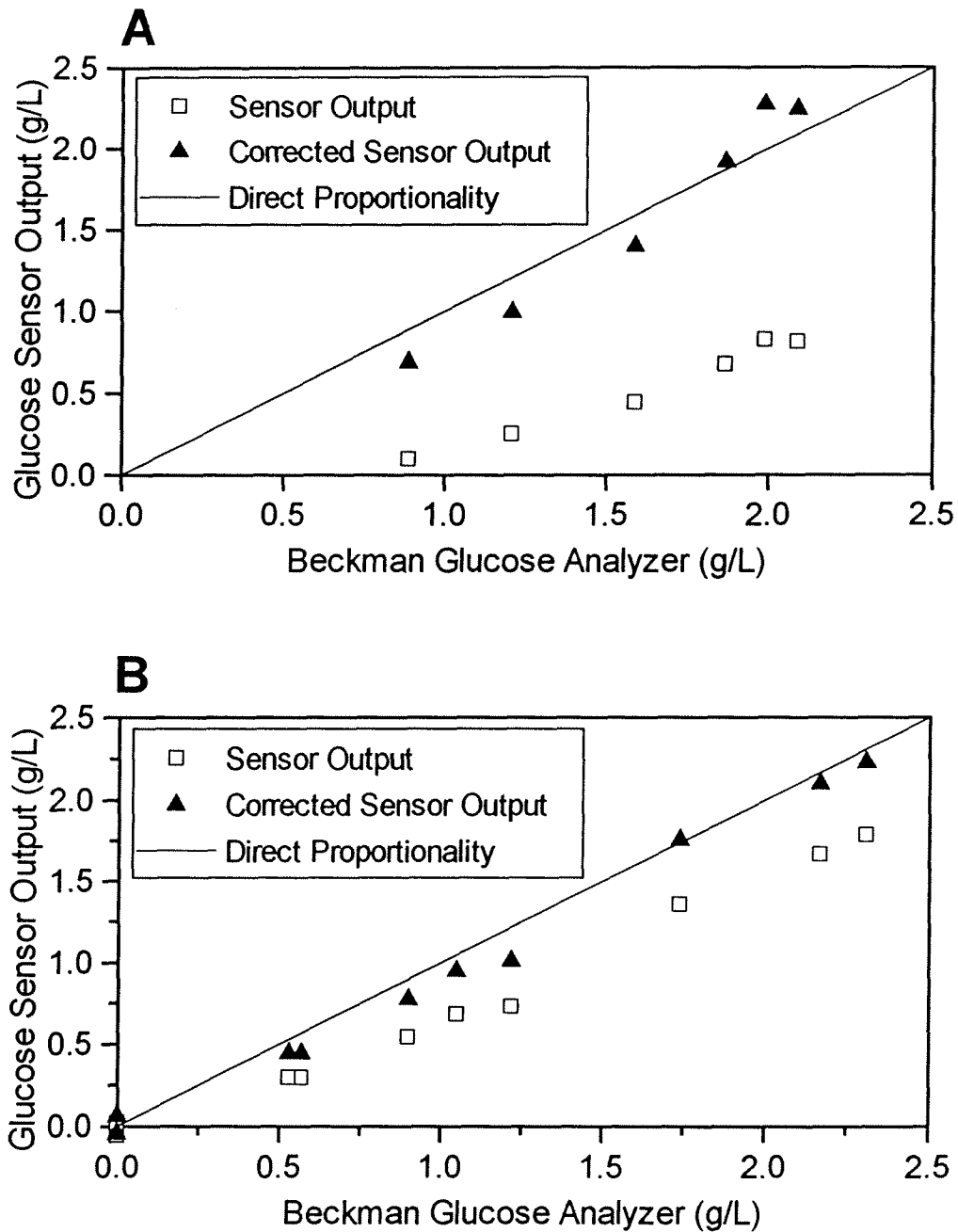


Figure 5.15: Cross-correlation plots of the prototype glucose sensor output and the Beckman off-line glucose analyzer results using the data from Figure 5.14. **A.** First enzyme loading. Data recorded during the period of transient fluctuations in the sensor signal at the outset of the experiment was not included. **B.** Second enzyme loading. One extreme outlier (which was measured at the instant of glucose feeding) was removed.

methods often will produce different results and the most accurate analytical method cannot easily be determined. This is especially true in the case of biological systems, which are frequently more difficult to measure accurately than simple physical or chemical systems. Comparison of the off-line glucose analyzer results immediately after inoculation (2.17 g/L) with the glucose sensor output (1.98 g/L) and the calculated medium glucose concentration (2.40 g/L, based on the volume of medium and the amount of glucose added) reveals a significant discrepancy in both methods. The choice of the most accurate and/or reliable analytical method must often be based on experience. In this experiment, the results from the Beckman glucose analyzer were used as the standard for comparison for reasons of practicality, availability, and relative ease of use.

To determine the useable lifetime of the enzyme component of the sensor, periodic internal calibration checks could be performed to determine at what point the activity of the enzyme had deteriorated to an unsatisfactory degree. In this experiment, the results from off-line glucose analysis of medium samples were used as a reference in an attempt to identify drift in the prototype sensor output which could be attributed to enzyme deactivation over time. This approach makes the assumption that the results from the off-line glucose analyzer were stable and reliable over time. With respect to this, care was taken to recalibrate the glucose analyzer before analyzing each medium sample. It was expected that if some systematic discrepancy existed between the off-line glucose analyzer and the glucose sensor output, the error would be consistent over time unless some process of membrane or electrode fouling or enzyme deactivation modified the results from one (or both) of the sensor(s). Figure 5.16 shows that the ratio of the off-line glucose analyzer results and the uncorrected glucose sensor output was relatively constant for a period of up to 6 hours after the initial loading of the enzyme at the outset of the experiment. After this period, the sensor output began to drift significantly in the case of the first enzyme loading. This may have been an indication of a decay in enzyme activity, although in the case of the second enzyme loading, the experiment was terminated 6.5

hours after loading the fresh enzyme, at which time the sensor signal had not yet shown any discernible signs of drift or decay. This suggests that continuous glucose monitoring could possibly be performed for at least 6 hours before elution and replacement of the enzyme would be necessary. However, further characterization is required to verify these results.

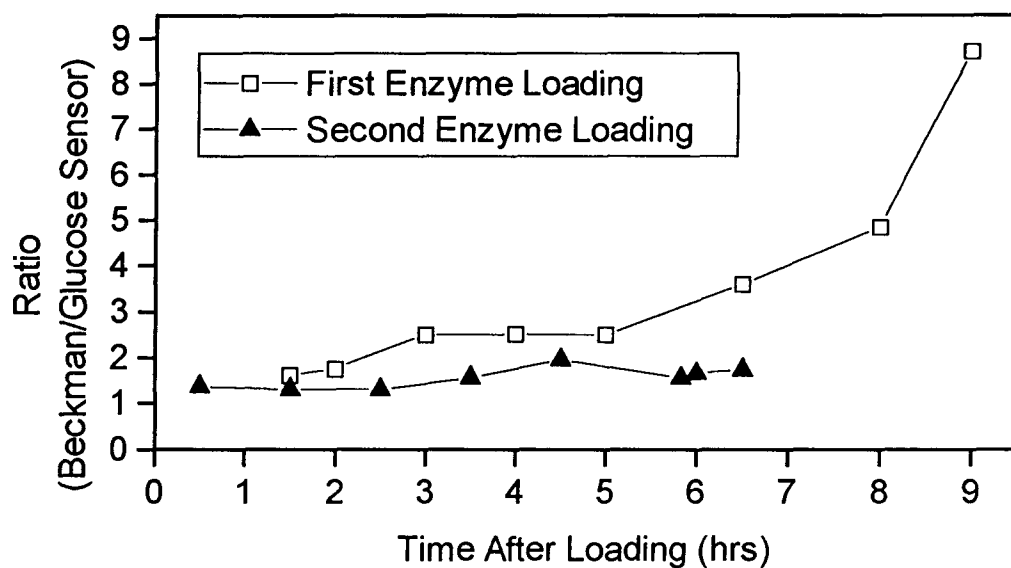


Figure 5.16: Ratio of the Beckman glucose analyzer results and the prototype glucose sensor output calculated at various points in time after fresh enzyme was loaded. The uncorrected sensor data from Figure 5.14 was used for calculation.

CHAPTER 6

CONCLUSION

6.1 CONCLUDING REMARKS

The results presented in this thesis are the first to demonstrate the concept, feasibility, and utility of a regenerable biosensor based on reversible immobilization of the enzyme using CBD technology. The design and construction of a prototype glucose biosensor based on this technology and the use of the prototype in a real microbial fermentation represent a significant step toward a practical, industrially acceptable probe design, and also toward better instrumentation for fermentation monitoring and control. The following objectives have been achieved:

1. Glucose oxidase and the cellulose binding domain have been successfully conjugated. The GOx-CBD conjugate was synthesized chemically using a glutaraldehyde linkage and retained the activity of glucose oxidase and the binding affinity of the cellulose binding domain.
2. The concept of repeatedly loading and eluting the GOx-CBD conjugate from a cellulose matrix on a platinum electrode was shown, demonstrating the feasibility of a regenerable biosensor based on reversible immobilization of the enzyme using CBD technology. The loading and elution protocols were defined and a number of cellulose-based materials were evaluated as potential immobilization matrices.
3. A prototype glucose biosensor and reagent flow system were designed and built with the capacity for loading and elution of the enzyme-CBD conjugate in order to regenerate the sensor during a fermentation. Enzyme loading and elution protocols were developed for *in situ* enzyme replacement using the reagent flow system. The prototype glucose biosensor was used successfully to monitor medium glucose concentration during

a fed-batch cultivation of *E. coli* in a 20 L fermenter, demonstrating the potential of the proposed biosensor system for on-line bioprocess monitoring and control.

In addition, a custom-designed membrane system suitable for use in microbial fermentations was developed for the biosensor prototype. The membrane system consisted of a sterilizable, glucose-permeable, outer Nafion membrane and a cellulose acetate coating on the platinum indicating electrode. This membrane system was shown to effectively reject interfering species and minimize the sensor background signal while maintaining high sensitivity and fast sensor response time. The prototype sensor with this membrane system was used for 16.5 continuous hours in a microbial fermentation without failure or discernible deterioration.

An empirical model for the sensor calibration curve was developed based on the Michaelis-Menten equation for enzyme kinetics. The sensor calibration curve could be characterized in terms of the apparent kinetic parameters K_m' and I_{max} and the sensor baseline current. The model was used successfully during fermentation monitoring as a conversion function to transform the measured sensor current into the corresponding medium glucose concentration.

A sensor system was proposed which addressed the sterilizability and stability problems of enzyme-based biosensors. The proposed sensor system could potentially perform the complete process of diagnosis, regeneration, and recalibration under computer control without interrupting the fermentation, including the automated, *in situ*, replacement of the enzyme. The prototype glucose biosensor described in this thesis has been developed with all of the necessary design characteristics in mind, however, it was beyond the scope of this project to completely develop all of the features of the proposed system. Furthermore, the system functions described could be executed manually using the present version of the prototype, and the modifications required to automate the system have been discussed.

The development of more advanced and sophisticated fermentation processes has given rise to an immediate need for improved instrumentation. In particular, four important motivations for bioprocess monitoring have been outlined by Locher et al. (1992):

1. Data collection during a bioprocess enables visualization of changes in bioprocess parameters in order to discuss observed phenomena.
2. Storage of collected data enables documentation of a series of experiments for later comparison.
3. The collected data can be used to evaluate the accuracy of mathematical models for research.
4. The output from bioprocess monitoring can be used for automatic process control by expert systems.

Thus, there is a need for monitoring techniques which can provide precise, high quality measurements of important bioprocess parameters, and the prototype described here has been shown to be useful for glucose monitoring in experimental systems, even at its present stage of development. The realization of a reliable, on-line system for glucose analysis has enormous potential for glucose monitoring in bioprocesses and the evolution of new fermentation control strategies. In batch culture, the prototype sensor system could be used in experimental fermentations to monitor glucose consumption profiles for the purpose of research, documentation, or model analysis. In fed-batch culture, the sensor could be used to replace open-loop glucose control systems with closed, feedback control loops which indicate medium glucose exhaustion and trigger glucose infusion. Alternatively, the full potential of the glucose sensor system could be realized using feedback control to maintain the medium glucose concentration at a set value. The rate of glucose infusion could be matched to the rate of glucose consumption in order to avoid fluctuation of the medium glucose concentration and maintain a constant glucose level. Thus, the prototype sensor system could be used in pilot-scale fermentations for the

investigation and optimization of the growth rate and product production of industrial/commercial fermentations, based on glucose control.

The technology for a regenerable enzyme-based biosensor for glucose using glucose oxidase conjugated to CBD has been developed. However, the approach is not restricted to the glucose sensor application presented here. In principle, it should be straightforward to conjugate other oxidase-type enzymes to CBD, such that the same sensor hardware could be used to measure different analytes in different fermentations, or at different stages of the same fermentation, depending on which enzyme-CBD conjugate solution is perfused through the cellulose matrix. A multiple enzyme sensor for analytes requiring a multi-enzyme system (see Table 1.1) may also be realized by incorporating two or more different enzyme-CBD conjugates in the same perfusate.

6.2 FUTURE WORK

Many possibilities exist for the optimization of the present version of the prototype. The importance of accurate calibration of the sensor has been discussed with respect to fermentation monitoring and further development of the procedure for sensor calibration during a fermentation is essential. It would be helpful to study the effects of the analyte matrix on the calibration constants of the sensor. In addition, internal calibration protocols that can be used to perform periodic calibration checks during the course of the fermentation, such as the scheme proposed by Bradley and Schmid (1992), remain to be investigated. In addition, further work is required toward the completion of a sterilization protocol, such as the design of a pressurization manifold for the interior of the sensor. The loading and elution protocols can also be optimized to increase the efficiency of these procedures.

The protocols that have been developed can be automated following acquisition of the necessary equipment. The sensor system could then be interfaced with a personal

computer which would monitor the sensor output and use the data in computer algorithms for sensor calibration, self-diagnosis, and regeneration. A computer-controlled glucose infusion pump could also be added to the system and control algorithms could be developed for feedback control of glucose concentration during bioprocesses, as envisioned at the outset of this project. The equipment for incorporating electrode and membrane cleaning into the regeneration cycle also remains to be developed, although the experimental results thus far have not indicated that these procedures would be necessary on a frequent basis for this system.

In addition, there are possibilities for enhancing the sensor performance. Increasing the amount of enzyme activity loaded for a given sensor configuration would be analogous to increasing I_{\max} and would result in a higher sensor current and greater sensitivity. This could be accomplished by using a concentrated GOx-CBD conjugate sample for the loading protocol or a cellulose matrix with a higher binding capacity. Other methods to increase the sensor signal include using a larger indicating electrode area and/or a higher electrode bias potential. It would also be possible to amplify the sensor signal, as the signal noise observed was very low (less than 1% of the measured sensor current). Any noise that is recorded is of sufficiently high frequency that it could easily be filtered with a low-pass filter.

The use of continuous internal buffer flow through the enzyme chamber has been reported by Cleland and Enfors (1984a), Bradley and Schmid (1991), and Brooks et al. (1987/88) and should be investigated for the sensor prototype. There are numerous advantages to this technique. Dilution of the analyte in the enzyme chamber can extend the range of concentrations that can be measured by the sensor. The operating concentration range can be varied to suit the sensor application by varying the dilution rate. A loss of sensitivity may result, as some of the influx of glucose and the hydrogen peroxide produced at the enzyme are carried away. However, harmful reaction products, enzyme inhibitors, electrochemical poisons, and other interferents are also washed away,

and a constant chemical environment is maintained within the enzyme chamber. In addition, an oxygenated buffer could potentially be used as an oxygen source for the enzyme during fermentation monitoring in anaerobic or low dissolved oxygen environments.

The hardware configuration of the prototype sensor may also be advantageous for the implementation and study of electro-enzymatic sensors mediated by alternate electron acceptors, such as ferrocene derivatives (Cass et al., 1984). Substitution of electron acceptors other than oxygen for the electron transfer between glucose oxidase and the indicating electrode can enable sensor operation at a lower electrode bias potential and in anaerobic or low dissolved oxygen media. Experiments could be performed to test this concept using solubilized mediators in the internal buffer of the enzyme chamber.

Furthermore, experimental work on the optimization and further characterization of the glucose oxidase-CBD conjugates should continue. The feasibility and utility of developing a genetically engineered fusion protein to replace chemical conjugation should also be investigated. It would be ideal if a stable, consistent source of conjugate, such as a lyophilized powder, could ultimately be obtained. Finally, the application of the CBD-immobilization approach to other oxidase enzyme systems should be explored in order to develop a range of sensor systems for different analytes which are based on the same generic sensor hardware and can be used effectively for the improvement of bioprocess monitoring and control.

NOMENCLATURE SUMMARY

A	Electrode area
C_i, c_i	Concentration of species i
C_O^*	Bulk solution oxygen concentration
D_i	Diffusion coefficient for species i
$D_{m,i}$	Membrane diffusion coefficient for species i
E_a	Applied potential
E^0	Standard half-cell potential or electromotive force
F	Faraday constant
I	Sensor current
I_O	Sensor baseline current
I_{max}	Maximum sensor current
J_i	Mass flux of species i
$J_{d,i}$	Mass flux of species i due to diffusion
K_d	Dissociation constant
K_m	Michaelis constant
K_m'	Apparent Michaelis constant
K_S, K_O	Michaelis constant for substrate and oxygen
L	Enzyme membrane thickness
MWCO	Molecular weight cut-off
R	Reaction rate
S, P, O	Concentration of substrate, product, and oxygen
S^0, P^0, O^0	Bulk solution concentration of substrate, product, and oxygen

$S_i^*(t), P_i^*(t)$	Boundary function for concentration of substrate or product at the interface between membrane layer i and $i+1$ as a function of time
U_i	Absolute mobility of species i
V	Enzyme reaction velocity
V_{\max}	Maximum enzyme reaction velocity
d_i	Width of membrane layer i
i_g	Glucose-dependent sensor current
k	Constant of proportionality ($k = V_{\max}/K_m$)
l	number of membrane layers
n_p	Number of ion equivalents of product
r^2	Correlation coefficient for linear regression
t	Time
x	X-axis position
z, z_i	Number of charge equivalents per mole of species i
α_o	Equilibrium partition coefficient for oxygen
$d\phi/dx$	Potential gradient
μ	Solution ionic strength
v_x	Solution velocity in the x -direction

REFERENCES

- Bailey, J.E.; Ollis, D.F. *Biochemical Engineering Fundamentals*, 2nd ed.; McGraw-Hill: New York, 1986.
- Bard, A.J.; Faulkner, L.R. *Electrochemical Methods: Fundamentals and Applications*; John Wiley & Sons: New York, 1980.
- Benthin, S.; Nielsen, J.; Villadsen, J. Anomeric Specificity of Glucose Uptake System in *Lactococcus cremoris*, *Escherichia coli*, And *Saccharomyces cerevisiae*: Mechanism, Kinetics, And Implications. *Biotechnol. Bioeng.* **1992**, *40*, 137-146.
- Bradley, J.; Anderson, P.A.; Dear, A.M.; Ashby, R.E.; Turner, A.P.F. Glucose Biosensors for the Study and Control of Baker's Compressed Yeast Production. In *Computer Applications in Fermentation Technology: Modelling and Control of Biotechnological Processes*; Fish, N.M., Fox, R.I., Thornhill, N.F., Eds.; Elsevier Applied Science: New York, 1988; pp 47-51.
- Bradley, J.; Kidd, A.J.; Anderson, P.A.; Dear, A.M.; Ashby, R.E.; Turner, A.P.F. Rapid Determination of the Glucose Content of Molasses Using a Biosensor. *Analyst* **1989a**, *114*, 375-379.
- Bradley, J.; Turner, A.P.F.; Schmid, R.D. An *In situ* Fermenter Probe for Baker's Yeast Propagation Monitoring. In *GBF Monographs. Biosensors: Application in Medicine, Environmental Protection and Process Control*; Schmid, R.D., Scheller, R., Eds.; VCH: New York, 1989b; Vol. 13, pp 85-88.
- Bradley, J.; Schmid, R.D. Biosensors For *In situ* Fermentation Monitoring of Glucose Concentration. *Proc. Biosensors 90*, May 1990, Singapore, p 255.
- Bradley, J.; Schmid, R.D. Optimisation of a Biosensor For *In situ* Fermentation Monitoring of Glucose Concentration. *Biosensors & Bioelectronics* **1991**, *6*, 669-674.
- Bradley, J.; Stöcklein, W.; Schmid, R.D. Biochemistry Based Analysis Systems for Bioprocess Monitoring and Control. *Process Contr. Qual.* **1991**, *1*, 157-183.

- Bright, H.J.; Porter, D.J.T. Flavoprotein Oxidases. In *The Enzymes*, 3rd ed.; P.D. Boyer, Ed.; Academic Press: New York, 1975; Vol. 3, pp 421-506.
- Brillhart, K.L.; Ngo, T.T. Simple And Rapid Procedure For "Sandwich" Enzyme ImmunoAssay Development Using Biotin Labeled Microwells (AvidPlate-Biotin). *Anal. Lett.* **1991**, *24*(12), 2157-2169.
- Brooks, S.L.; Ashby, R.E.; Turner, A.P.F.; Calder, M.R.; Clarke, D.J. Development of an On-Line Glucose Sensor For Fermentation Monitoring. *Biosensors* **1987/88**, *3*, 45-56.
- Brooks, S.L.; Higgins, I.J.; Newman, J.D.; Turner A.P.F. Biosensors For Process Control. *Enzyme Microbiol. Technol.* **1991**, *13*, 946-955.
- Bühler, H.; Ingold, W. Measuring pH and Oxygen in Fermenters. *Process Biochem.* **1976**, *11*(3), 19-24.
- Cass, A.E.G.; Davis, G.; Francis, G.D.; Hill, H.A.O.; Aston, W.J.; Higgins, I.J.; Plotkin, E.V.; Scott, L.D.L.; Turner, A.P.F. Ferrocene-Meditated Enzyme Electrode For Amperometric Determination of Glucose. *Anal. Chem.* **1984**, *56*, 667-671.
- Chaplin, M.F.; Bucke, C. *Enzyme Technology*; Cambridge University Press: Cambridge, 1990; pp 197-219.
- Clark, L.C. Monitor And Control of Blood And Tissue Oxygen Tensions. *Trans. Amer. Soc. Artif. Intern. Organs.* **1956**, *2*, 41.
- Clark, L.C.; Lyons, C. Electrode Systems For Continuous Monitoring in Cardiovascular Surgery. *Ann. N.Y. Acad. Sci.* **1962**, *102*, 29-45.
- Clark, L.C. Membrane Polarographic Electrode System And Method With Electrochemical Compensation. US Patent 3 539 455, **1970**.
- Cleland, N.; Enfors, S.O. Control of Glucose Fed-Batch Cultivations of *E. coli* by Means of an Oxygen Stabilized Enzyme Electrode. *Eur. J. Appl. Microbiol. Biotechnol.* **1983**, *18*, 141-147.
- Cleland, N.; Enfors, S.O. Externally Buffered Enzyme Electrode For Determination of Glucose. *Anal. Chem.* **1984a**, *56*, 1880-1884.

- Cleland, N.; Enfors, S.O. Monitoring Glucose Consumption in an *Escherichia coli* Cultivation With an Enzyme Electrode. *Anal. Chim. Acta.* **1984b**, *163*, 281-285.
- Coutinho, J.B.; Gilkes, N.R.; Warren R.A.J.; Kilburn, D.G.; Miller, R.C. Jr. The Binding of *Cellulomonas fimi* Endoglucanase C (CenC) to Cellulose and Sephadex is Mediated by The N-Terminal Repeats. *Molec. Microbiol.* **1992**, *6*, 1243-1252.
- Cronenberg, C.C.H.; van den Huevel, J.C. Determination of Glucose Diffusion Coefficients in Biofilms With Micro-Electrodes. *Biosensors & Bioelectronics* **1991**, *6*, 255-262.
- de Alwis, U; Wilson, G.S. Strategies For The Reversible Immobilization of Enzymes by Use of Biotin-Bound Anti-Enzyme Antibodies. *Talanta* **1989**, *36*, 249-253.
- De Baetselier, A.; Vasavada, A.; Dohet, P.; Ha-Thi, V.; De Beukelaer, M.; Erpicum, T.; De Clerck, L.; Hanotier, J.; Rosenberg, S. Fermentation of a Yeast Producing *A. niger* Glucose Oxidase: Scale-Up, Purification and Characterization of The Recombinant Enzyme. *Bio/Technology* **1991**, *9*, 559-561.
- Demain, A.L. Cellular And Environmental Factors Affecting The Synthesis And Excretion of Metabolites. *J. Appl. Chem. Biotechnol.* **1972**, *22*, 345-362.
- Dixon, M.; Webb, E.C. *Enzymes*; Academic Press: New York, 1964.
- Enfors, S.O. Oxygen-Stabilized Enzyme Electrode For D-Glucose Analysis in Fermentation Broths. *Enzyme Microbiol. Technol.* **1981**, *3*, 29-32.
- Enfors, S.O.; Molin, N. Enzyme Electrodes for Fermentation Control. *Process Biochem.* **1978**, *13*, 9-11.
- Enfors, S.O.; Nilsson, H. Design And Response Characteristics of an Enzyme Electrode For Measurement of Penicillin in Fermentation Broth. *Enzyme Microbiol. Technol.* **1979**, *1*, 260-264.
- Filippini, C.; Sonnleitner, B.; Fiechter, A.; Bradley, J.; Schmid, R. On-Line Determination of Glucose in Biotechnological Processes: Comparison Between FIA And an *In situ* Enzyme Electrode. *J. Biotechnol.* **1991**, *18*, 153-160.

- Fortier, G.; Brassard, E.; Bélanger, D. Optimization of a Polypyrrole Glucose Oxidase Biosensor. *Biosensors & Bioelectronics* **1990**, *5*, 473-490.
- Foulds, N.C.; Lowe, C.R. Enzyme Entrapment in Electrically Conducting Polymers. *J. Chem. Soc. Faraday Trans.* **1986**, *82*, 1259-1264.
- Frame, K.K.; Hu, W.-S. Kinetic Study of Hybridoma Cell Growth in Continuous Culture: II. Behavior of Producers And Comparison to Nonproducers. *Biotech. Bioeng.* **1991**, *38*, 1020-1028.
- Frederick, K.R.; Tung, J.; Emerick, R.S.; Masiarz, F.R.; Chamberlain, S.H.; Vasavada, A.; Rosenberg, S.; Chakraborty, S.; Schopfer, L.M.; Massey, V. Glucose Oxidase From *Aspergillus niger*: Cloning, Gene Sequence, Secretion From *Saccharomyces cerevisiae* and Kinetic Analysis of a Yeast-Derived Enzyme. *J. of Biol. Chem.* **1990**, *265*, 3793-3802.
- Freitag, R. Applied Biosensors. *Curr. Opin. Biotech.: Anal. Biotech.* **1993**, *4*, 75-79.
- Gibson, T.D.; Woodward, J.R. Protein Stabilization in Biosensor Systems. In *Biosensors & Chemical Sensors: Optimizing Performance Through Polymeric Materials*; Edelman, P.G., Wang, J., Eds.; ACS: Washington, DC, 1992; pp 40-55.
- Gilkes, N.R.; Henrissat, B.; Kilburn, D.G.; Miller, R.C. Jr.; Warren, R.A.J. Domains in Microbial β -1,4-Glycanases: Sequence Conservation, Function, And Enzyme Families. *Microbiol. Rev.* **1991**, *55*, 303-315.
- Gilkes, N.R.; Jarvis, E.; Henrissat, B.; Tekant, B.; Miller, R.C. Jr.; Warren, R.A.J.; Kilburn D.G. The Adsorption of a Bacterial Cellulase And Its Two Isolated Domains to Crystalline Cellulose. *J. Biol. Chem.* **1992**, *267*(10), 6743-6749.
- Guilbault, G.G.; Lubrano, G.L. An Enzyme Electrode For The Amperometric Determination of Glucose. *Anal. Chim. Acta* **1973**, *64*, 439-455.
- Guilbault, G.G.; Luong, J.H. Biosensors: Current Status And Future Possibilities. *Sel. Elec. Rev.* **1989**, *11*, 3-16.

- Guilbault, G.G.; Montalvo, J. A Urea-Specific Enzyme Electrode. *J. Am. Chem. Soc.*, **91**, 1969, 2164.
- Hall, E.A.H. *Biosensors*; Prentice Hall: Englewood Cliffs, New Jersey, 1991; pp 216-218.
- Hansen, E.H.; Mikkelsen, H.S. Enzyme-Immobilization by The Glutardialdehyde Procedure. An Investigation of The Effects of Reducing The Schiff-Bases Generated, as Based on Studying The Immobilization of Glucose Oxidase to Silanized Controlled Pore Glass. *Anal. Lett.* **1991**, *24*(8), 1419-1430.
- Hardjito, L.; Greenfield, P.F.; Lee, P.L. Recombinant Protein Production Via Fed-Batch Culture of The Yeast *Saccharomyces cerevisiae*. *Enzyme Microb. Technol.* **1993**, *15*, 120-126.
- Harlow, E.; Lane, D. *Antibodies: A Laboratory Reference Manual*; Cold Spring Harbor Laboratory: Cold Spring Harbor, New York, 1988; Ch. 12.
- Harrison, D.J.; Turner, R.F.B.; Baltes, H.P. Characterization of Perfluorosulfonic Acid Polymer Coated Enzyme Electrodes And a Miniaturized Integrated Potentiostat For Glucose Analysis in Whole Blood. *Anal. Chem.* **1988**, *60*, 2002-2007.
- Hendry, S.P.; Higgins, I.J.; Bannister, J.V. Amperometric Biosensors. *J. Biotech.* **1990**, *15*, 229-238.
- Hecht, H.J.; Schomburg, D.; Kalisz, H.; Schmid, R.D. The 3D Structure of Glucose Oxidase From *Asperigillus niger*. Implications For The Use of GOD as a Biosensor Enzyme. *Biosensors & Bioelectronics* **1993**, *8*, 197-203.
- Holst, O.; Håkanson, H.; Miyabayashi, A.; Mattiasson, B. Monitoring of Glucose in Fermentation Processes Using a Commercial Glucose Analyser. *Appl. Microbiol. Biotechnol.* **1988**, *28*, 32-36.
- Huang, Y.L.; Li, S.Y.; Dremel, B.A.A.; Bilitewski, U.; Schmid, R.D. On-Line Determination of Glucose Concentration Throughout Animal Cell Cultures Based on Chemiluminescent Detection of Hydrogen Peroxide Coupled With Flow-Injection Analysis. *J. Biotechnol.* **1991**, *18*, 161-172.

- Ingold, W. CO₂ Measuring System Product Brochure, Ingold Electrodes Inc.,
Wilmington, MA, c. 1990.
- Janata, J. *Principles of Chemical Sensors*; Plenum Press: New York, 1989; pp 175-195.
- Jochum, P.; Kowalski, B.R. A Coupled Two-Compartment Model For Immobilized
Enzyme Electrodes. *Anal. Chim. Acta.* **1982**, *144*, 25-38.
- Kilburn, D.G.; Turner, R.F.B.; Coutinho, J.B.; Din, N.; Gilkes, N.R.; Greenwood, J.M.;
Hobbs, J.B.; Miller, R.C. Jr.; Ong, E.; Phelps, M.R.; Ramirez, C.; Warren, R.A.J.
Cellulose Binding Domains: Applications in Biotechnology. *Proc. Cellucon 92*, In
Press.
- Kittsteiner-Eberle, R.; Ogbomo, I.; Schmidt, H.-L. Biosensing Devices For The Semi-
Automated Control of Dehydrogenase Substrates in Fermentations. *Biosensors* **1989**,
4, 75-85.
- Kobos, R.K. Potentiometric Enzyme Methods. In *ISE's in Analytical Chemistry*; Freiser,
H., Ed.; Plenum: New York, 1980; Vol. 2, p.1.
- Kok, R.; Hogan, P. The Development of an *In situ* Fermentation Electrode Calibrator.
Biosensors **1987/88**, *3*, 89-100.
- Kole, M.M.; Ward, D.; Gerson, D.F. Simultaneous Control of Ammonium And Glucose
Concentrations in *Escherichia coli* Fermentations. *J. Ferment. Technol.* **1986**, *64*(3),
233-238.
- Leyboldt, J.K.; Gough, D.A. Model of a Two-substrate Enzyme Electrode For Glucose.
Anal. Chem. **1984**, *56*, 2896-2904.
- Linek, V.; Beneš, P.; Sinkule, J.; Holecek, O.; Malý, V. Oxidation of D-Glucose in The
Presence of Glucose Oxidase And Catalase. *Biotech. Bioeng.* **1980**, *22*, 2515-2527.
- Locher, G.; Sonnleitner, B.; Fiechter, A. On-Line Measurement in Biotechnology:
Exploitation, Objectives and Benefits. *J. Biotech.* **1992**, *25*, 55-73.

- Lüdi, H.; Garn, M.B.; Haemmerli, S.D.; Manz, A.; Widmer, H.M. Flow Injection Analysis And In-Line Biosensors For Bioprocess Control: A Comparison. *J. Biotech.* **1992**, *25*, 75-80.
- Mandenius, C.F.; Danielsson, B.; Mattiasson, B. Evaluation of a Dialysis Probe For Continuous Sampling in Fermentors And in Complex Media. *Anal. Chim. Acta* **1984**, *163*, 135-141.
- Maresse, C.A.; Miyawaki, O.; Wingard, L.B., Jr. Simultaneous Electrochemical Determination of Diffusion And Partition Coefficients of Potassium Ferrocyanide For Albumin-Glutaraldehyde Membranes. *Anal. Chem.* **1987**, *59*, 248-252.
- Mascini, M.; Palleschi, G. Design And Applications of Enzyme Electrode Probes. *Sel. Elec. Rev.* **1989**, *11*, 191-264.
- Merten, O.-W.; Palfi, G.E.; Steiner, J. On-Line Determination of Biochemical/Physiological Parameters in The Fermentation of Animal Cells in a Continuous or Discontinuous Mode. In *Advances in Biotechnological Processes*; Mizrahi, A. Ed.; Alan R. Liss: New York, 1986; Vol. 6, pp 125-152.
- Miyabayashi, A.; Reslow, M.; Adlercreutz, P.; Mattiasson, B. A Potentiometric Enzyme Electrode For Monitoring in Organic Solvents. *Anal. Chim. Acta.* **1989**, *219*, 27-36.
- Moody, G.J.; Thomas, J.D.R. Amperometric Biosensors: A Brief Appraisal of Principles and Applications. *Sel. Elec. Rev.* **1991**, *13*, 113-124.
- Moore, R.B.; Martin, C.R. Procedure For Preparing Solution-Cast Perfluorosulfonate Ionomer Films And Membranes. *Anal. Chem.* **1986**, *58*, 2569-2570.
- Nakamura, S.; Hayashi, S.; Koga, K. Effect of Periodate on The Structure And Properties of Glucose Oxidase. *Biochem. Biophys. Acta* **1976**, *445*, 294-308.
- O'Neill, G.; Goh, S.H.; Warren, R.A.J.; Kilburn, D.G.; Miller, R.C. Jr. Structure of The Gene Encoding The Exoglucanase of *Cellulomonas fimi*. *Gene* **1986**, *44*, 325-330.
- Ogbomo, I.; Prinzing, U.; Schmidt, H.L. Prerequisites For The Control of Microbial Processes by Flow Injection Analysis. *J. Biotechnol.* **1990**, *14*(1), 63-70.

- Ong, E.; Gilkes, N.R.; Miller, R.C. Jr.; Warren, R.A.J.; Kilburn, D.G. Enzyme Immobilization Using a Cellulose-Binding Domain: Properties of a β -Glucosidase Fusion Protein. *Enzyme Microb. Technol.* **1991**, *13*, 59-65.
- Ong, E.; Gilkes, N.R.; Miller, R.C. Jr.; Warren, R.A.J.; Kilburn, D.G. The Cellulose-Binding Domain (CBD_{Cex}) of an Exoglucanase From *Cellulomonas fimi*: Production in *Escherichia coli* And Characterization of the Polypeptide. *Biotech. Bioeng.* **1993**, *42*, 401-409.
- Ong, E.; Gilkes, N.R.; Warren, R.A.J.; Miller, R.C. Jr.; Kilburn, D.G. Enzyme Immobilization Using The Cellulose-Binding Domain of a *Cellulomonas fimi* Exoglucanase. *Bio/Technology* **1989**, *7*, 604-607.
- Patkar, A.; Seo, J.-H. Fermentation Kinetics of Recombinant Yeast in Batch And Fed-Batch Cultures. *Biotech. Bioeng.* **1992**, *40*, 103-109.
- Pieters, B.R.; Bardeletti, G. Enzyme Immobilization on a Low-Cost Magnetic Support: Kinetic Studies on Immobilized And Coimmobilized Glucose Oxidase And Glucoamylase. *Enzyme Microb. Technol.* **1992**, *14*, 361-370.
- Reach, G.; Wilson, G.S. Can Continuous Glucose Monitoring be Used For The Treatment of Diabetes? *Anal. Chem.* **1992**, *64*, 381-386.
- Renneberg, R.; Trott-Kriegeskorte, G.; Lietz, M.; Jäger, V.; Pawlowa, M.; Kaiser, G.; Wollenberger, U.; Schubert, F.; Wagner, R.; Schmid, R.D.; Scheller, F.W. Enzyme Sensor-FIA-System For On-Line Monitoring of Glucose, Lactate And Glutamine in Animal Cell Cultures. *J. Biotech.* **1991**, *21*, 173-186.
- Rishpon, J.; Shabtai, Y.; Rosen, I.; Zibenberg, Y.; Tor, R.; Freeman, A. *In situ* Glucose Monitoring in Fermentation Broth by "Sandwiched" Glucose-Oxidase Electrode (SGE). *Biotech. Bioeng.*, **1990**, *35*, 103-107.
- Rogers, M.J.; Brandt, K.G. Multiple Inhibition Analysis of *Aspergillus niger* Glucose Oxidase by D-Glucal And Halide Ions. *Biochem.* **1971**, *10*, 4636-4641.

- Romette, J.-L.; Froment, B.; Thomas, D. Glucose-Oxidase Electrode. Measurements of Glucose In Samples Exhibiting High Variability In Oxygen Content. *Clin. Chim. Acta* **1979**, *95*, 249-253.
- Romette, J.-L. Mammalian Cell Culture Process Control: Sampling And Sensing. *BGF Monographs* **1987**, *10*, 81-86.
- Sansen, W.; Suls, J.; Lambrechts, M.; Claes, A.; Jacobs, P.; Kuypers, M.H. Anaerobic Operation of a Glucose Sensor by Use of Pulse Techniques. *Biosensors* **1992**, 156-162.
- Sawyer, D.T.; Roberts, J.L. Jr. *Experimental Electrochemistry for Chemists*; John Wiley and Sons: New York, 1974; pp 39-41.
- Schulmeister, T. Mathematical Treatment of Concentration Profiles And Anodic Current of Amperometric Multilayer Enzyme Electrodes. *Anal. Chim. Acta* **1987**, *198*, 223-229.
- Schulmeister, T. Mathematical Modelling of the Dynamic Behaviour of Amperometric Enzyme Electrodes. *Sel. Elec. Rev.* **1990**, *12*, 203-260.
- Schultz, J.S. Sophisticated Descendants of The Canary in The Coal Mine Are Based on Molecular Components of Plants And Animals Bound to Microscopic Electrodes or Optical Fibers. *Scientific American* **1991**, *264*, 64-69.
- Sigma catalogue, 1993, Sigma Chemical Co., St. Louis, MO, U.S.A., pp 2104-2106.
- Sittampalam, G.; Wilson, G.S. Surface-Modified Electrochemical Detector For Liquid Chromatography. *Anal. Chem.* **1983**, *55*, 1608-1610.
- Smith, M.; Bajpai, R. Fed-Batch Control of *Escherichia coli* Fermentation to High Cell Density. *Proc. 15th Ann. Biochem. Eng. Symp.* **1985**, *15*, 34-44.
- Stamm, W.W.; Seidler, W.; Kahlert, W.; Kappel, W. On-Line Monitoring of Glucose in Batch Fermentations of *Escherichia coli* With a Commercially Available Biosensor Analyzer - Fermentation Control System. *Proc. 2nd World Cong. Biosensors*, May 1992, Geneva, p 506.

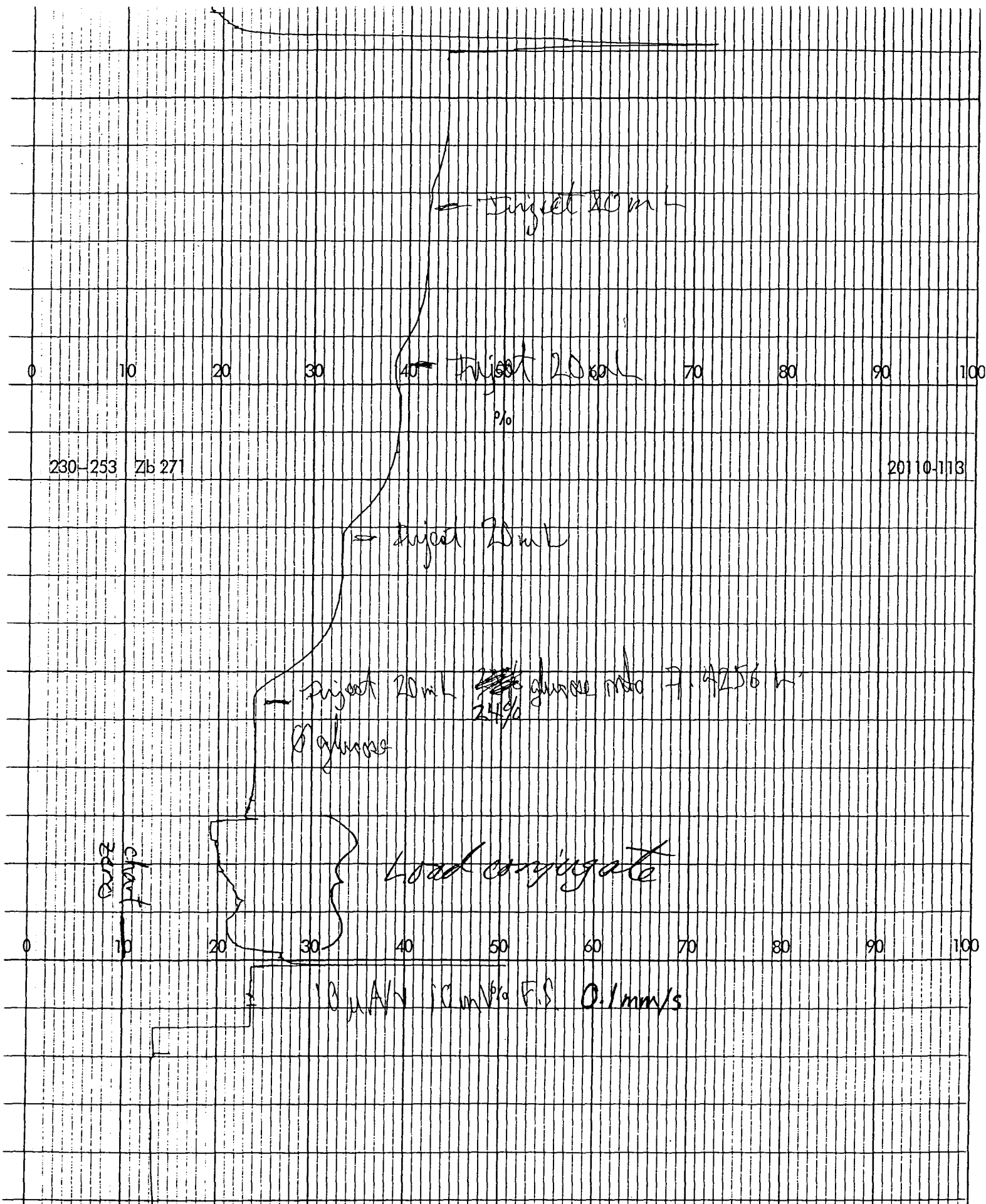
- Stoecker, P.W.; Yacynych, A.M. Chemically Modified Electrodes as Biosensors. *Sel. Elec. Rev.* **1990**, *12*, 137-160.
- Tran-Minh, C.; Broun, G. Construction And Study of Electrodes Using Cross-Linked Enzymes. *Anal. Chem.* **1975**, *47*, 1359-1364.
- Turner, A.P.F., Karube, I., Wilson, G.S. Eds.; *Biosensors: Fundamentals and Applications*. Oxford University Press: Oxford, 1987.
- Urdike, S.J.; Hicks, G.P. The Enzyme Electrode. *Nature* **1967**, *214*, 986-988.
- Valero, F; Lafuente, J.; Poch, M.; Solà, C.; Araujo, A.N.; Lima, J.L.F.C. On-Line Fermentation Monitoring Using Flow Injection Analysis. *Biotech. Bioeng.* **1990**, *36*, 647-651.
- Wang, J.; Hutchins, L.D. Thin-Layer Electrochemical Detector With a Glassy Carbon Electrode Coated With a Base-Hydrolyzed Cellulosic Film. *Anal. Chem.* **1985**, *57*, 1536-1541.
- Wang, J. Permselective Coatings For Amperometric Biosensing. In *Biosensors and Chemical Sensors: Optimizing Performance Through Polymeric Materials*; Eddman, P.G., Wang, J., Eds.; ACS: New Mexico State University, 1992; Symposium Series 487, pp 125-132.
- Whittle, D.J.; Kilburn, D.G.; Warren, R.A.J.; Miller, R.C. Jr. Molecular Cloning of a *Cellulomonas fimi* Cellulase Gene in *Escherichia coli*. *Gene* **1982**, *17*, 139-145.
- Wilson, R.; Turner, A.P.F. Glucose Oxidase: An Ideal Enzyme. *Biosensors & Bioelectronics* **1992**, *7*, 165-185.
- Wirth, M.; Li, S.Y.; Schumacher, L.; Lehmann, J. Screening For And Fermentation of High Producer Cell Clones From Recombinant BHK Cells. In *Advances in Animal Cell Biology and Technology for Bioprocesses*; Spier, R.E., Griffiths, J.B., Stephenne, J., Gooy, P.J., Eds.; Butterworth: Sevenoaks, Kent, England, 1989; pp 44-51.
- Yamasaki, Y. The Development of a Needle-Type Glucose Sensor For Wearable Artificial Endocrine Pancreas. *Medical Journal of Osaka University* **1984**, *35*, 25-34.

Ylilammi, M.; Lehtinen, L. Numerical Analysis of a Theoretical One-Dimensional Amperometric Enzyme Sensor. *Med. & Biol. Eng. & Comput.* **1988**, 26, 81-87.

APPENDIX
SAMPLE STRIP CHART RECORD

**Recorded during first calibration of the biosensor prototype for glucose monitoring
in a fermentation of *E. coli***

Conditions: Prototype with Nafion/cellulose acetate membrane system
 First enzyme loading
 Fresh minimal medium (M-9)
 No cells



230-253

Zb 271

20110-1113